



universität  
wien

# MASTERARBEIT

Titel der Masterarbeit

Evaluating capacity and drainage behavior of alpine  
ground water storages – Recession observations in the  
upper Poschiavino Area / Switzerland in winter 2013/14

Verfasser

Marius Floriancic, BSc

angestrebter akademischer Grad

Master of Science (MSc)

Wien, 2014

Studienkennzahl lt. Studienblatt:

A 855 655

Studienrichtung lt. Studienblatt:

Masterstudium Geographie

Betreuerin / Betreuer:

Dr. Felix Naef



---

## Erklärung

Hiermit versichere ich,

- dass die ich die vorliegende Masterarbeit selbstständig verfasst, andere als die angegebenen Quellen und Hilfsmittel nicht benutzt und mich auch sonst keiner unerlaubter Hilfe bedient habe,
- dass ich dieses Masterarbeitsthema bisher weder im In- noch im Ausland in irgendeiner Form als Prüfungsarbeit vorgelegt habe
- und dass diese Arbeit mit der vom Begutachter beurteilten Arbeit vollständig übereinstimmt.

Wien, August 2014

---

Marius Floriancic

---

---

## Danksagung

Im Laufe des Studiums, während spannender Exkursionen sowie bei meinen Praktika konnte ich unzählige Erfahrungen sammeln und lernte zahlreiche interessante Personen kennen. An dieser Stelle möchte ich mich bei all jenen bedanken, die mich während meines Studiums und beim Verfassen dieser Arbeit unterstützt haben. Allen voran danke ich meinem „Betreuerteam“ Felix Naef, Maarten Smoorenburg und Michael Margreth für die unzähligen Stunden spannender Diskussionen und Hilfestellungen. Durch eure hervorragende Betreuung hatte ich erst die Möglichkeit diese Arbeit erfolgreich zu beenden, eure ständige Motivation und Hilfe beim Bewältigen der Herausforderung waren ein wesentlicher Antrieb vor allem in den „dunkelsten Stunden vor der Dämmerung“.

Des Weiteren möchte ich mich bei allen Kollegen und Mitarbeitern des Instituts für Umweltingenieurwissenschaften bedanken: Wolfgang Kinzelbach für die finanzielle Unterstützung, Vera Löhle für die Unterstützung in oft kurzfristigen bürokratischen Belangen, Daniel Braun und Lucien Boilley für Hilfestellungen bei der Laborarbeit, Thomy Keller für die Vorbereitungen der Feldkampagnen und selbstverständlich bei der „Zmittagcrew“ für die spannenden, motivierenden und lustigen Tischgespräche in der Mensa. Ein grosser Dank geht an meinen Mitbewohner Gero Bauser, der mich in Zürich aufgenommen, bekocht und sehr unterstützt hat.

Für Unterstützung bei den herausfordernden Feldarbeiten möchte ich mich vor allem bei Familie Foppoli und den Mitarbeitern des „Chalet della Stazione“ bedanken die mich während den Aufenthalten im winterlichen Puschlav bestens beherbergt, gepflegt und in allen Belangen unterstützt haben. Ausserdem möchte ich mich bei Marco Passini (Comune di Poschiavo), der Firma „Fratelli Lanfrachi“ und Romeo Lardi (Giardino dei Ghiacciai Cavaglia) bedanken. Für die Finanzierung meines mehrmonatigen Auslandsaufenthalts und den Feldarbeiten möchte ich mich beim Institut für Umweltingenieurwissenschaften, den Firmen Soilcom GmbH und HyBest GmbH sowie bei der Kärnter Industriellenvereinigung bedanken ohne deren finanzielle Unterstützung diese Arbeit nicht zustande gekommen wäre.

Außerdem möchte ich mich bei den zahlreichen Personen bedanken, die mich während meines Studiums unterstützt haben: Christian Maslo der in mir die Leidenschaft für Hydrologie entfacht und mich letztendlich nach Zürich vermittelt hat, Robert Peticzka und Franz Holawe für die jahrelange Unterstützung während meines Studiums und die zahlreichen motivierenden Gespräche, Rainer Bell für unvergesslichen Erlebnisse auf den Exkursionen nach Nepal, Rumänien und ins Salzkammergut, der ganzen Arbeitsgruppe ENGAGE für die spannenden Projekte bei denen ich mitarbeiten durfte und nicht zuletzt bei meinen Studienkollegen an Universität Wien und BOKU für eine unvergessliche Studienzeit.

Mein grösster Dank gilt meinen Eltern denen ich diese Arbeit widmen möchte. Meine Ausbildung, Exkursionen und Auslandsaufenthalte, zahlreiche Reisen wären ohne eure grenzenlose Unterstützung nicht möglich gewesen.

---

---

# Table of Contents

<b>Erklärung</b> .....	<b>iii</b>
<b>Danksagung</b> .....	<b>v</b>
<b>List of figures</b> .....	<b>xi</b>
<b>List of tables</b> .....	<b>xv</b>
<b>Abbreviations</b> .....	<b>xvii</b>
<b>Kurzfassung</b> .....	<b>xix</b>
<b>Abstract</b> .....	<b>xxi</b>
<b>1 Introduction</b> .....	<b>1</b>
1.1 General introduction.....	1
1.2 Objectives and hypotheses.....	2
1.3 Structure of the thesis.....	3
<b>2 Theoretical background</b> .....	<b>4</b>
2.1 The low flow value Q347.....	4
2.2 Storage, drainage and travel times.....	4
2.3 Recession analysis.....	5
<b>3 Research Area</b> .....	<b>6</b>
3.1 Selection of the study area.....	6
3.1.1 Decision criteria.....	6
3.1.2 Evaluation of existing data.....	8
3.2 The upper Poschiavino Area.....	9
3.2.1 The hydrology of the catchment.....	11
3.2.2 The geology of the catchment.....	11
3.2.3 Main subcatchments.....	12
<b>4 Methodological Approach</b> .....	<b>16</b>
4.1 Available data.....	16
4.2 Mapping of storages.....	16
4.3 Discharge measurements.....	18
4.3.1 Salt dilution.....	18

---

4.3.2	Bucket measurements.....	19
4.4	Measurement of electric conductivity .....	21
4.4.1	Continuous measurements .....	21
4.4.2	Field campaigns.....	21
4.5	Lake gauges.....	21
4.6	Ion composition of water samples .....	22
4.7	Model calculations.....	22
4.8	Organization of field work .....	23
<b>5</b>	<b>Results .....</b>	<b>24</b>
5.1	Measurements on catchment scale .....	24
5.2	Comparison on subcatchment scale.....	25
5.2.1	Discharge and Conductivity.....	25
5.2.2	Storage mapping .....	28
5.2.2.1	Subcatchment A .....	28
5.2.2.2	Subcatchment B .....	30
5.2.2.3	Subcatchment C .....	31
5.2.2.4	Subcatchment D .....	33
5.2.3	Potential storage volume .....	35
5.2.4	Comparison of storage and discharge behavior .....	37
5.3	Spatially higher resolved measurements .....	37
5.3.1	Scale issues.....	37
5.3.2	Variation of ion composition along Poschiavino.....	40
5.3.3	Influence of the rockslide area.....	41
5.3.4	The influence of Raibler sediment series on discharge behavior .....	44
5.4	Additional results.....	47
5.4.1	Evaluation of influence of snowmelt .....	47
5.4.2	Influence of the pass road on ion composition .....	48
<b>6</b>	<b>Interpretation and discussion .....</b>	<b>51</b>
6.1	Spatial variability in discharge during recession .....	51
6.2	Spatial scale issues.....	52



---

6.3	Different storage types.....	53
<b>7</b>	<b>Perspectives and summary.....</b>	<b>54</b>
7.1	Perspectives.....	54
7.2	Summary.....	55
<b>8</b>	<b>References.....</b>	<b>57</b>
<b>9</b>	<b>Appendix.....</b>	<b>61</b>

---

---

---

## List of figures

<b>Figure 1:</b> Flow duration curve of Poschiavino LaRösa for 2004 until 2013 (Data: FOEN).....	4
<b>Figure 2:</b> Measured discharge for Alpbach / Erstfeld for winter seasons 2003/04 until 2012/13 (Data: FOEN) .....	8
<b>Figure 3:</b> Measured discharge for Poschiavino / LaRösa for winter seasons 2003/04 until 2012/13 (Data: FOEN) .....	9
<b>Figure 4:</b> Study area Poschiavino / LaRösa (Data: swisstopo / ETH Zürich).....	10
<b>Figure 5 &amp; Figure 6:</b> FOEN gauging station LaRösa, after (left) and before bricking of the riverbed and sealing cracks at the orographic right side (right) (Figure 6 – Andrea Crose / FOEN).....	11
<b>Figure 7:</b> Geological map of the study area Poschiavino / La Rösa (Data: swisstopo / ETH Zürich).....	12
<b>Figure 8:</b> Map of the four main subcatchments including location and direction of impressions of the subcatchments (Figure 8 – 15) (Data: swisstopo / ETH Zürich) .....	13
<b>Figure 9 &amp; Figure 10:</b> Impressions of subcatchment A – see Figure 8 for location and perspective .....	14
<b>Figure 11 &amp; Figure 12:</b> Impressions of subcatchment B – see Figure 8 for location and perspective .....	14
<b>Figure 13 &amp; Figure 14:</b> Impressions of subcatchment C – see Figure 8 for location and perspective .....	15
<b>Figure 15 &amp; Figure 16:</b> Impressions of subcatchment D – see Figure 8 for location and perspective .....	15
<b>Figure 17:</b> Storage map in subcatchment C: besides field observation and a DEM, aerial photographs (A) and geological maps (B) (see Figure 7 for legend) were used to generate a storage map (C). Geomorphological type, depth (<1m, 1-5m and >5m) and permeability (high, medium, low and zero) were classified. (Data: swisstopo) .....	17
<b>Figure 18 &amp; Figure 19:</b> Bucket measurements at MP D5 and MP A 21 .....	19
<b>Figure 20:</b> Overview of the measuring locations of discharge (Data: swisstopo / ETH Zürich) .....	20

---

<b>Figure 21 &amp; Figure 22:</b> Lake gauges (left – in western part of subcatchment A, right – subcatchment C).....	21
<b>Figure 23:</b> Overview of the locations of EC monitoring and lake gauges (Data: swisstopo / ETH Zürich) .....	22
<b>Figure 24 &amp; Figure 25:</b> snow accumulation during winter season 2013/14.....	23
<b>Figure 26:</b> Q, $Q_s$ and EC at the gauging station LaRösa from 9 Nov 13 to 02 April 14 (Discharge data: FOEN) .....	24
<b>Figure 27:</b> Discharged volume between 27 November 13 and 11 March 14 .....	25
<b>Figure 28:</b> Q, $Q_s$ and EC in the four subcatchments during the winter season 2013/14.....	26
<b>Figure 29:</b> The four subcatchments show different recession behavior during the winter season 2013/14. In the beginning specific discharge ( $l/s\ km^2$ ) is similar but the drainage behavior of the four catchments differs - quick recession in the western part (A and B), high winter discharge and slow recession in the eastern part (C and D) .....	27
<b>Figure 30:</b> Depth of the quaternary deposits for subcatchment A.....	29
<b>Figure 31:</b> Discharged volume (highlighted in grey) between 27.11. – 11.03. for subcatchment A.....	29
<b>Figure 32:</b> Depth of the quaternary deposits in subcatchment B – marked: area covered by sedimentary rocks .....	30
<b>Figure 33:</b> Discharged volume between 27.11. – 11.03. for subcatchment B.....	31
<b>Figure 34:</b> Depth of the quaternary deposits for subcatchment C.....	32
<b>Figure 35:</b> Discharged volume between 27.11. – 11.03. for subcatchment C.....	33
<b>Figure 36:</b> Depth of the quaternary deposits in subcatchment D – highlighted: alluvial plain LaRösa.....	34
<b>Figure 37:</b> Discharged volume between 27.11. – 11.03. for subcatchment D .....	34
<b>Figure 38:</b> Estimated storage potential in mm for the research area .....	36
<b>Figure 39:</b> Variation of discharge (Q), specific discharge ( $Q_s$ ) and electric conductivity (EC) along Poschiavino from measurement point C to the gauging station on 22 February 2014.	38
<b>Figure 40:</b> Spatial variation of specific discharge ( $Q_s$ ) for every single MP in subcatchment D on 22 February based on subcatchment areas defined by surface topography .....	39
<b>Figure 41:</b> Hillshade of subcatchment D .....	40

---

<b>Figure 42:</b> Variation of water chemistry along Poschiavino between 22 February 13 and 12 March 14 .....	41
<b>Figure 43:</b> Variation of specific discharge and electrical conductivity in subcatchment C on 12 March 14 .....	42
<b>Figure 44:</b> Measured values of EC and Q between X7 and C.....	43
<b>Figure 45:</b> Area covered by sedimentary rocks and crystalline lithology and relevant sampling points.....	45
<b>Figure 46:</b> Total amount (mg/l) of Mg, Ca and SO <sub>4</sub> ions at sampling points in subcatchment B and C.....	46
<b>Figure 47:</b> Evaluation of the electric conductivity probes for the main measurement points between 19 Dec until 03 April 14.....	47
<b>Figure 48:</b> The Bernina Pass Road in the upper Poschiavino area.....	49
<b>Figure 49:</b> Variation of Na, Cl and EC during snowmelt at MP A and the gauging station .....	49

---

---

## List of tables

**Table 1:** List of gauging stations considered for this project (Data: FOEN / swisstopo)..... 7

**Table 2:** Comparison of discharged volume and the estimated range of storage volume for main subcatchments ..... 35

**Table 3:** Estimated discharge from Raibler sediment series from ion composition from January 14 to March 14..... 44

---



---

## Abbreviations

**BU** ... Bucket measurement

**EC** ... electrical conductivity ( $\mu\text{S}/\text{cm}$ )

**FOEN** ... Federal Office of the Environment (BAFU – Bundesamt für Umwelt)

**m asl** ... meters above mean sea level

**MeteoSwiss** ... Federal Office of Meteorology and Climatology (Bundesamt für Meteorologie und Klimatologie)

**MK** ... measurement campaign

**MP** ... measuring point

**Q** ... discharge ( $\text{l}/\text{s}$ )

**Qs** ... specific discharge ( $\text{l}/\text{s km}^2$ )

**SD** ... salt dilution measurement

**swisstopo** ... Federal Office of Topography (Bundesamt für Landestopografie)



---

## Kurzfassung

Die Abschätzung der Wasserverfügbarkeit in alpinen Einzugsgebieten bei Niederwasser ist wesentlich für viele wirtschaftliche und ökologische Fragestellungen. Besseres Verständnis über die Wasserspeicherung in Böden und quartären Sedimenten könnte die Abschätzung von Niederwasserverhalten und Hochwasserretention erheblich verbessern. Selbst steile alpine Gebiete reagieren auf Grund der vorhandenen Speicher gedämpft auf Niederschlagsereignisse oder weisen auch in Niederwasserperioden einen hohen Abfluss auf. Nicht nur das Volumen dieser Speicher, sondern auch die Zeit der Entwässerung ist wichtig um die Dynamik der Abflussabnahme zu verstehen. In den Wintermonaten können Rücklaufprozesse von Abflüssen in alpinen Einzugsgebieten gut untersucht werden, da die Speicher kaum durch Regen oder Schneeschmelze aufgefüllt werden.

Um zu untersuchen, wie das Verhalten eines Einzugsgebiets mit der räumlichen Verteilung von Speichern zusammen hängt, wurden während der Wintersaison 2013/14 in 7 Messkampagnen in verschiedenen Teileinzugsgebieten des Oberlaufs des Poschiavino, räumlich hoch aufgelöst, Abflussmessungen durchgeführt. Das Einzugsgebiet in der Südost Schweiz ist etwa 14 km<sup>2</sup> gross und weist sehr unterschiedliche Teileinzugsgebiete auf. Ausserdem wurden elektrische Leitfähigkeiten, sowie Ionenzusammensetzung gemessen, um verschiedene Speichertypen und die Herkunft des Wassers zu identifizieren und klassifizieren. Um die Auswirkungen von Speichern auf das Verhalten bei Niederwasser zu untersuchen, wurden die unterschiedlichen Ablagerungen kartiert und nach ihrer Mächtigkeit und Typen klassifiziert. Ausserdem wurde versucht das Speicherpotential der Ablagerungen abzuschätzen.

Räumliche Variationen in Drainagezeit und abgeflossenem Volumen konnten in den einzelnen Teileinzugsgebieten identifiziert werden (zwischen 54mm und 200mm in vier Monaten). Die Untersuchungen sind auf Teileinzugsgebietsebene limitiert, da unterirdischer Abfluss und punktuelle Zuflüsse die Beobachtungen auf kleinerer Skala verfälschen. Rücklaufkurven, kombiniert mit zeitlicher Veränderung in der Ionen-Zusammensetzung, wurden verwendet, um Drainage-Zeiten und Speichervolumen zu klassifizieren. Die unterschiedlichen Volumina und die zeitliche Variabilität der Abflüsse konnten auf kartierte Speichereigenschaften zurückgeführt werden. Zusammengefasst konnte gezeigt werden, dass das Verständnis über Speicher und Drainageprozesse in alpinen Einzugsgebieten helfen könnte, Herausforderungen bei der Vorhersage von Niederwassermenge, aber auch bei der Hochwasserabschätzung zu bewältigen.

---

---

## Abstract

Estimation of water availability in alpine catchments during low flow conditions is important for many economic and environmental services. Better understanding of water storage timescales of soils and quaternary deposits may improve flood prediction and low flow estimation in mountainous catchments. Even steep slopes can react damped to precipitation events and sustain baseflow during dry periods due to large storage. Not only the storage volume, but also the drainage time scale is important for understanding recession dynamics. To explore how low flow behavior relates to spatial organization of storage potential a detailed field study of winter low flows was carried out in the upper Poschiavino catchment in southeast Switzerland, a 14km<sup>2</sup> basin with strongly contrasting subcatchments.

Winter months provide good opportunities for studying flow recession in alpine catchments because there is little groundwater recharge from rainfall and snowmelt. Therefore, discharge time series were obtained for different nested subcatchments in 7 campaigns throughout the 2013/14 winter season. Electrical conductivity and various ion composition of stream water were measured to identify different drainage types and their origin. To study the effect of storage on low flow, sediment cover type and thickness were mapped what allowed classifying storage potential throughout the catchment.

Substantial spatial variation in drainage timescales and contributed volumes between the different subcatchments (54mm vs. 200mm discharged in four months) could be observed. Subsurface flow and point source contributions complicate small scale studies of recession flow, suggesting this process should be studied at subcatchment rather than hillslope-scale. The recession analyses combined with time series of ion composition allowed detecting different drainage timescales and an estimation of storage volumes. The variability of low flow discharge and differences in recession behavior can be attributed to the mapped storage potential. The observations show that understanding storage and drainage behavior of areas with large storage potential helps assessing catchment-scale flood and low flow problems.

(see also FLORIANCIC et al., 2014a and FLORIANCIC et al., 2014b)

---

---

# 1 Introduction

## 1.1 General introduction

Better understanding of storage and drainage of soils and quaternary deposits can help to improve flood prediction and low flow estimation. Yet, particularly in mountainous terrain, knowledge of storage potential and drainage behavior of different geomorphological settings is limited. Even steep slopes can react delayed to precipitation events and sustain baseflow during dry periods due to large storage (SMOORENBURG et al., 2013). To improve understanding of the processes involved it is essential to address differences in drainage to different physical properties of deposits. This could help assessing catchment scale low flow and flood problems.

Knowledge of formation of low flow is essential for water management strategies like sustainable drinking water supply, energy production, artificial snow production in alpine regions for winter tourism but also for environmental reasons (MWAKALILA et al., 2002). Discharge during dry periods varies even on small scales, some areas are contributing more than others (MARGRETH et al., 2013). These differences and the impact on water availability get more severe with changing climate conditions (OUYANG, 2012) (PUSHPALATHA et al., 2011). PUSHPALATHA et al. (2011) suggest that hydrological droughts have even higher economic consequences than flood events. Different approaches for low flow estimations on watershed scale were provided in the last decades: On the one hand numerous rainfall-runoff models, which are used for all possible flow conditions (SINGH and FREVERT, 2002) on the other hand approaches focusing especially on low flow (e.g. PUSHPALATHA et al., 2011). In Switzerland low flow ( $Q_{347}$  – see chapter 2) in alpine watersheds is estimated based on duration curves (in catchments with an at least 10 year observation period) or by a method developed by ASCHWANDEN (1992) based on regression and regionalization (MARGRETH et al., 2013). Due to lack of measurements and a limited understanding of the interaction of storage and drainage processes in alpine watersheds the mentioned approaches do not produce satisfying results (MARGRETH et al., 2013).

Drainage and storage processes characterizing low flow discharge behavior also contain important information for understanding different response of alpine watersheds to flood events. Although storage processes of catchments are essential for estimating runoff (e.g. BRUTSAERT, 2005; KIRCHNER, 2009; KIRCHNER, 2006;), due to lack of information on the complex subsurface processes involved (SAYAMA et al., 2011), only few attempts estimating the volumes of these water storages can be found. Even in steep alpine watersheds quaternary deposits can have dampening effects during flood runoff (SMOORENBURG et al.,

---

2013). Recently published, process based researches, focused on the storage capacity and the drainage processes of these hillslope storages, due to their importance for catchment description, inter-comparison, classification and explaining non-linearities in rainfall-runoff transformation (PFISTER et al., 2014). Different watershed scale rainfall-runoff approaches, focusing on the functions of landscapes, proposed a threshold like activation of hillslopes (e.g. SAYAMA et al., 2011; SMOORENBURG et al., 2013;). Further studies found that storages have to be filled before they release water (e.g. McGUIRE and McDONNELL, 2010; SAYAMA et al., 2011). Although there have recently been published different approaches on quantification of flood retention potential and storage dynamics on watershed scale, knowledge about these processes should be broadened.

## **1.2 Objectives and hypotheses**

Drainage processes depend on interaction of numerous storages. Much work has already been done analyzing and mapping the upper layers, especially on different physical properties of soils and estimation of dominant subsurface flood runoff processes in lower altitude areas (SCHERRER and NAEF, 2003) (WEILER and NAEF, 2003) (SCHERRER et al., 2007) (SCHMOCKER-FACKEL et al., 2007) (KIENZLER and NAEF, 2008). With higher altitude deeper layers and deposits become more significant for drainage processes, therefore SMOORENBURG et al., 2013 also considered deeper layers like quaternary deposits. All these investigations aimed to understand runoff formation and the retention behavior of hillslope storages during intense precipitation.

The aim of the thesis is to improve the understanding of storage and drainage processes in alpine catchments during low flow conditions. The connection between discharge recession and different storage properties should be examined. The characterizing processes should be observed and linked to physical properties of the landscape, like type and depth of the deposits, slope length, bedrock permeability and groundwater recharge. Different storages should be identified and classified regarding their drainage behavior. The main idea was to conduct spatially detailed discharge measurements in a small heterogeneous watershed during a period of recession and depletion and link the differences in drainage behavior to various landscape properties. Quantification of storage volume should be done based on the recession observation and water chemistry analyses. Observation of storage depletion is only possible in dry periods. In middle Europe alpine catchments at high altitude provide good opportunities for studying flow recession during winter months, because there is hardly any groundwater recharge from rainfall or snowmelt and storages are depleted by drainage only. Therefore winter measurement campaigns should be conducted in a high altitude alpine catchment. The research was guided by the following main hypotheses:



- 
- Can we relate spatial differences in low flow behavior within a small alpine catchment to distribution and physical properties of hillslope storages that can be identified by geomorphological mapping?

Water chemistry evaluation and model calculations (electric conductivity, ion capacity recession gradient and different product equations) were used to classify discharge and storage types regarding drainage timescales and water storage capacity.

- Is it possible to classify different storage / drainage types and quantify storage capacity by water chemistry evaluation and model calculations based on the collected data?

For a small research area a high resolution storage map was produced and discharge measurements were made. On small scale challenges regarding the topographic delineation of subsurface catchment borders are expected.

- What is the smallest possible organization unit of the hydrological research, what is the smallest organization unit on which reliable results can be gathered?

### **1.3 Structure of the thesis**

In chapter 2 the relevant hydrological concepts influencing the thesis are explained. Chapter 3 gives a geological and hydrological overview about the research area and a description of its characteristic features. In chapter 4 the applied methodological approaches are explained. All investigations are explained, and analyzed for reliability of the results. In chapter 5 discharge and conductivity measurements on different scales will be presented and mapped storage potential is compared to observed recession behavior. Results of conductivity monitoring, ion composition analyses and experimental calculations are explained. In chapter 6 the outcomes are discussed and further estimations are interpreted. The knowledge gained from field campaigns is linked to possible improvements for flood and low flow predictions. Ideas for further research are raised in chapter 7, followed by a final summary of the thesis.

---

## 2 Theoretical background

The hydrological concepts used are explained in this part of the thesis, mainly the use of  $Q_{347}$ , the connection between storage, drainage and travel times and the concept of flow recession.

### 2.1 The low flow value $Q_{347}$

In Switzerland residual flow in rivers is based on the  $Q_{347}$ , defined as the discharge reached or exceeded at least 347 days a year over the last 10 years (see Figure 1). The value should not be influenced by artificial storage, supplies or extraction and based on measured values (ASCHWANDEN and KAN, 1999). For all measured rivers  $Q_{347}$  is published in the hydrological yearbook as a base for water management in Switzerland (ASCHWANDEN and KAN, 1999).

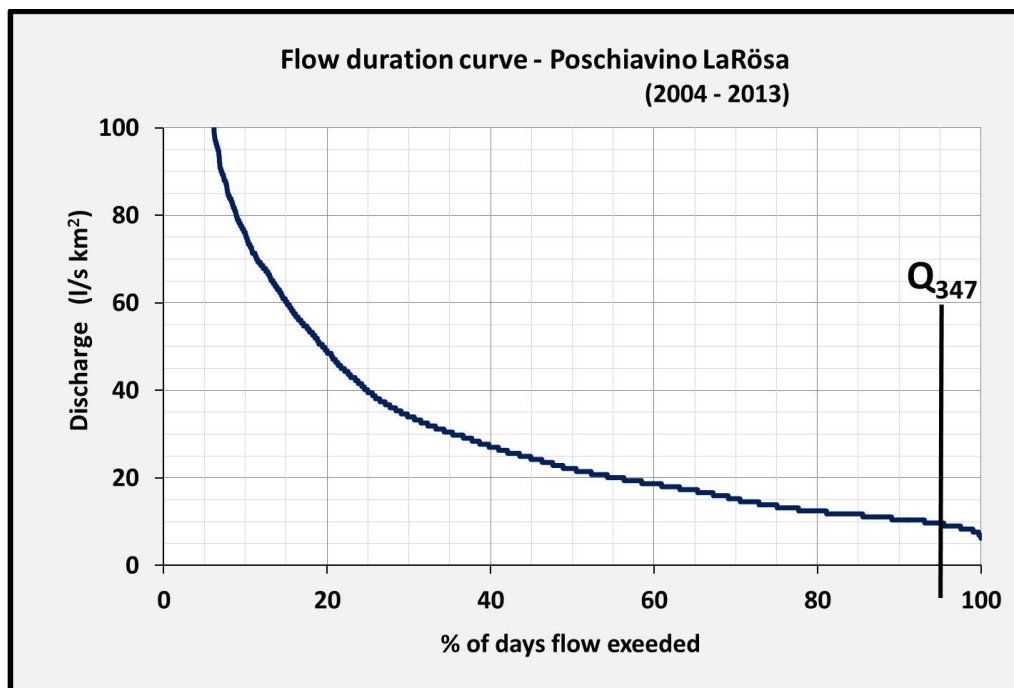


Figure 1: Flow duration curve of Poschiavino LaRösa for 2004 until 2013 (Data: FOEN)

### 2.2 Storage, drainage and travel times

Recent physically based approaches in catchment hydrology focused on storage potential and storage and drainage timescales in different geological settings. Water storage is the nonlinear variable in most simple rainfall-runoff approaches (PFISTER et al., 2014). Therefore a lot work concentrated on analyzing and mapping the upper subsurface layers (SCHERRER and NAEF, 2003) (WEILER and NAEF, 2003) (SCHERRER et al., 2007)

---

(SCHMOCKER-FACKEL et al., 2007) (KIENZLER and NAEF, 2008). SMOORENBURG et al. (2013) found that even steep alpine slopes have dampening effects on flood runoff due to large storage (mainly quaternary deposits). Not only these storage volumes but especially the timescale of drainage and traveltimes through the sediment are important when estimating contribution from different hillslopes.

The most relevant storage is groundwater, where water is stored (and transported) in highly permeable rocks or deposits called aquifers (JOHNSTON and McCARTNEY, 2010). Water is also stored in the unsaturated zone or in wetlands like swamp areas. When looking at the recession dynamics the traveltimes of water through storages has to be considered. Traveltime is defined as the time a water particle needs to flow through a hillslope, from infiltration of precipitation to drainage into the streamflow. Traveltimes are often used for characterizing catchment-scale flow and transport processes. (BOTTER et al., 2011). These processes of transport involved in runoff generation are crucial for understanding the main hydrological processes of a catchment (UHLENBROOK et al., 2002).

## **2.3 Recession analysis**

Knowledge of discharge and drainage processes of hillslope storages and the delay of contribution to the river network is essential for water budgets and threshold behavior of catchments (TALLAKSEN, 1995). The variations in streamflow are attributed to different drainage behavior of hillslopes and storage elements (KIRCHNER, 2009). A useful and acknowledged tool to interpret catchment characteristics is recession analysis. The concept of flow recession analysis dates back to BOUSSINESQ (1877) MAILLET (1905) used for estimation of groundwater storage.

During dry periods stream flow is fed by drainage from different groundwater storages and other delayed sources as soils, quaternary deposits and bedrock fractures. This outflow and gradual depletion during dry periods results in the recession rate and can be plotted as recession curves (see TALLAKSEN, 1995; KIRCHNER, 2009;). Therefore recession curves characterize catchment storage and drainage properties. The most challenging aspect is identification of the contributing sources. Measuring and modelling of these drainage processes especially on small scale and during unsaturated conditions is extremely challenging (HEWLETT, 1961) (TALLAKSEN, 1995).

---

## 3 Research Area

### 3.1 Selection of the study area

#### 3.1.1 Decision criteria

Observation of depletion of storages is only possible during dry periods. In middle Europe such periods exist in high altitude alpine areas during winter months. Due to the lack of liquid precipitation there is no / only little recharge of the storages.

An essential working step was finding an appropriate study area. To work on the research hypothesis and to get reliable results following points were considered when deciding for the research area:

First of all, the report of MARGRETH et al., 2013 on flow recession in Switzerland was evaluated. Available gauging data (daily mean discharge in  $\text{m}^3/\text{s}$ ) for alpine catchments in Switzerland from FOEN (Federal Office for the Environment) were collected (<http://www.hydrodaten.admin.ch/de/>). As a result there should be a dense data set of discharge measurements and a high spatial resolution map of storage types, therefore only catchments smaller than  $100 \text{ km}^2$  were selected. To avoid the refill of the storages due to liquid precipitation and major influence of snowmelt only catchments with a gauging station above 1000 m asl were selected. It is estimated that below this elevation, snowmelt and rain events also take place during winter months and have influence to storage recession. The possible observation periods would be shorter and without a frequent discharge observation the recession curves would be flattened due to inflow to the storages of the catchment.

Fifteen of the FOEN gauging stations were selected to take a closer look at (Table 1). Because winter discharge occurs on low rates, uncertainties in the discharge measurements can have major effects on the results. These mainly derive from bedload and suspended matter accumulated at the measuring station changing the rating curves and the calculated discharge. Low flow measurements are critical, therefore the gauging station must be equipped properly. Pictures of the gauging stations and personal contact with the responsible keepers helped to identify reliable stations. Stations having a low flow channel or a concrete / bricked riverbed are less influenced by sediment accumulation. Because discharge measured during the winter is used, also the influence of ice at the gauge had to be considered. According to available information three of the selected stations are known to be iced during the winter months and are not freed from ice during winter season, another three do not have a low flow channel or a bricked / concrete riverbed.

In a further step the geology of the catchment was examined using existing information from swisstopo (Federal Office of Topography – <http://map.geo.admin.ch>) and gauging station background information of FOEN (<http://www.hydrodaten.admin.ch/de/>). The catchments were organized according to the main geology (crystalline, flysch, limestone or dolomite). It

was assumed that crystalline catchments could be better delineated than carstic watersheds consisting of limestone or dolomite.

Because the aim of the research is to identify different storages types the geomorphologic heterogeneity within the catchment was also taken into consideration. The idea was to identify nested subcatchments, showing different storage and drainage behavior. Additionally also the mean  $Q_{347}$  of the last twenty years was looked at. Catchments having a high  $Q_{347}$  were assumed to have large storages. To allow frequent discharge observations during winter months, accessibility to the catchment must be given.

**Table 1:** List of gauging stations considered for this project (Data: FOEN / swisstopo)

Decision Scheme							
name of the creek	location gauging station	catchment size (km <sup>2</sup> )	m asl	info FOEN	main geology	$Q_{347}$	Accessibility
Allenbach	Adelboden	28.8	1.297	ok	flysch	8.33	Poor
Alpbach	Erstfeld	20.6	1.022	ok	<i>crystalline</i>	4.85	Poor
Dischmabach	Davos	43.3	1.668	ice	<i>crystalline</i>	6.45	Med
Goneri	Oberwald	40.0	1.385	ice	<i>crystalline</i>	9.25	Med
Lonza	Blatten	77.8	1.520	ok	<i>crystalline</i>	6.17	Poor
Orbe	LeChenit	44.4	1.040	ok	limestone	2.03	Med
Ova da Cluozza	Zernez	26.9	1.509	ok	dolomite	5.20	Poor
Ova dal Fuorn	Zernez	55.3	1.707	ice	dolomite	5.97	Poor
Rein da Sumvigt	Sumvigt	21.8	1.490	ok	<i>crystalline</i>	7.34	Poor
Poschiavino	LaRösa	14.1	1.860	ok	<i>crystalline</i>	9.93	Good
Rhone	Gletsch	38.9	1.761	lfch miss	<i>crystalline</i>	4.11	Poor
Riale di Roggiasca	Roveredo	8.1	980	lfch miss.	<i>crystalline</i>	3.72	Poor
Rosegbach	Pontresina	66.5	1.766	lfch miss.	<i>crystalline</i>	1.35	Med
Rotenbach	Plaffeien	1.65	1.275	ok	flysch	6.12	Med
Schwändli-bach	Plaffeien	1.38	1.220	ok	flysch	0.38	Med

ice ... gauging station with icing problems  
lfch miss. ... gauging station does not have a low flow channel or bricked riverbed

### 3.1.2 Evaluation of existing data

Furthermore different analyses on the reliability of the existing data were made. Discharge data (FOEN - <http://www.hydrodaten.admin.ch/de/>) of the last ten years were used to study the recession behavior and rating curves for the catchments Alpbach, Dischmabach, Goneri, Lonza, Rein da Sumvig, Poschiavino, Riale di Roggiasca and Rosegbach.

For all these catchments the rating curves were stable, at least for the last 10 years. In addition recession curves, based on daily mean values were derived to get an idea of the discharge behavior during the winter months. To avoid recharge of the storages there should be no liquid precipitation and no snowmelt in the potential research area. Of course recession could be observed frequently, but to study the storage and drainage behavior of a catchment during low flow conditions it's essential to be able to observe a long recession period.

When having a closer look at the evaluation of winter discharge at the gauging station Erstfeld at Alpbach (Figure 2), it's obviously that there is frequent influence of rain and snowmelt events during the winter months. Due to the low main altitude of the catchment and the height of the gauging station (1022 m asl) discharge shows frequent increase also during winter months and recession was observable for short periods only.

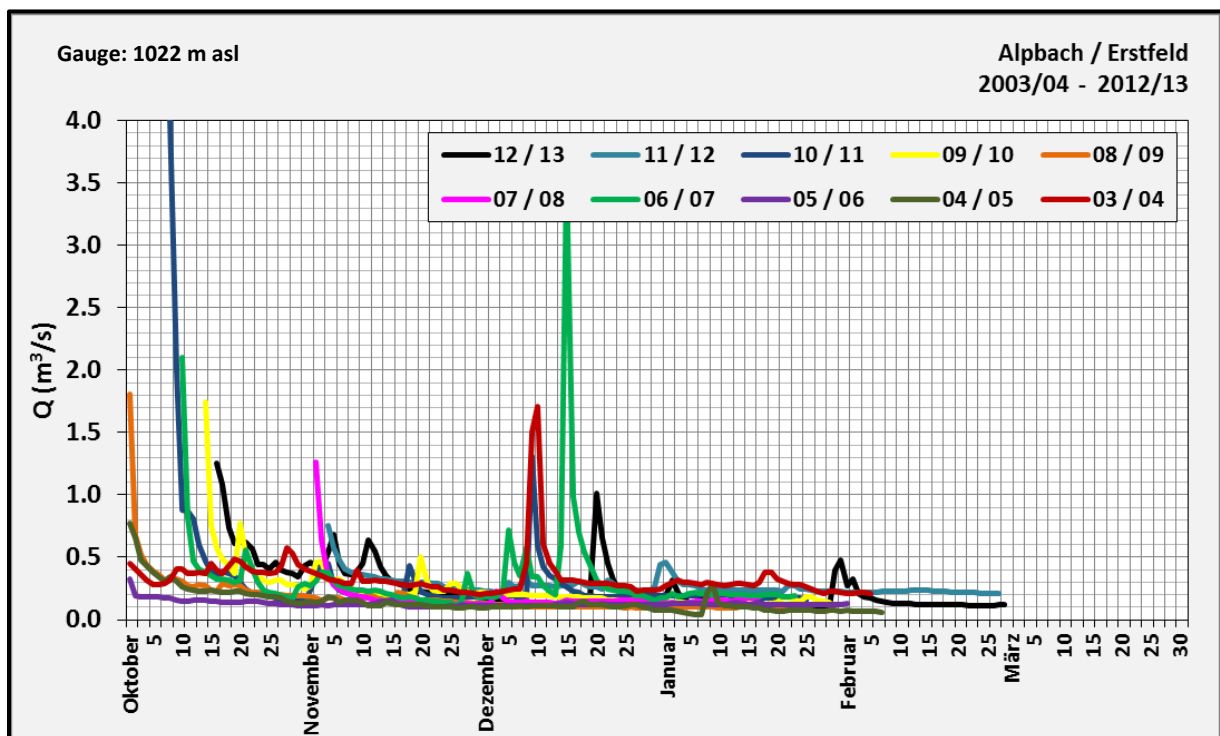
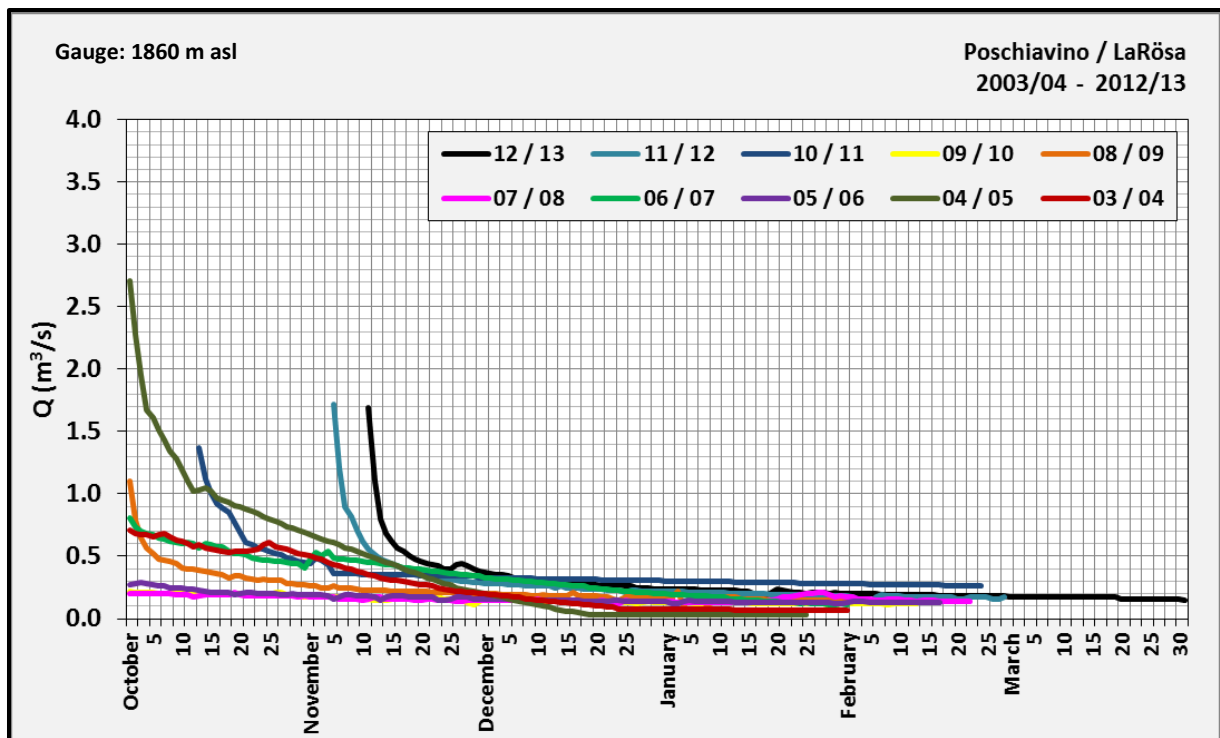


Figure 2: Measured discharge for Alpbach / Erstfeld for winter seasons 2003/04 until 2012/13 (Data: FOEN)



**Figure 3:** Measured discharge for Poschiavino / LaRösa for winter seasons 2003/04 until 2012/13 (Data: FOEN)

The gauge of the upper Poschiavino catchment lies at 1860 m asl and measurements do not show any major rain or snowmelt events during the last 10 winter seasons. The recession curves show long periods of decreasing discharge, beginning at least mid-November (Figure 3). Considering all collected information, quoted in chapters 3.1.1 and 3.1.2 the upper Poschiavino area was selected for the research.

### 3.2 The upper Poschiavino area

The research area spreads over 14.4 km<sup>2</sup> in the southeast of Switzerland in the region Puschlav of the Kanton Graubünden (see Figure 4). It is the headwater of the 238 km<sup>2</sup> Poschiavino catchment which merges after about 30 km into the Adda river (part of Po watershed). The northwestern limit of the catchment corresponds with the border to Italy. The highest point is Piz Ursera with 3032 m asl, the lowest point is the FOEN gauging station at the end of the Plan da LaRösa (1860 m asl) (see Figure 4). The catchment mean altitude is 2283 m asl.

Almost half of the area is used as alpine grazeland; Due to the high elevation only 6% of the area is covered by coniferous forests (FOEN - <http://www.hydrodaten.admin.ch/de/>).

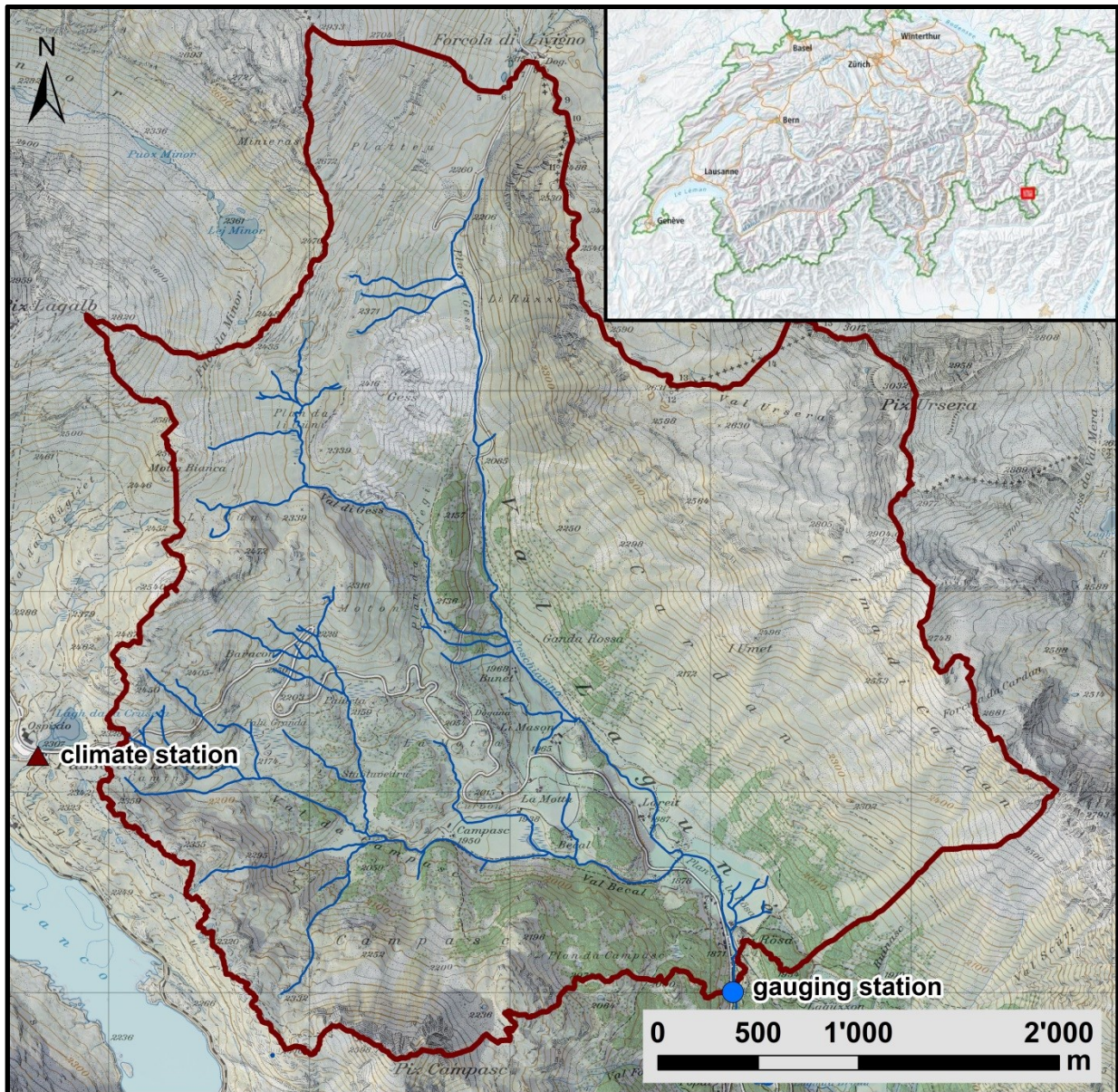


**Figure 4:** Study area Poschiavino / LaRösa (Data: swisstopo / ETH Zürich)

The main soil types are lithosols and regosols (shallow weakly developed soils lacking defined horizons) with very poor storage capacity and high permeability (FOEN - <http://www.hydrodaten.admin.ch/de/>).

The next climate station is at Passo di Bernina, about 200 meters outside the catchment at 2.207 m asl. The mean annual precipitation is 1.738mm (1981 – 2010). The annual mean temperature (1981 – 2010) is 0.2°C, reaching maximum in July and August and minimum in January and February. Due to high snow accumulation (annual mean 792cm) and the high elevation snow cover lasts at average for 217 days (mean 1981 – 2010) (MeteoSwiss - <http://www.meteosuisse.admin.ch/>). Mean annual height of evapotranspiration (1973 – 1992) is around 300mm per year (MENZEL et al., 1999).



---

### 3.2.1 The hydrology of the catchment

The main river Poschiavino stretches from north to south through the research area, with two main inflows from orographic right (Passo del Bernina and Plan da li Cüni). The eastern part of the catchment covered by thick quarterly sediments shows almost no surface discharge.

The general hydrological behavior of catchments in Switzerland is classified according to ASCHWANDEN and WEINGARTNER (1985). The upper Poschiavino area is assigned to the south alpine regime nival meridional, characterized by a discharge maximum in spring due to snowmelt.



**Figure 5 & Figure 6:** FOEN gauging station LaRösa, after (left) and before bricking of the riverbed and sealing cracks at the orographic right side (right) (Figure 6 – Andrea Crose / FOEN)

The mean discharge at LaRösa is  $0.55 \text{ m}^3/\text{s}$  (1970 – 2013) varying between  $0.94 \text{ m}^3/\text{s}$  (1977) and  $0.31 \text{ m}^3/\text{s}$  (2007). The specific discharge is  $39 \text{ l/s km}^2$ . In 2013 the mean annual discharge was  $0.67 \text{ m}^3/\text{s}$  (FOEN - <http://www.hydrodaten.admin.ch/de/>). According to personal information of the responsible keeper Andrea Crose (FOEN) there had been problems at the station with undercurrent in the last years. In April 2013 the bricked riverbed was repaired to avoid losses and measuring errors (see Figure 5 & 5).

The  $Q_{347}$  over the period 1970 – 2012 was  $0.14 \text{ m}^3/\text{s}$ , the specific  $Q_{347}$   $10 \text{ l/s km}^2$ . Due to uncertainties in the measurements mentioned above, the  $Q_{347}$  might be even a little higher.

### 3.2.2 The geology of the catchment

The catchment is situated in the Bernina- and Campo nappes from the Middle and Lower East Alpine. It is strongly influenced by glacial activity. Along the main river the border of the two nappes is surmised. The western half of the catchment is characterized by Lower East Alpine crystalline formations, mainly green orthogneiss, and a variety of quarterly

sediments. The eastern and northern parts of the catchment are characterized by Middle East Alpine layers consisting of paraslates and ortho and injection gneiss overlapped by thick quarterly sediments. At some locations gabbroides and amphibolites emerge. In the eastern part of the catchment two areas of creeping landmasses and a rockslide could be found. In the northern part of the catchment lower East Alpine sediments are exposed. They consist of Triassic flat marine carbonates, mainly dolomite and gypsum, and could be divided into the Raibler Series and main dolomite. Raibler Series are characterized by various thin layers in steady alternation due to environmental changes during sedimentation. In the research area these are mainly derived from dolomites, rauhwacke and gypsum in a very frequent sequencing (see Figure 7) (NAEF, 1987). Numerous moraines are indicated in the geological map suggesting high influence of glaciation in the area. Half of the catchment is overlaid by quaternary sediments.

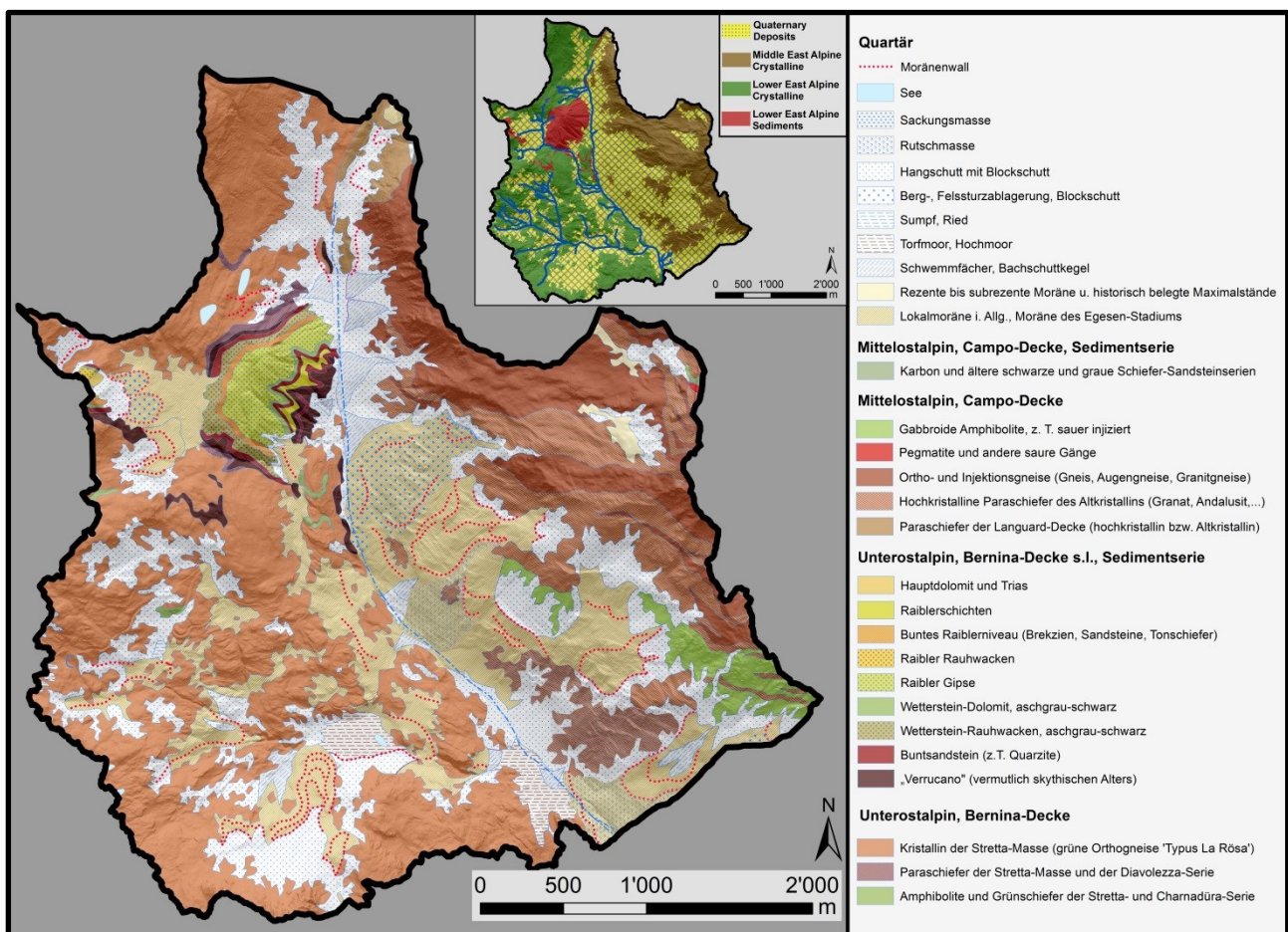
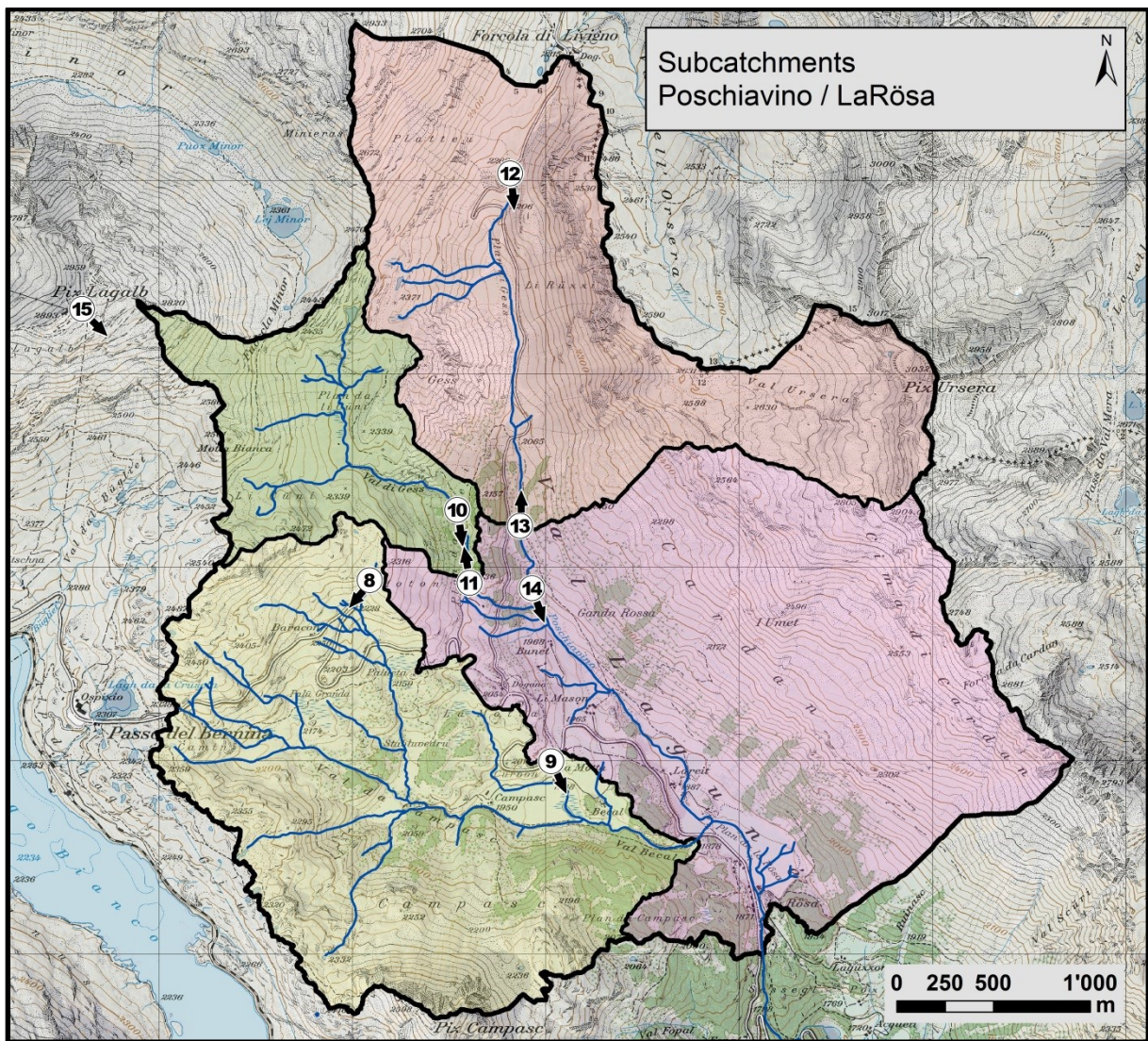


Figure 7: Geological map of the study area Poschiavino / La Rösa (Data: swisstopo / ETH Zürich)

### 3.2.3 Main subcatchments

The research area was divided in four main subcatchments (see Figure 8). Subcatchment A is characterized by numerous small creeks, swampy areas and a homogeneous crystalline

geology. It has a heterogeneous morphology due to quaternary sediments like moraines and talus deposits. In the lower part (at the swamp area of Val da Campasc) all the creeks flow into one tributary of the Poschiavino. Subcatchment B is also the watershed of an orographic right tributary of the main creek, most of the catchment is characterized by the same quaternary deposits and geology as found in subcatchment A, but some parts of B are situated in the Lower East Alpine Sediments (Raibler formations). After a large swamp / plain area (Plan da li Cüni) all the conveyors merge to pass through a steep canyon (Val di Gess). Subcatchment C is the headwater of the catchment. It contains Raibler formations in the south western part and thick talus and moraine deposits in large parts of the catchment. In some sections the Poschiavino is even covered by deposits. The fourth subcatchment (D), is characterized by a steep slope showing no tracer of surface discharge because of thick quaternary sediments lying on quiet homogeneous crystalline nappes. In the lower part there is a large alluvial aquifer / Plan LaRösa.



**Figure 8:** Map of the four main subcatchments including location and direction of impressions of the subcatchments (Figure 8 – 15) (Data: swisstopo / ETH Zürich)

---

## Subcatchment A



**Figure 9 & Figure 10:** Impressions of subcatchment A – see Figure 8 for location and perspective

## Subcatchment B



**Figure 11 & Figure 12:** Impressions of subcatchment B – see Figure 8 for location and perspective

---

### Subcatchment C



**Figure 13 & Figure 14:** Impressions of subcatchment C – see Figure 8 for location and perspective

### Subcatchment D



**Figure 15 & Figure 16:** Impressions of subcatchment D – see Figure 8 for location and perspective

---

## 4 Methodological Approach

### 4.1 Available data

First data of the research area were collected to get an overview of existing information:

- geological information of the vector dataset GeoCover (Bernina-Gruppe) based on investigations of Rudolf Staub (1912 – 1945) at a scale of 1:50.000
- digital elevation models (DEM) in 2m and 25m resolution
- vector data (1:25.000) of landuse, hydrology, buildings and traffic routes
- a topographical map and aerial photographs (swisstopo – available via ETH VPN)

Preliminary investigations of the hydrological behavior were based on data of FOEN (<http://www.hydrodaten.admin.ch/de/>). The data contain daily mean values of discharge ( $\text{m}^3/\text{s}$ ) and daily mean water level values (m asl). FOEN additionally provided discharge values (l/s) and water level measurements (m asl) in 10 minute resolution and the valid rating curves.

### 4.2 Mapping of storages

The aim of the project was to identify different storages and estimate their main physical properties like mean depth, permeability and area. This should help classifying the deposits regarding their storage and drainage behavior and get a map of the spatial distribution of storage potential. Based on the DEM, aerial photographs, geological maps and field observations the whole watershed was mapped regarding geomorphological type, thickness and estimated permeability (see Figure 17). The mapping scheme was inspired by the methodology of SMOORENBURG et al., (2013) developed for a geomorphology based flood prediction model on dominant runoff processes. Six geomorphological types were differentiated: alluvium, talus slope, outcrop, swamp area, glacial till and debris slope assigning three thickness classes: < 1m, 1-5m and > 5m and the permeability classes high, medium, low and zero based on surface observation (see Figure 17).

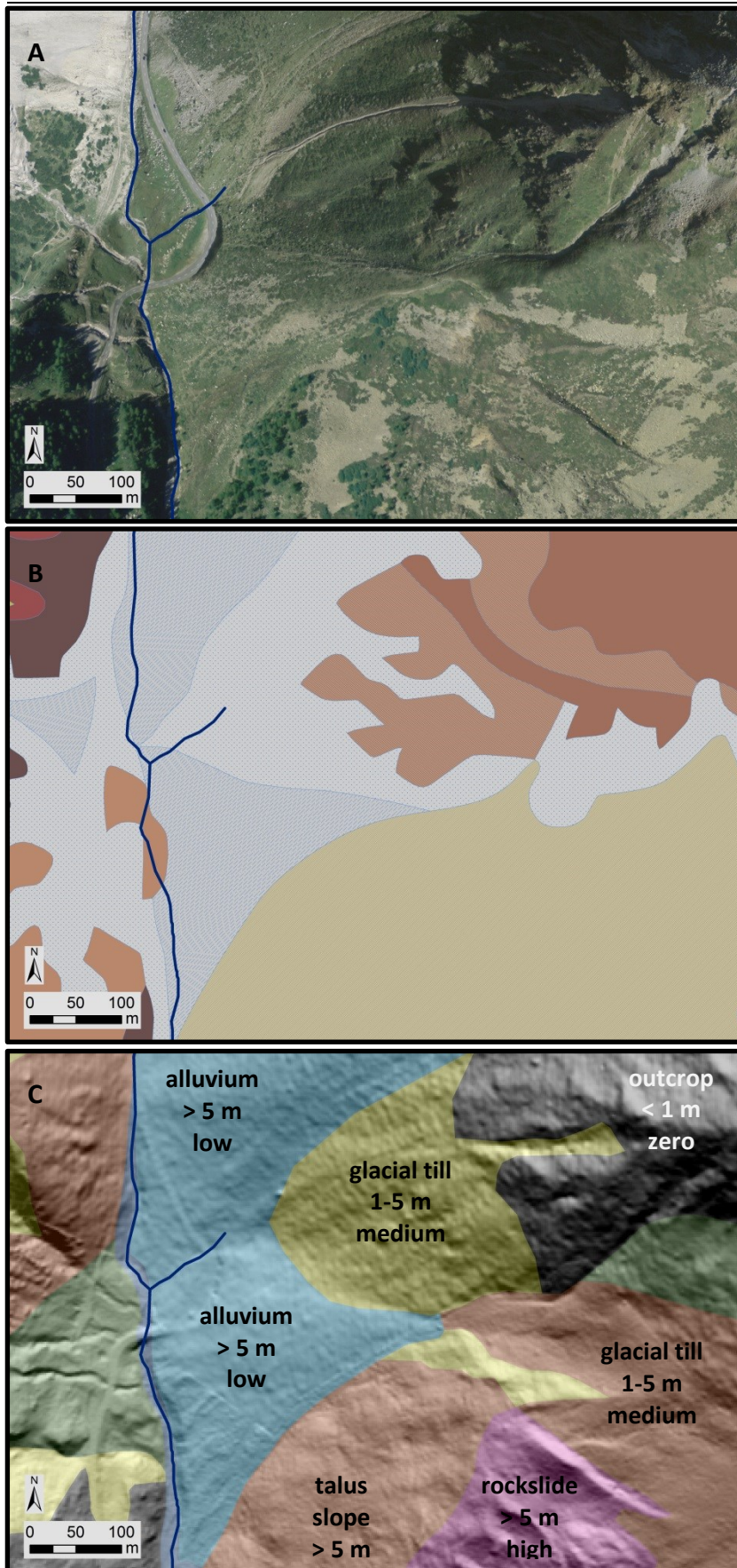


**Figure 17:** Storage map in subcatchment C: besides field observation and a DEM, aerial photographs (A) and geological maps (B) (see Figure 7 for legend) were used to generate a storage map (C). Geomorphological type, depth (<1m, 1-5m and >5m) and permeability (high, medium, low and zero) were classified. (Data: swisstopo)

---

Based on the DEM, aerial photographs, geological maps and field observations the whole watershed was mapped regarding geomorphological type, thickness and estimated permeability (see

Figure 17). The mapping scheme was inspired by the methodology of SMOORENBURG et al., (2013) developed for a geomorphology based flood prediction model on dominant runoff processes. Six geomorphological types were differentiated: alluvium, talus slope, outcrop, swamp area, moraine and debris slope assigning three thickness classes: < 1m, 1-5m and > 5m and permeability classes high, medium, low and zero based on surface observation (see Figure 17).

### **4.3 Discharge measurements**

Discharge was measured every three weeks with high spatial resolution at up to 57 locations during the winter 2013/14 from November to April (Figure 20). Measuring discharge in a high alpine catchment is challenging. Due to heterogeneous river morphology usage of current meter can be difficult. Low temperatures can lead to icing of the weir and measurement structures, the variation in flow velocity results in uncertainties when applying standard weir equations (MOORE, 2004). Therefore tracer dilution and a volumetric bucket approach were used.

#### **4.3.1 Salt dilution**

The tracer dilution method is based on tracer injection and measuring the dilution after complete mixing downstream (MOORE, 2004). The tracer can be injected constantly or by gulp injection. The accuracy of both methods depends on complete mixing of stream water and tracer in a short distance with as little pool volume as possible and no backwater areas (MOORE, 2004). For this project gulp injection was used and all measurement sites were selected preliminary in autumn. The mixing length in the stream was chosen regarding the proposal of DAY (1977) to use the flow width 25 times. Gulp injection is easily applicable because no additional equipment for injection is needed and it can be done at temperatures far below zero. As tracer salt solution (NaCl + H<sub>2</sub>O) was used as it has low aquatic toxicity at the concentration needed (WOOD and DYKES, 2002) and can easily be measured as electrical conductivity. It is cheap (MOORE, 2004), works well in steep, highly turbulent streams and produces reliable results up to 10m<sup>3</sup>/s (MOORE, 2005). After injecting the cloud of salty water (longitudinal dispersion) is measured as variation of electric conductivity (EC) at a point downstream (MOORE, 2005). Accuracy depends on the variation of electrical conductivity, therefore MOORE (2005) suggests the salt solution should increase EC by 100% - 200% at streams with a background EC below 100 µS/cm and 400% above 100 µS/cm



---

background EC. For the salt used a calibration curve was derived in the laboratory, salt was weighed and packed with high accuracy in the laboratory and dissolved in stream water using an electric drill and a remand wing at the measurement sites. Downstream EC was measured and logged with at least two calibrated devices (types: WTW Multi 3420 or WTW Multi 340i) in intervals of 5 seconds in the main part of the flow as suggested by MOORE (2005). Additionally water temperature was logged, because EC varies by temperature. Calibration of the devices was done frequently using 0.01 molar Potassium Chloride as suggested by the manufacturer. The error of the method is less than 5% under good conditions (DAY, 1976). Errors occur when salt is not completely dissolved, if the solution is not mixed across the whole channel or when the flow path is covered by ice and snow (MOORE, 2005). For high alpine conditions during winter times measuring error was estimated to be below 10%. When comparing the results of the two probes at the same point, the error was always below 5%.

### 4.3.2 Bucket measurements

Bucket measurements were used mainly at tube outlets with low discharge, found along the Bernina Pass road (see Figure 20). Volumetric discharge measurement are most reliable when measuring small discharges (TURNIPSEED and SAUER, 2010). It is based on the time a container of a calibrated volume needs to be filled completely or up to a certain depth (RANTZ, 1982).



Figure 18 & Figure 19: Bucket measurements at MP D5 and MP A 21

Four different sized containers were calibrated in the lab (by weighing the full container with high precision) for usage depending on the discharge. The time until complete filling of the container was measured. The outlet of the tube was often too low to place the bucket

beneath; therefore a gutter was used to lead the water into the bucket (see Figure 18 & 19). The measurement error is lower if the time for filling the container is longer. The measurement was repeated at least two times (if filling time exceeded 4 minutes) three times (from 1 to 4 minutes) and five times (below one minute).

At measurement point D2, an orographic left tributary, the presented volumetric method was not possible, due to high discharge and low elevation difference between the tubes and the riverbed of the receiving waters. A bigger bucket was weighed, held beneath the tube for short time (recorded with a stopwatch) then the whole bucket was weighed again. The difference in weight would be the discharged volume in a certain time period. This method was applied at least six times to minimize errors. Afterwards the minimum and the maximum were dismissed; the remaining four values were used to calculate the mean. After applying the mentioned statistical approaches, the error could be minimized to below 5%.

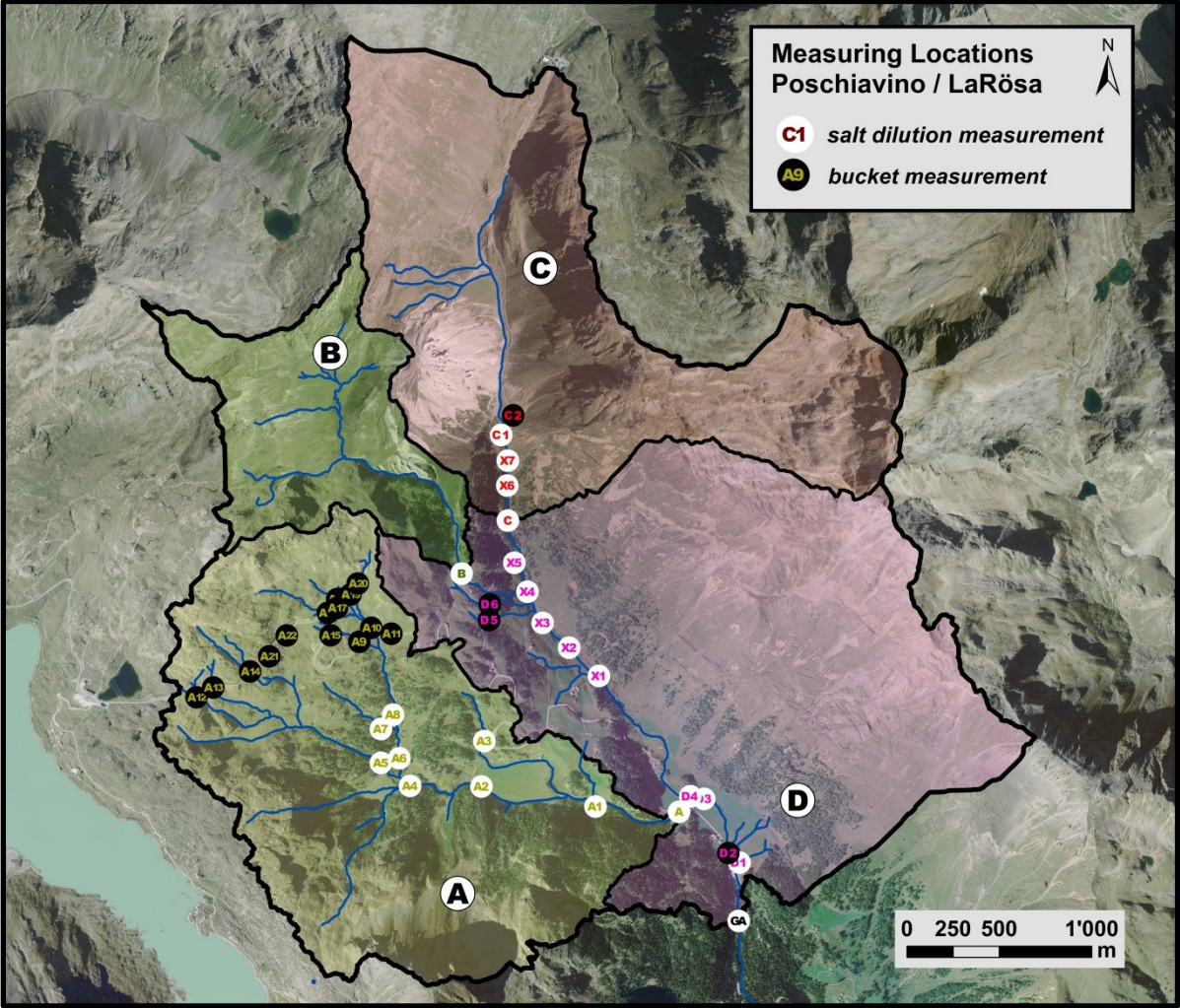


Figure 20: Overview of the measuring locations of discharge (Data: swisstopo / ETH Zürich)

---

## 4.4 Measurement of electric conductivity

### 4.4.1 Continuous measurements

Electric conductivity probes were installed at certain points (see Figure 23) to record hourly values from December to March. To evaluate the influence of snow melt during the recession period and to survey electric conductivity 9 probes (HOBO U24 Conductivity Logger) were installed (Gauge, D3, D4, A, A2, A4, A6, B and C) on 19 December. Calibration curves for all loggers were derived before installing and after removing them from the creeks by observing the increase of EC by adding a certain amount of calibrated salt solution every 2 minutes for 20 minutes. The calibration was additionally observed with another calibrated device (WTW Multi 3420).

### 4.4.2 Field campaigns

Electric conductivity was observed along the main creeks every three weeks at the measurement sites and at additional locations using the calibrated devices WTW Multi 3420 and WTW Multi 340i. Calibration was done frequently using 0.01M KCl (as determined by the manufacturer). A spatial dataset of electric conductivity for the observation period could be derived.

## 4.5 Lake gauges

Lake gauges were installed at four small lakes (see Figure 21 & 22 for examples and Figure 23 for location of the lake gauges). Due to low air temperatures (up to  $-29^{\circ}\text{C}$ ) in November 2013 three of the lakes froze up to the ground, the fourth lake gauge at Val di Campasc was lost due to massive snow accumulation after 19 December.



**Figure 21 & Figure 22:** Lake gauges (left – in western part of subcatchment A, right – subcatchment C)

## 4.6 Ion composition of water samples

Water samples were taken at the main measurement points and at various tributaries and springs every three weeks from January to March for ion composition analyses. Plastic conical centrifuge tubes were used to take one sample for each point, completely filled to avoid the influence of air inside the tube. The samples were stored in the refrigerator until they were analyzed by ion chromatography, using organic polymers and eluent ions (FEDOTOVA and GÜNTHER, 2013). Every sample was analyzed two times.

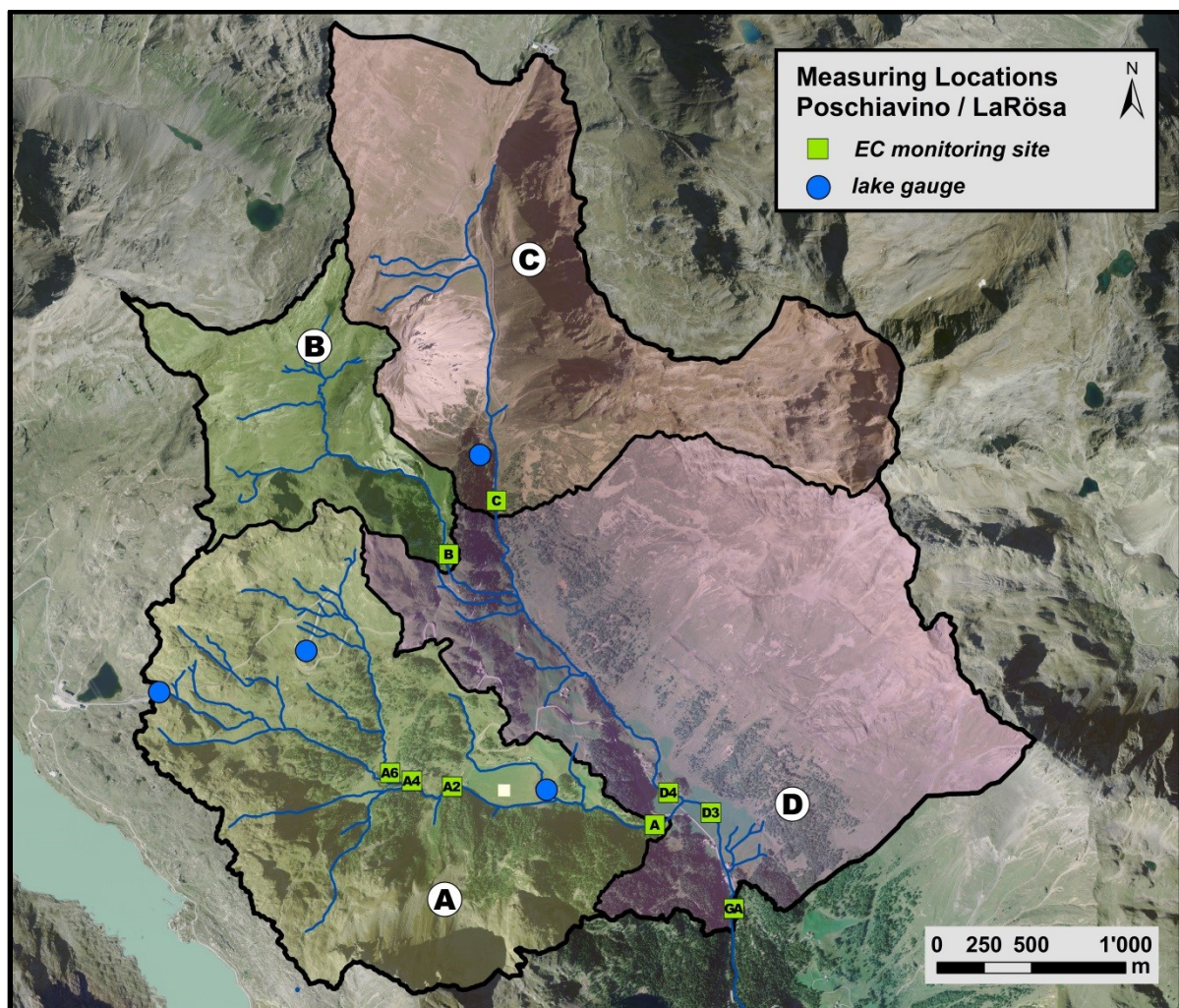


Figure 23: Overview of the locations of EC monitoring and lake gauges (Data: swisstopo / ETH Zürich)

## 4.7 Model calculations

The collected data was used as input for various mathematical approaches for storage quantification and drainage type separation. Quantification of storage volumes throughout the catchment was based on mapped thickness of deposits and qualitative permeability

---

estimation. The contribution from sedimentary rocks was estimated using natural ion tracers ( $\text{SO}_4$  and Mg) in the water samples. Product equations could be used for estimating the contribution from a rockslide area. Recession curves and product equations were used to divide different storage types regarding their drainage behavior the gradient of the plotted recession curves was used.

#### 4.8 Organization of field work

An important major part of the project was the field work in a hostile environment. Many permissions and support had to be organized. The nine measurement campaigns were carefully prepared beforehand and coordinated regarding weather conditions. Although much effort was put into the preparation for field work, measurement campaigns were challenging during winter season 2013/14. 9m to 10m of snow were accumulated during winter and temperatures were often below  $-20^\circ\text{C}$ .

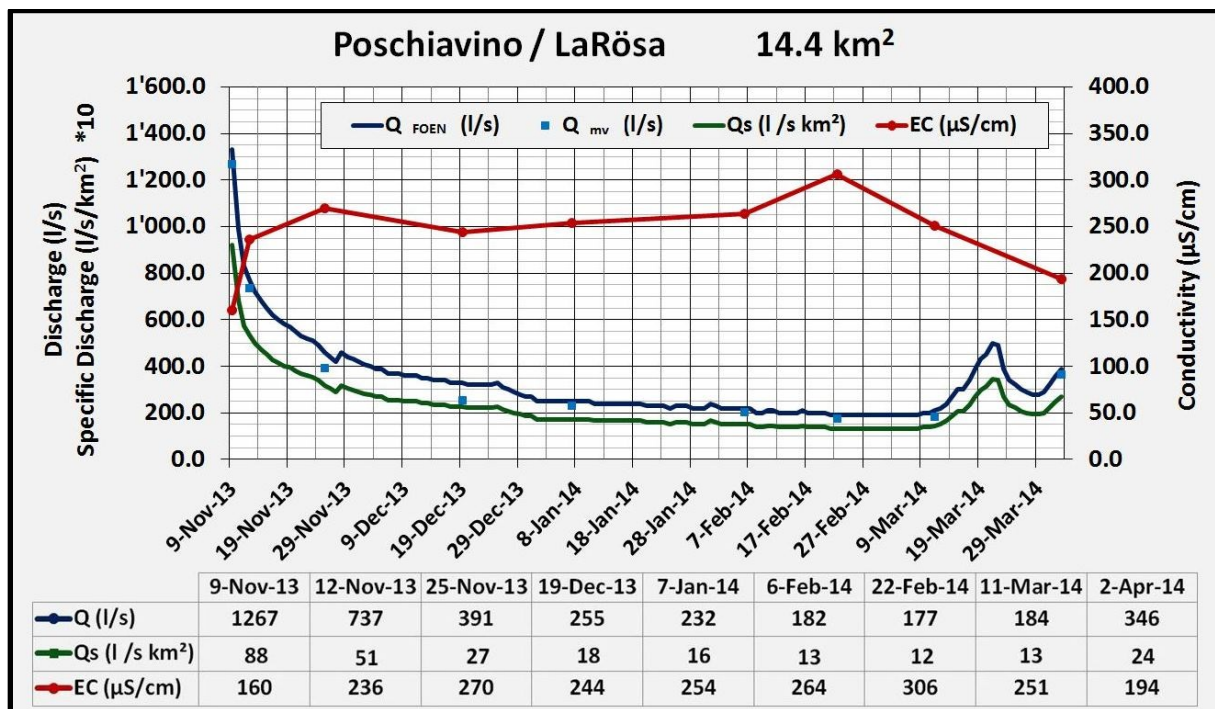


Figure 24 & Figure 25: snow accumulation during winter season 2013/14

## 5 Results

### 5.1 Measurements on catchment scale

First the results of the measurement campaigns during winter season 2013/14 were analyzed on catchment scale. Salt dilution measurements were applied 9 times from 09 November 13 until 02 April 14 at the FOEN gauging station LaRösa. In Figure 26 the results for discharge provided by FOEN (dark blue graph), measured discharged (light blue, dashed) specific discharge (green) and electrical conductivity (red) were plotted. Obviously a quick recession until the end of November followed by a dampened recession until mid of March took place. After the measurement campaign launched on 11 March increase in discharge due to snowmelt is visible, but as explained in chapter 5.2 ( Comparison on subcatchment scale) not all parts of the catchment reacted to increasing temperatures. Regarding the FOEN discharge measurements the peak was reached on 22 March. Discharge decreased from November to March from 1267 l/s to 177 l/s. Specific discharge ( $Q$  l/s km<sup>2</sup>) reached the minimum at 12.3 l/s km<sup>2</sup> which is above the expected mean of the catchment given by FOEN. This could be explained by the renovation of the riverbed at the gauging station or by more precipitation during summer and autumn leading to a higher content in the storages. A quick increase of the electric conductivity time series could be observed reaching a peak at the end of November. Electric conductivity again increased after the 19 December 13 to reach the highest peak in the end of February (306  $\mu$ S/cm). Afterwards conductivity decreased again due to the influence of snowmelt especially in the parts of the catchment influenced by the pass road.



**Figure 26:** Q, Q<sub>s</sub> and EC at the gauging station LaRösa from 9 Nov 13 to 02 April 14 (Discharge data: FOEN)

Between 27 November 13 and 11 March 14 165mm were discharged in the research area (see Figure 27). As no significant recharge of the storages occurred through liquid precipitation or snowmelt in this period, the storages in the catchment were depleted by 2.4 million m<sup>3</sup>. In this three and a half months, almost 1/10 of mean annual precipitation of 1738mm were discharged. When comparing the measured values during the field campaigns to the daily mean values measured by FOEN (see Figure 26), the results fit very well except in the period from 25 November until 7 January, when the plotted discharge curve of daily mean values by FOEN increases. The difference could be assigned to inaccurate measurements by FOEN, by plotting the relation of discharge and stage (rating curve) for the relevant period which does not show reliable results.

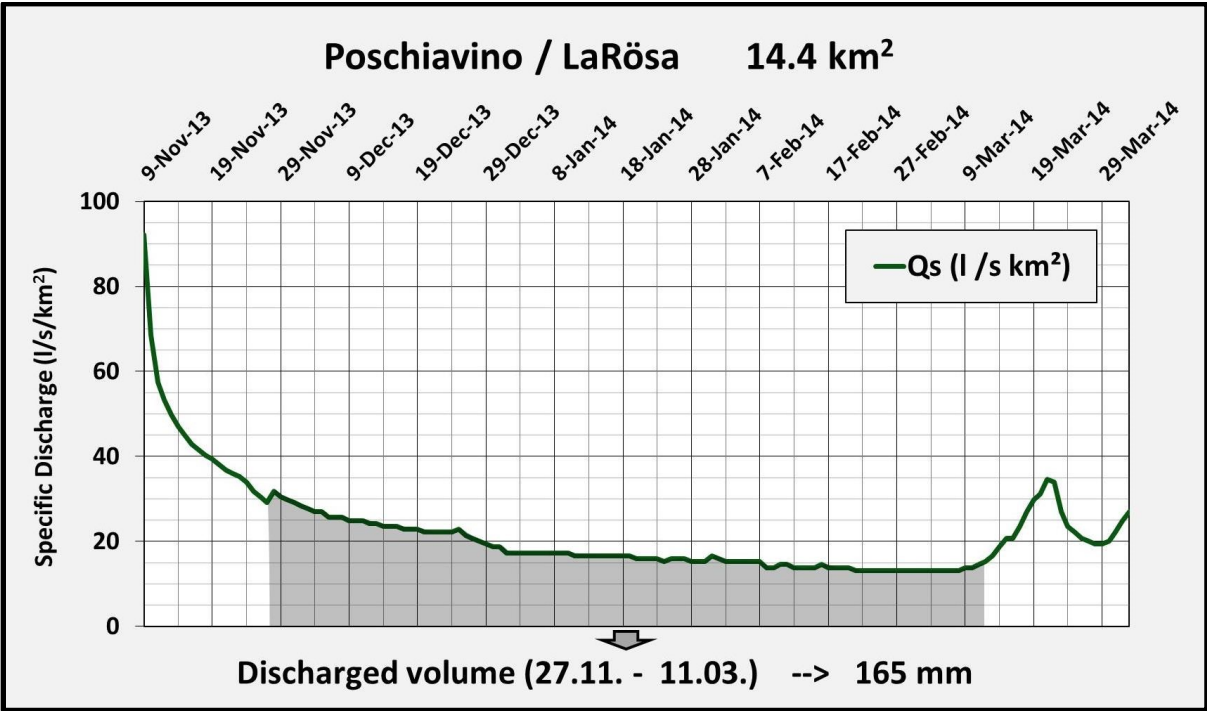


Figure 27: Discharged volume between 27 November 13 and 11 March 14

## 5.2 Comparison on subcatchment scale

### 5.2.1 Discharge and Conductivity

The differences in drainage behavior between the watersheds A, B, C and D are evaluated on subcatchment scale. They show different recession behaviors (see Figure 28). The western part (A and B) and the eastern part (C and D) behave differently. Subcatchment A and B both show a quick recession in autumn and a low winter discharge. In subcatchment B electric conductivity is much higher than in A, discharge is a little higher. Subcatchment C and D show a slower recession over the observation period. As observed at the gauging station electric conductivity decreases between the measuring campaigns of 22 November and 19

December in subcatchment C. The results for subcatchment D are not measured values but are calculated as the difference between the gauging station and the measured values of subcatchments A, B and C. Therefore there are no measured values for electric conductivity. Considering the sum of uncertainties of the four salt dilution measurements (gauge, A, B and C) the plotted recession curve for subcatchment D shows slow recession behavior and high winter discharge.

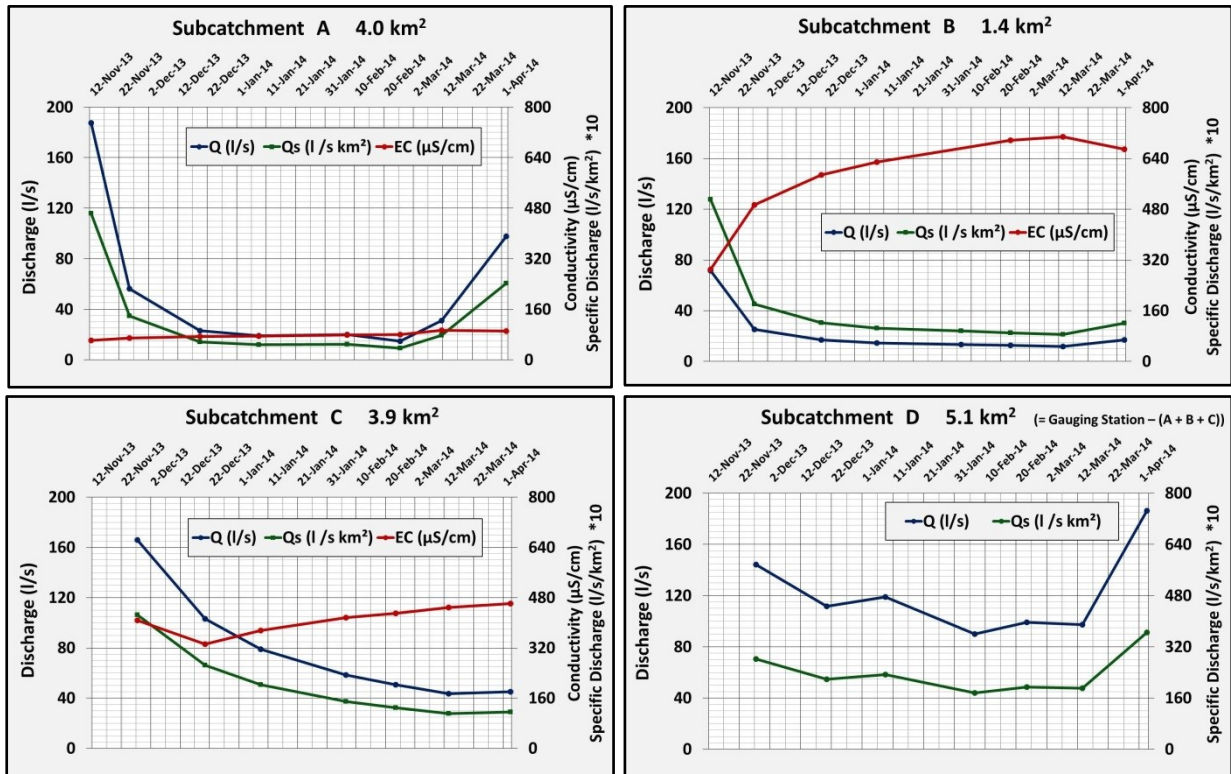
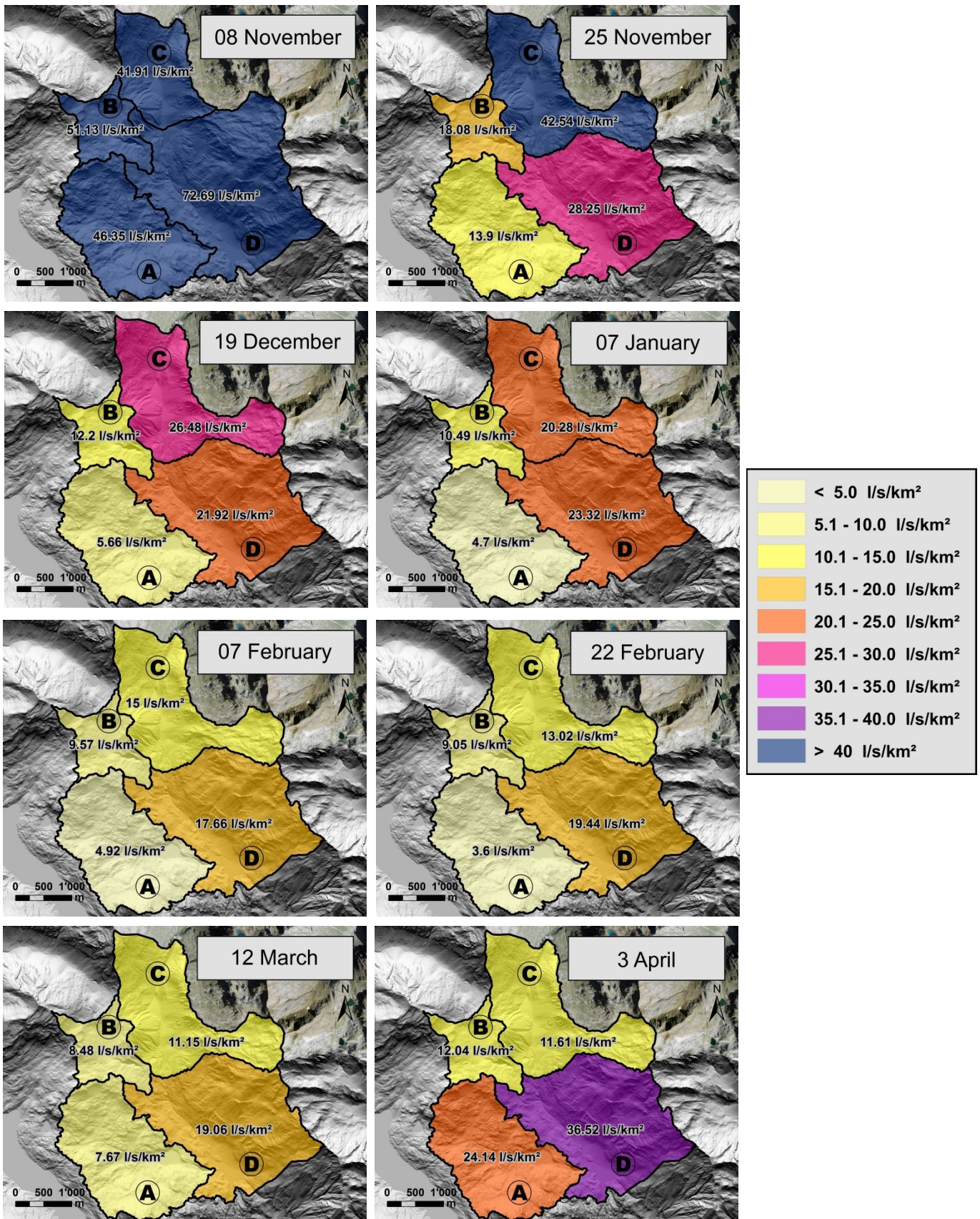


Figure 28: Q, Q<sub>s</sub> and EC in the four subcatchments during the winter season 2013/14

An overview of the spatial distribution of low flow behavior in the research area and the variations during the observation period is shown in the maps of specific discharge (l/s km<sup>2</sup>) for the subcatchments (see Figure 29). At 8 November 13, all subcatchments show a discharge of more than 40 l/s km<sup>2</sup>. At the 28 November a much smaller discharge is visible in the western part of the catchment (subcatchments A and B). Subcatchment C shows the highest specific discharge followed by subcatchment D. Until 19 December 13 subcatchment A (from 14 l/s/km<sup>2</sup> to 6 l/s/km<sup>2</sup>) was going through much higher decrease in specific discharge than subcatchment B (from 15 l/s km<sup>2</sup> to 12 l/s km<sup>2</sup>). In subcatchment C (from 43 l/s km<sup>2</sup> to 26 l/s km<sup>2</sup>) a stronger recession can be detected than in D (from 28 l/s/km<sup>2</sup> to 22 l/s/km<sup>2</sup>), but the headwater area C remains the part of the watershed with the highest contribution. It changes with the beginning of January 14: subcatchment D then shows the highest specific discharge, remaining with the highest contribution for the rest of the observation period. Subcatchment A only shows smooth recession until the end of February 14 (from 6 l/s km<sup>2</sup> to 4 l/s km<sup>2</sup>).





**Figure 29:** The four subcatchments show different recession behavior during the winter season 2013/14. In the beginning specific discharge ( $l/s\ km^2$ ) is similar but the drainage behavior of the four catchments differs - quick recession in the western part (A and B), high winter discharge and slow recession in the eastern part (C and D)

---

Also in subcatchment B specific discharge decreases only marginally from 12 l/s km<sup>2</sup> to 8 l/s km<sup>2</sup> until 12 March 14. Subcatchment D shows about the same mean value from end of December to mid-March with about 20 l/s km<sup>2</sup> for three months. It shows only minor recession). During the measurement campaign on 22 February subcatchment A reaches the lowest point, all other catchments show further decreasing discharge. Although until 12 March discharge decreases in subcatchments B, C and D some influence of snowmelt can be observed. This leads to a more flattened recession curve. Due to major influence of snowmelt along the pass road in subcatchment A (see also chapter 5.4.2) discharge rises in that part of the research area. Looking at the measurement on 3 April 14 one can observe rising discharge in all four subcatchments, however increase is larger in the catchments A and D influenced by lower altitude and the pass road. Subcatchments B and C only show a small increase in specific discharge (Figure 29).

## **5.2.2 Storage mapping**

In the following the results of the measurements are compared to the mapped storages in the catchment.

### **5.2.2.1 Subcatchment A**

In subcatchment A many slopes are covered by debris material but outcrop is frequently visible. Numerous glacial relicts like terminal moraines, glacial cirques or moraine debris can be identified. In glacial cirques, swamp areas developed over time. The largest swamp area, which also has a small lake due to artificial drainage systems, is at Val Campasc where all conveyors gather into one main creek of subcatchment A (see Figure 30). The surface material appears to be pretty rough and high permeable, except in the area of talus slopes identified in the northern and southern part of the catchment (green - Figure 30). According to the spatial distribution of storage thickness in subcatchment A (Figure 30) wide areas have no or only small storage potential. About 63% of the watershed is covered by sediments estimated to be less than 1m in depth. Only 17% are between 1 and 5m and 13% above 5m in thickness. Another indication for the low storage capacity are numerous swamp areas in this subcatchment. Swamps arise only when there is a water stowing horizon, which in case of subcatchment A is bedrock.

In subcatchment A we find a low storage potential due to thin sediment deposits. This low storage potential results in a quick recession behavior in November (Figure 31), a low winter discharge and a quick increase in discharge due to snowmelt starting at the end of February. Discharged volume during the main recession period from 27 November 13 to 11 March 14 is only 54mm, about one third of the mean value of the catchment (142mm). The electric conductivity is low compared to the values at the gauging station and shows only small increase during the measurement campaign (from 69 μS/cm to 79 μS/cm).

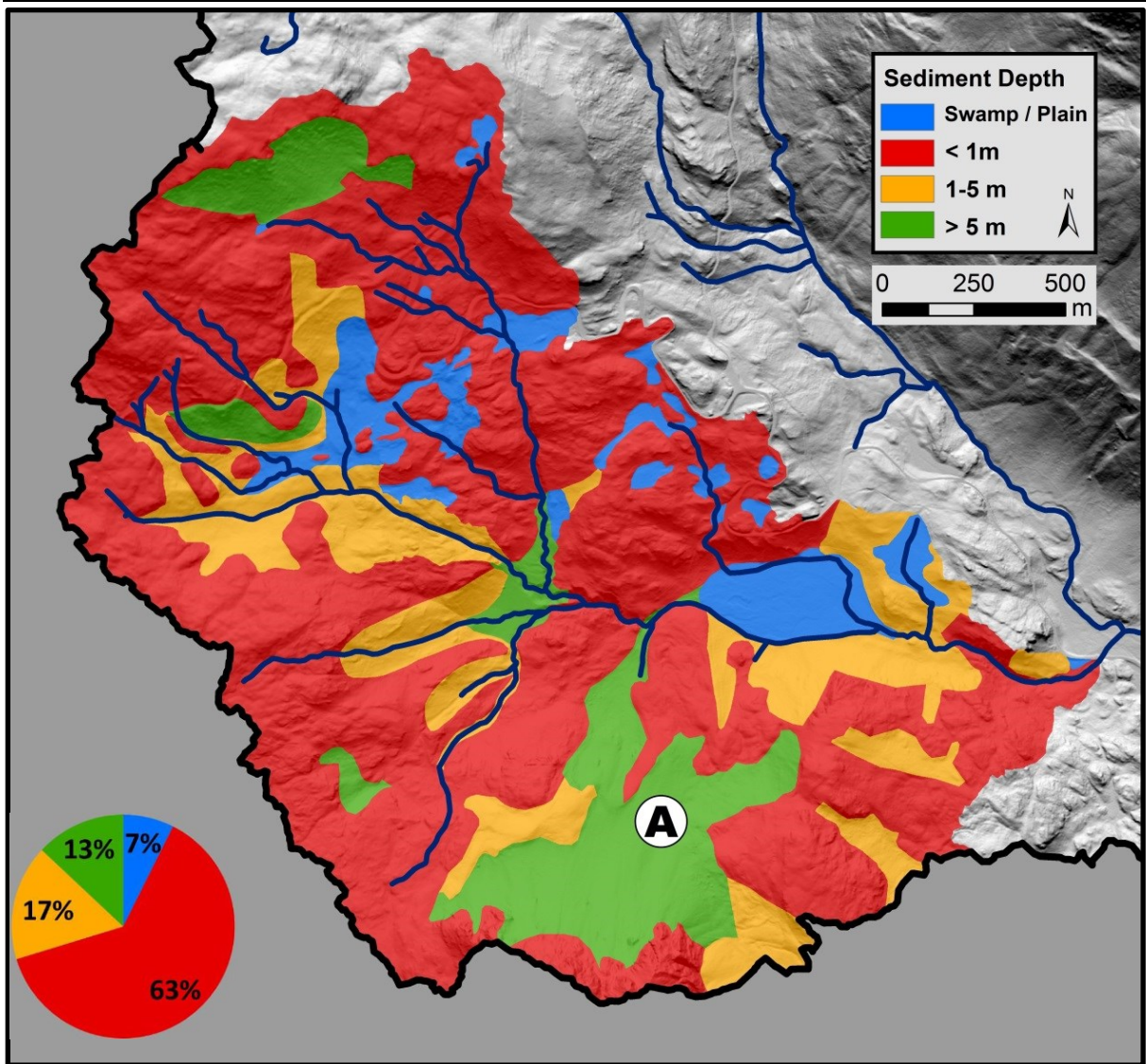


Figure 30: Depth of the quaternary deposits for subcatchment A

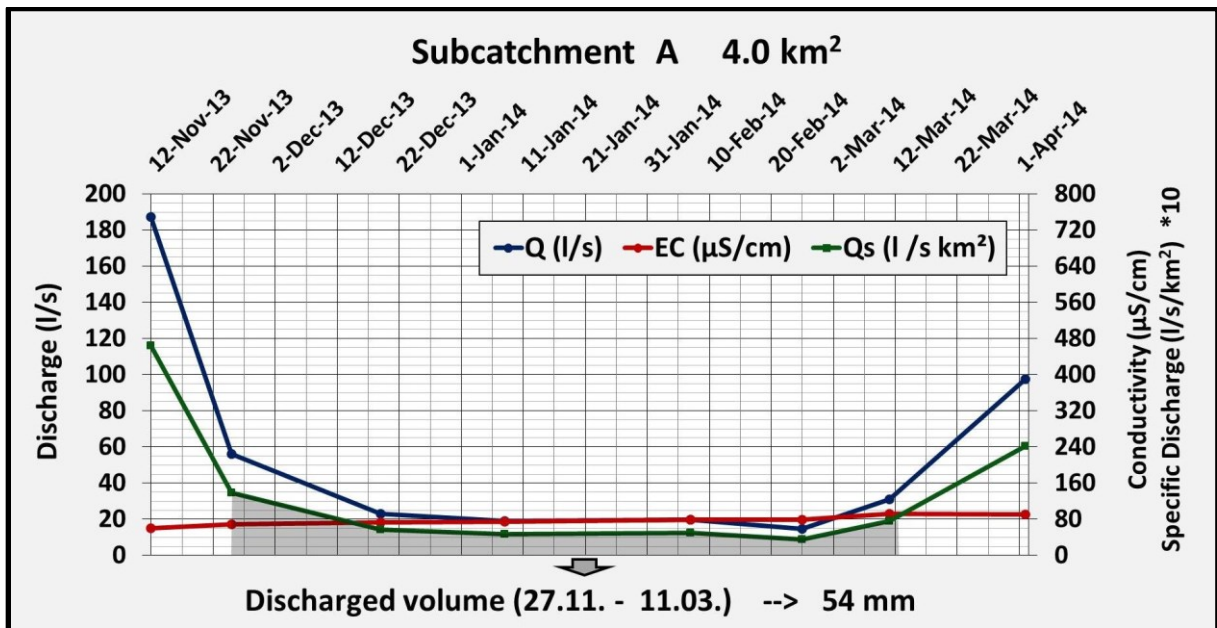


Figure 31: Discharged volume (highlighted in grey) between 27.11. – 11.03. for subcatchment A

The Bernina pass road - leading through the catchment – seems to influence the discharge. Because the street's drainage system is conveying meltwater directly into small creeks, a quick discharge increase can be observed with increasing temperatures. This is also visible when looking at ion composition of the collected water samples. During snowmelt we find a higher conductivity due to increased concentration of sodium and chloride ions, coming from applied NaCl at the pass road.

### 5.2.2.2 Subcatchment B

In subcatchment B geomorphological conditions are similar to those observed in subcatchment A. Numerous glacial relicts like moraine debris form a thin cover on bedrock. Outcrop is visible in many parts. In some areas moraine debris cover is a little thicker than in subcatchment A but as permeable.

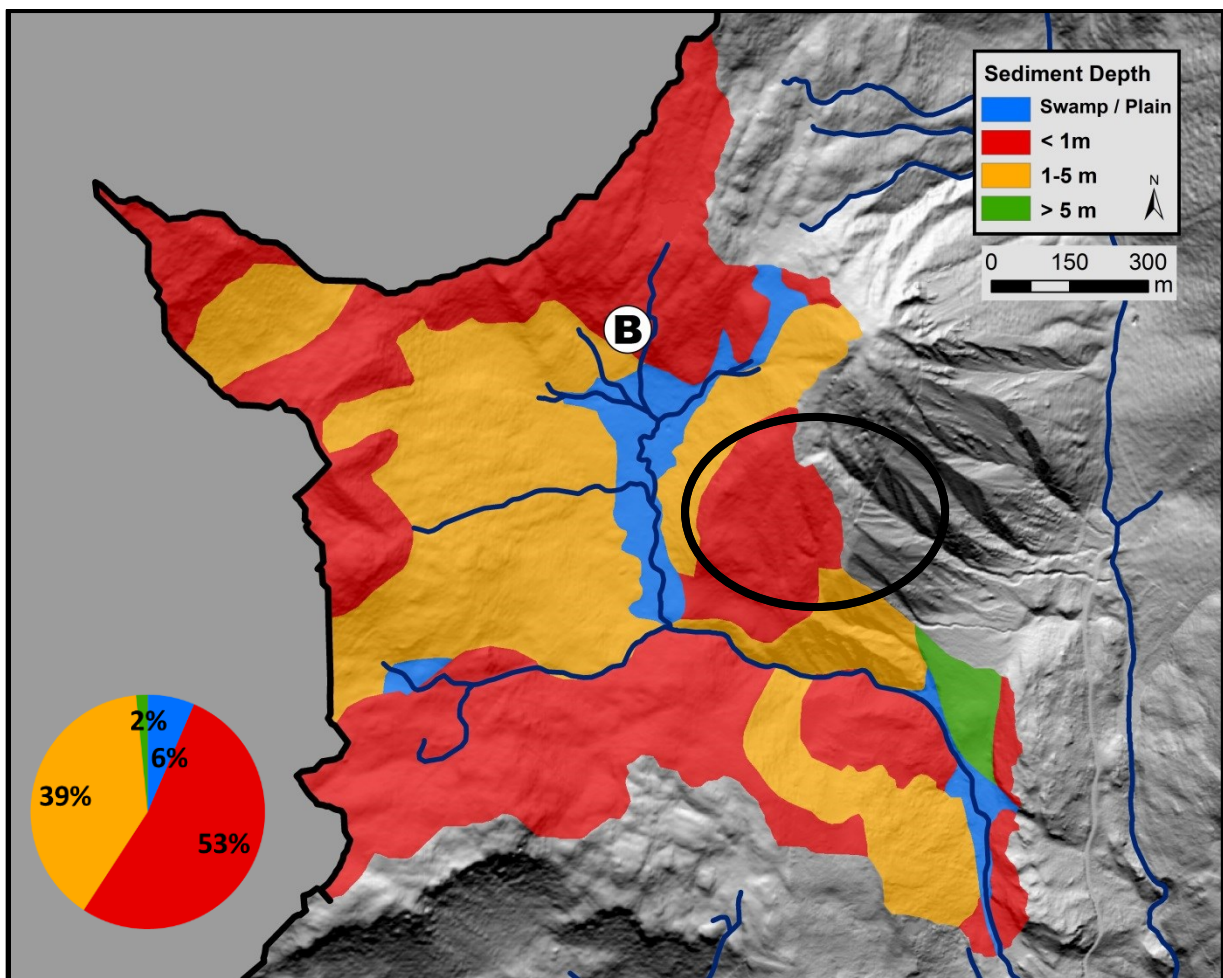


Figure 32: Depth of the quaternary deposits in subcatchment B – marked: area covered by sedimentary rocks

Additionally we find Lower East Alpine sedimentary rocks, mainly gypsum and rauhwacke, building a less permeable surface visible in numerous gullies in the eastern part of the

catchment. These sedimentary rocks are known to have high storage potential due to numerous cavities. Subcatchment B is characterized by storage properties similar to subcatchment A. 53% of the area is covered by sediments below 1m thickness. 29% of the area is covered by sediments between 1 and 5m, only 2% by deposits of more than 5m. Swampy areas exist mainly at Plan di Cüni along the main creek where all the tributaries gather to one main creek (see Figure 32).

Subcatchment B has also a low storage potential, resulting in a quick recession in November and low winter discharge like subcatchment A. But winter discharge is higher in subcatchment B. The discharged volume during the observation period (101 mm) is twice the volume discharged in catchment A (see Figure 33). This can be traced back to sedimentary rocks, mainly gypsum and dolomites found in the eastern part of the catchment contributing about 40% of the total discharge (highlighted in Figure 32) as shown in chapter 5.3.4. Electric conductivity is about 8 times higher than in subcatchment A. High concentrations of calcium, magnesium and especially sulfate can be identified in the water samples. These are washed out from gypsum and other sedimentary rocks being the origin of the discharged water (see also chapter 5.3.4).

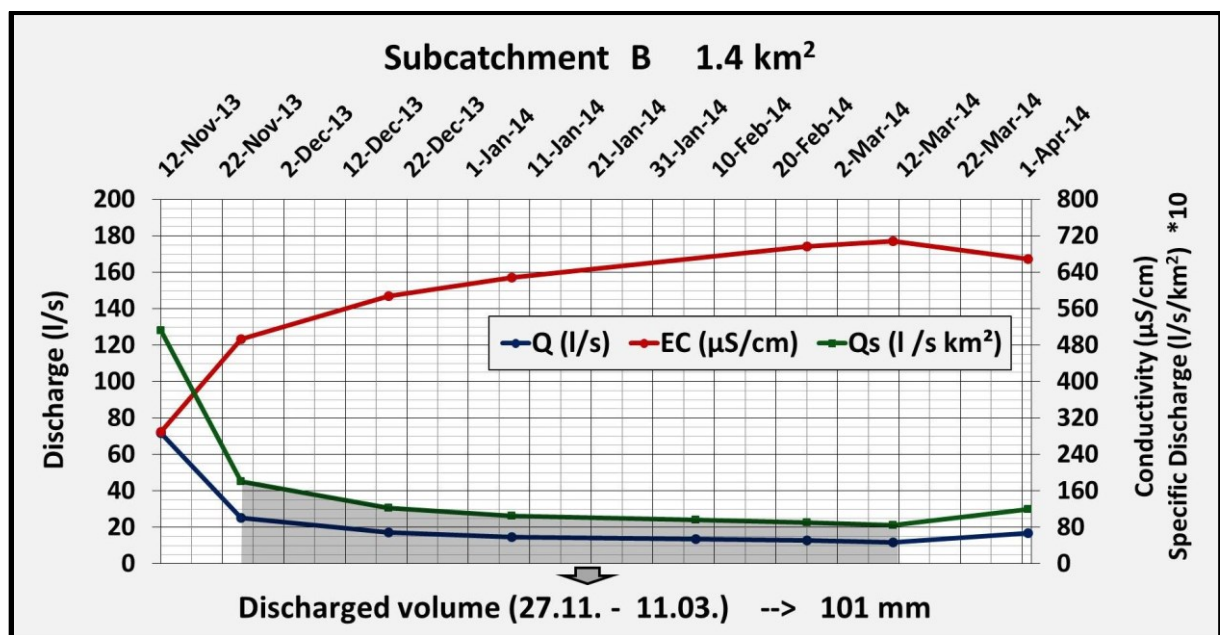
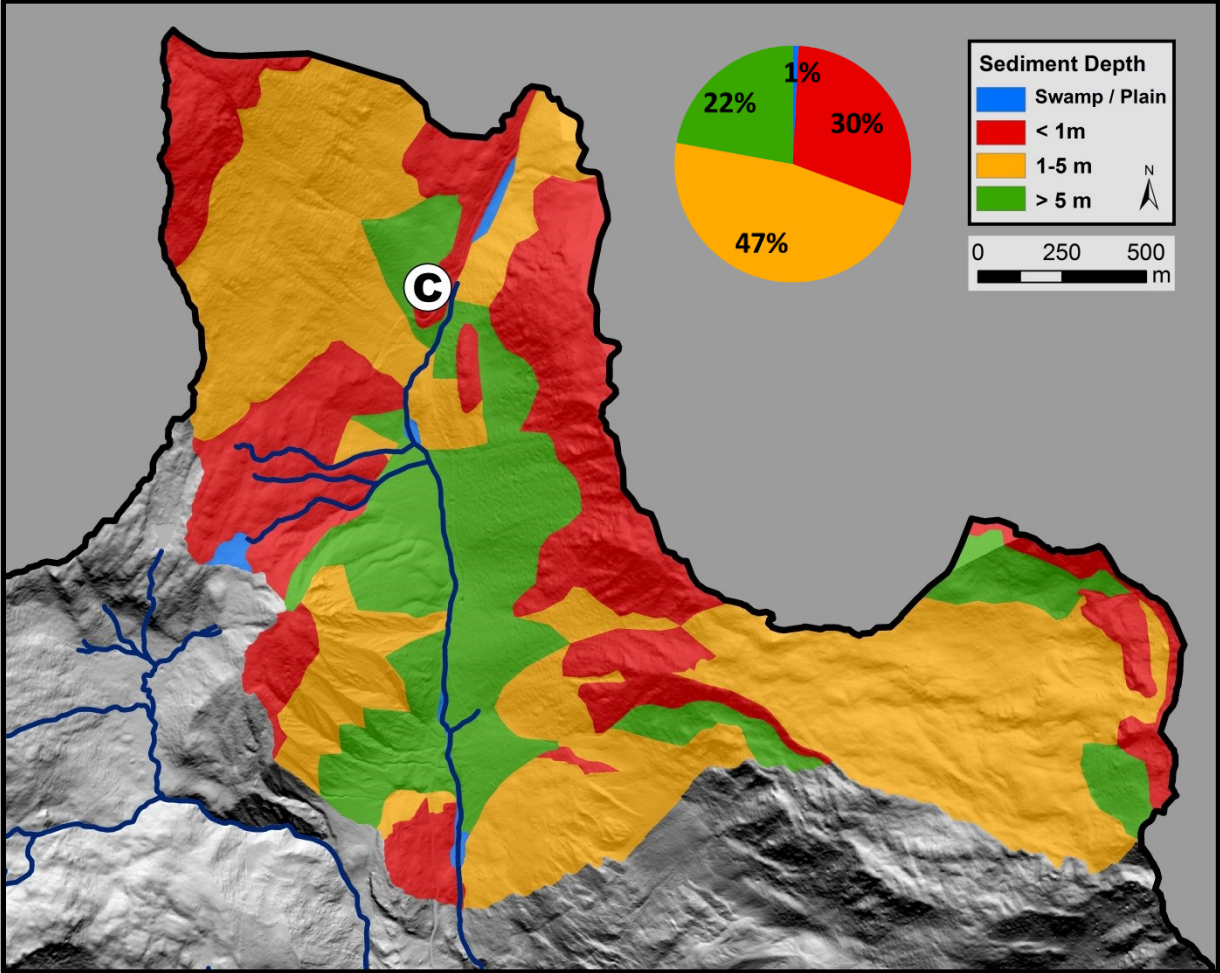


Figure 33: Discharged volume between 27.11. – 11.03. for subcatchment B

### 5.2.2.3 Subcatchment C

Along the main creek, large talus and alluvial deposits could be identified in subcatchment C. Coming from steep hillslopes on both sides of the riverbed, a lot of material was deposited. In some areas, the river is even covered by those sediments. In the upper parts of these hillslopes outcrop is visible. In the northwestern part a large slope covered with debris was identified, comparable to the main parts of subcatchment A and B. Visible gullies suggest low

permeability and surface runoff due to low storage capacity (see Figure 34). The southwestern part (orographic right of the main creek) is characterized by Raibler sediment series, strongly erodible sedimentary rocks of marine origin where surface runoff processes occur (visible steep gullies). The southeastern part of subcatchment C is a former glacial cirque, with some leftover ice lenses and a lot of moraine material and debris showing no surface discharge. In the southern part a rockslide is deposited.



**Figure 34:** Depth of the quaternary deposits for subcatchment C

Subcatchment C is characterized by a large storage potential, 22% of the covering deposits are above 5m in thickness and additionally 47% are between 1 and 5m in depth. There are only little swamp areas and 30% of the catchment’s area is outcrop or covered by less than 1m of sediment (see Figure 34). The storage potential in subcatchment C is much larger than in subcatchment A and B. Conductivity is also high, due to the influence of gypsum / sedimentary rocks in the western part of the catchment. There is dampened but persistent recession behavior and high winter discharge. Discharged volume (190mm) is almost four times as large as in subcatchment A (see Figure 35).

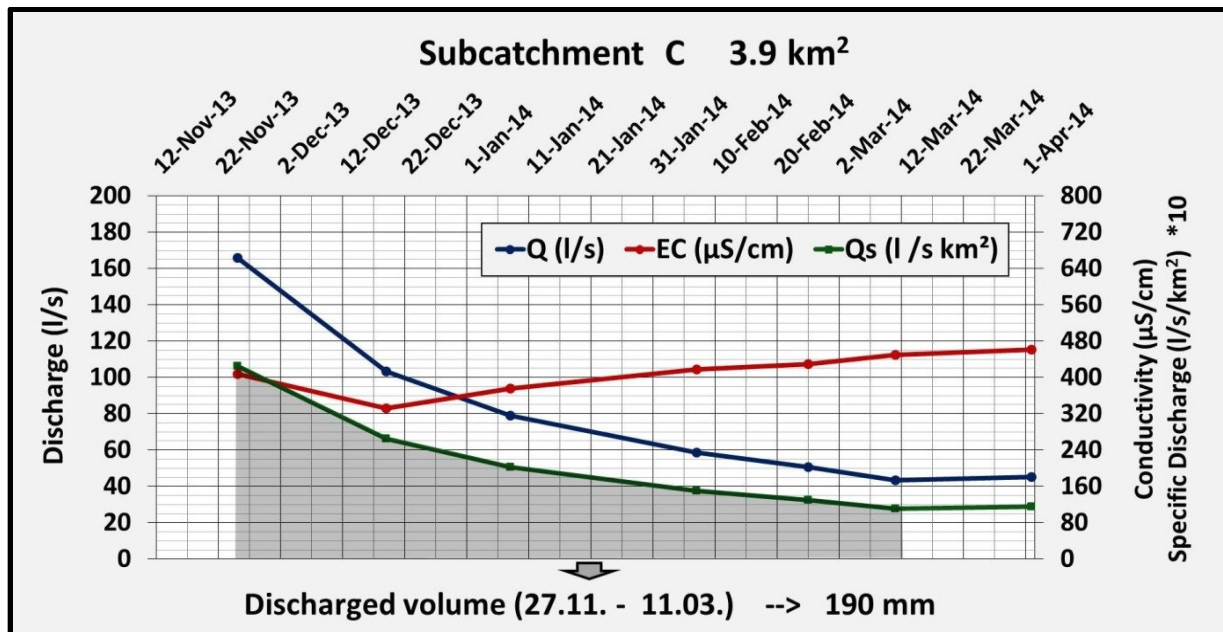


Figure 35: Discharged volume between 27.11. – 11.03. for subcatchment C

The storage potential in subcatchment C is much larger than in subcatchment A and B. Conductivity is also high, due to the influence of gypsum / sedimentary rocks in the western part of the catchment. There is dampened but persistent recession behavior and high winter discharge. Discharged volume (190mm) is almost four times as large as in subcatchment A (see Figure 35).

#### 5.2.2.4 Subcatchment D

Subcatchment D is divided into two parts by Poschiavino River. On the orographic right lie thin debris deposits with properties as found in subcatchments A and B, on the orographic left, which forms the major part of the catchment, a steep slope without any surface discharge is found. Orographic right one can detect numerous small inflows suggesting low permeability and low storage potential. The steep slope on the orographic left side is characterized by thick layers of debris, only little traces of surface runoff processes. Numerous cracks and neotectonics (see SUMMERFIELD, 1987) perpendicular to slope inclination can be detected. Between these neotectonic cracks sediment is deposited. On the slope a few small sliding areas with small springs, mainly in the lower part, can be found. In the lower parts along the river lies the large alluvial aquifer (“Plan LaRösa” - highlighted in Figure 36) at the valley bottom, visible as a wetland area / swampy plain with an artificial drainage system.

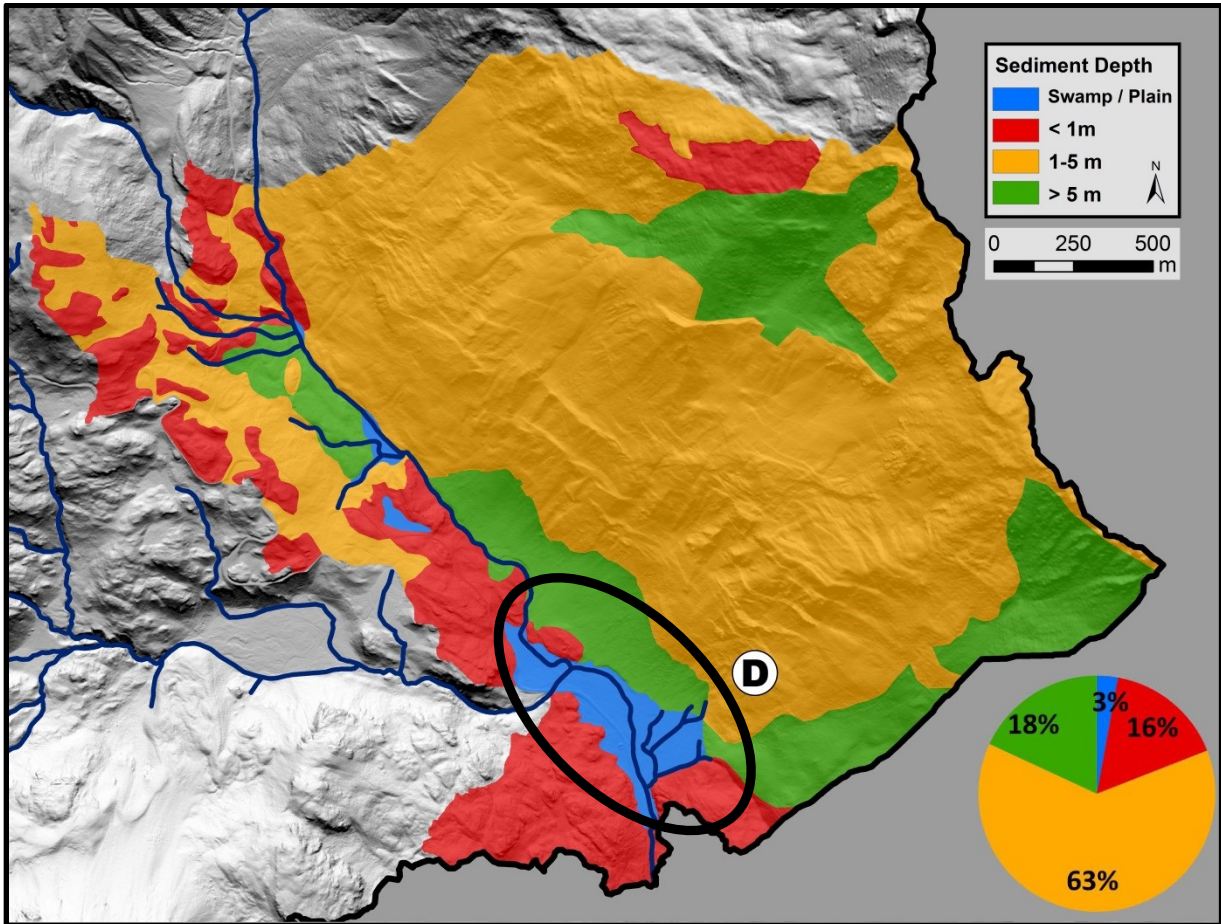


Figure 36: Depth of the quaternary deposits in subcatchment D – highlighted: alluvial plain LaRösa

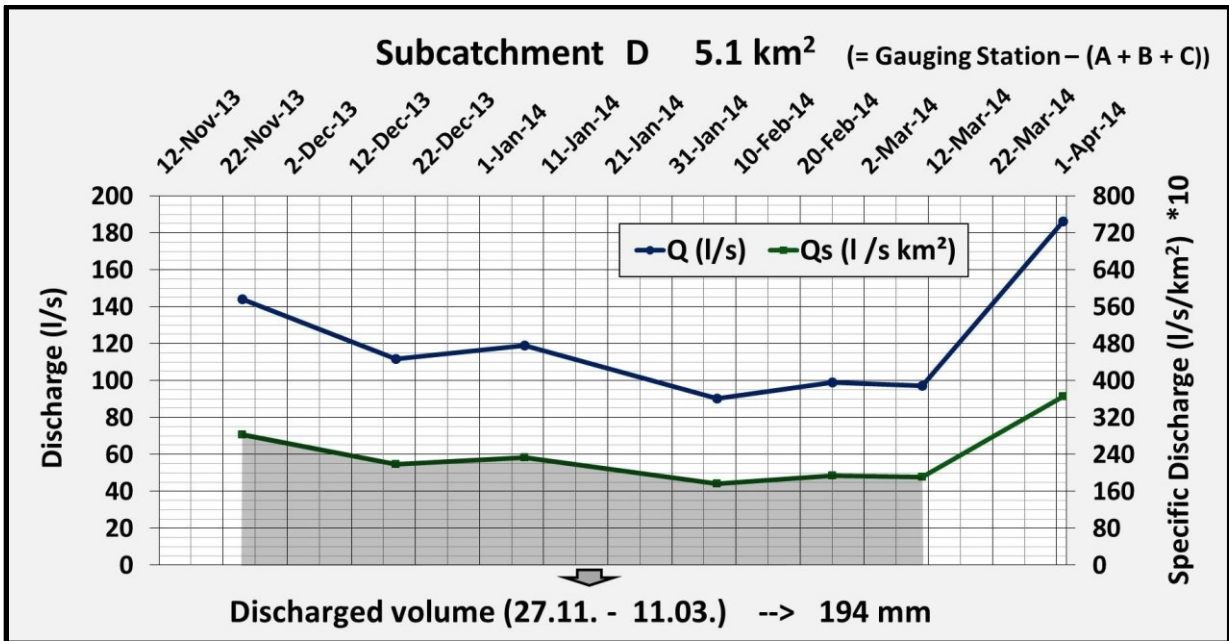


Figure 37: Discharged volume between 27.11. – 11.03. for subcatchment D



Subcatchment D, dominated by a steep slope without any surface discharge has approximately 18% of sediment cover of above 5m depth (see Figure 36). 63% of the deposits are between 1 and 5m, only 16% are below 1m thickness or outcrop. Additional influence on discharge from the valley bottom alluvial aquifer (“Plan LaRösa”), the visible cracks and neotectonics is plausible.

Due to the thick quaternary deposits the storage potential of the catchment is very high. During the measuring campaign slow, dampened recession could be observed. Considering the higher uncertainties in the calculated discharge values for subcatchment D, discharge in the main recession period nearly stabilized. The catchment shows the highest discharged volume of all four subcatchments (194mm).

### 5.2.3 Potential storage volume

Quantification of storage volumes was done based on mapped thickness of deposits and qualitative permeability estimation within a certain range. The depth classes <1m, 1-5m, >5m were averaged into 0.5m, 3m and 7m for minimum storage potential and 1m 5m and 10m for maximal storage potential and the values for porosity (low, medium, high) were quantified regarding literature (BLUME et al., 2010) as pore volume (10%, 20% and 30%). Regarding these values the storage capacity for every subcatchment was calculated.

**Table 2:** Comparison of discharged volume and the estimated range of storage volume for main subcatchments

subcatchment	discharged volume 27 November – 11 March	range of storage potential	% of annual precipitation
	in mm	in mm	(P minus ET)
A	54	370 – 540	26 – 37
B	101	250 – 420	17 – 29
C	190	670 – 1030	47 – 72
D	194	760 - 1190	53 – 82

Estimated storage volumes are much larger than volumes discharged in the main recession period (from 27 November to 11 March), which started long after the recharge of storages by a large big precipitation event. Especially short term storages had already been depleted when the observation started. The storage potential seems to be underestimated as no catchment could store total annual precipitation of 1738mm even when considering 300mm of mean annual evapotranspiration (see

Table 2). Subcatchment A has a storage potential between 370mm to 540mm, about 10% were discharged during the observation period. Subcatchment B has the lowest storage potential of 250mm to 420mm, which is less than 30% of total annual precipitation. Storage of the sedimentary rocks were not included in this calculations, therefore the storage

potential in B would be much higher. Subcatchment C and D have more potential storage volume, up to 72% of mean annual precipitation can be stored in subcatchment C, up to 82% in subcatchment D.

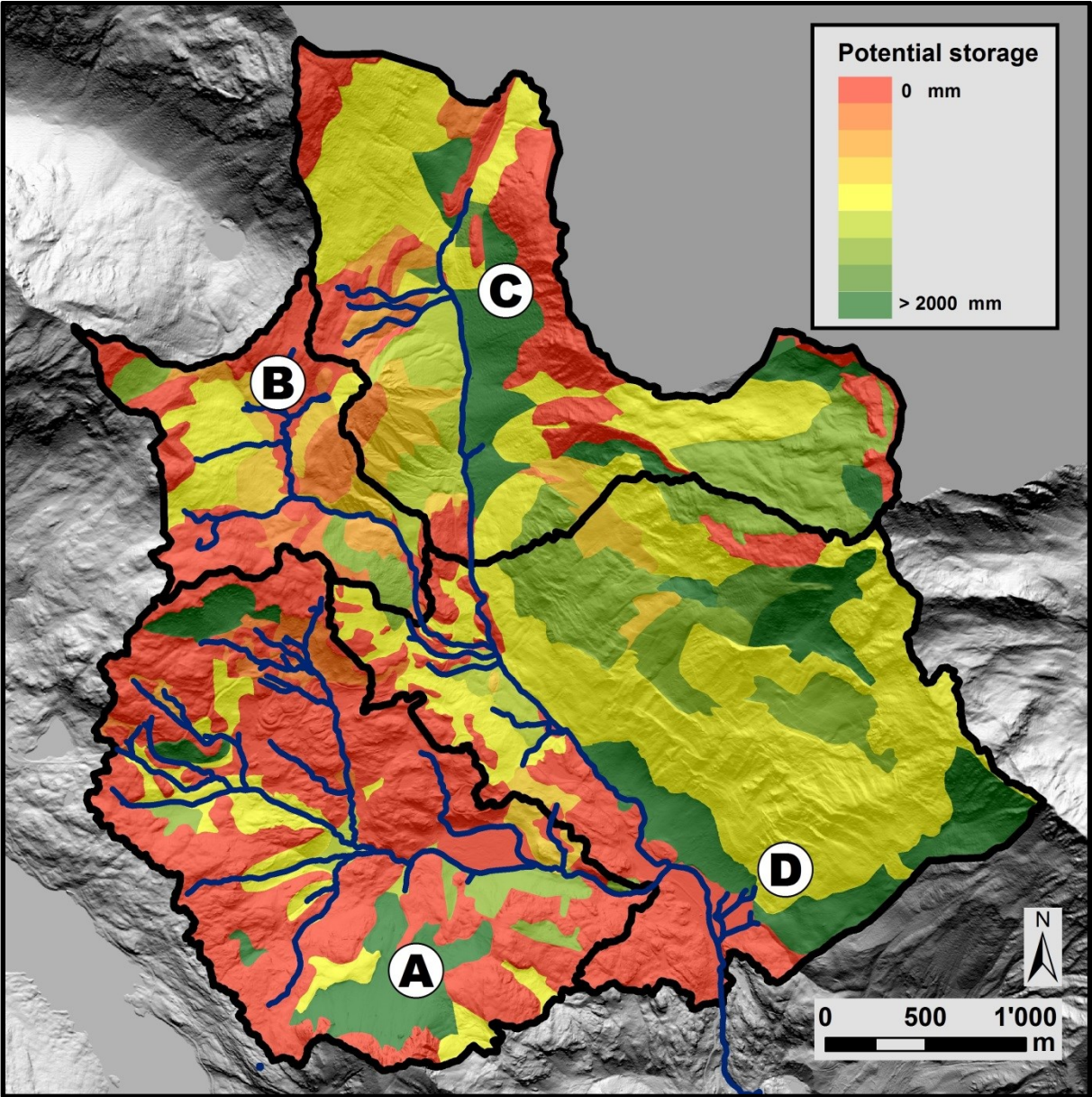


Figure 38: Estimated storage potential in mm for the research area

Uncertainties derive from generalized pore volume and thickness classes, mean precipitation (1738mm) and mean annual evapotranspiration (300mm). Another uncertainty is the traveltime through the sediments. It is estimated that deposits, although having only low porosity and high pore volume, beneath 1m thickness cannot hold water for a sufficient time period, sustaining baseflow during low flow conditions.

---

Of course generalizations were applied when calculating the potential storage but Figure 38 gives an overview of spatial distribution of the catchments' storages and the main source areas of winter discharge.

#### **5.2.4 Comparison of storage and discharge behavior**

The estimated depth of quaternary sediments is corresponding to discharged volumes during the winter months: The western part of the catchment with thin sediment cover shows quick recession in autumn and a low winter discharge, the eastern part covered by numerous thick deposits shows slow recession throughout the winter season. It is estimated that basically the thick quaternary deposits sustain the high winter discharge during times without liquid precipitation. The estimation of total storage volume, despite included uncertainties, gives an overview of the spatial distribution of contributing storages of the upper Poschiavino area.

### **5.3 Spatially higher resolved measurements**

Numerous measurements were done on smaller scales, so more interesting findings can be put forward to discussion:

#### **5.3.1 Scale issues**

Figure 39 shows discharge (blue line), specific discharge (green) and conductivity (red) measurements in high spatial resolution on 22 February along Poschiavino between MP C and the gauging station. Additionally identified conveyors from orographic left and right are indicated. On the X axis measurement points with their catchment areas are plotted.

Almost no difference in specific discharge between MP C and the gauging station ( $13 \text{ l/s km}^2$  vs.  $12 \text{ l/s km}^2$ ) can be found, but between those points differences are visible (from  $18 \text{ l/s km}^2$  at MP X1 to  $11 \text{ l/s km}^2$  at MP D3). Discharge rises and conductivity falls almost linear; the only exceptions looking at discharge are at measurement point X1 due to inflow of numerous springs from orographic left and at the gauging station suggesting more subsurface inflow from the groundwater aquifer "Plain LaRösa" (see Figure 41). Variation in Q, Qs and EC can be explained by observed features. Qs is rising till MP X4 due to numerous subsurface conveyors and springs mainly from orographic left.

Although between MP X4 and X3 the main creek of subcatchment B merges from orographic right, specific discharge decreases due to low specific discharge in subcatchment B (larger area but Qs smaller than  $16 \text{ l/s km}^2$ ). Conductivity decreases until X4. Due to high electric conductivity in subcatchment B EC rises a little till MP X3. Qs smoothly increases again until MP X2, also EC smoothly decreases until that MP. Between MP X2 and X1 numerous small

springs add a lot of water with lower electric conductivity from orographic left, what leads to visible increase in  $Q_s$  (from 14 l/s km<sup>2</sup> to 18 l/s km<sup>2</sup>) and decrease in EC (360  $\mu$ S/cm to 300  $\mu$ S/cm). Up to measuring point D4 no more conveyors merge, therefore of course  $Q_s$  decreases and EC and Q more or less remain at the same level. Before D3 the main creek from subcatchment A merges to Poschiavino (low conductivity and low discharge), therefore Q rises but  $Q_s$  (due to the large catchment area) decreases. Between MP D3 and the gauging station discharge increases a lot (130 l/s to 180 l/s) also specific discharge rises a little, due to conveyors from orographic left (D1 and D2) and contribution of "Plain LaRösa". Electric conductivity remains around 300 $\mu$ S/cm.

According to Figure 39 many point sources contribute to the river network resulting in a large spatial variation of specific discharge in the subcatchments within research area D (Figure 40).

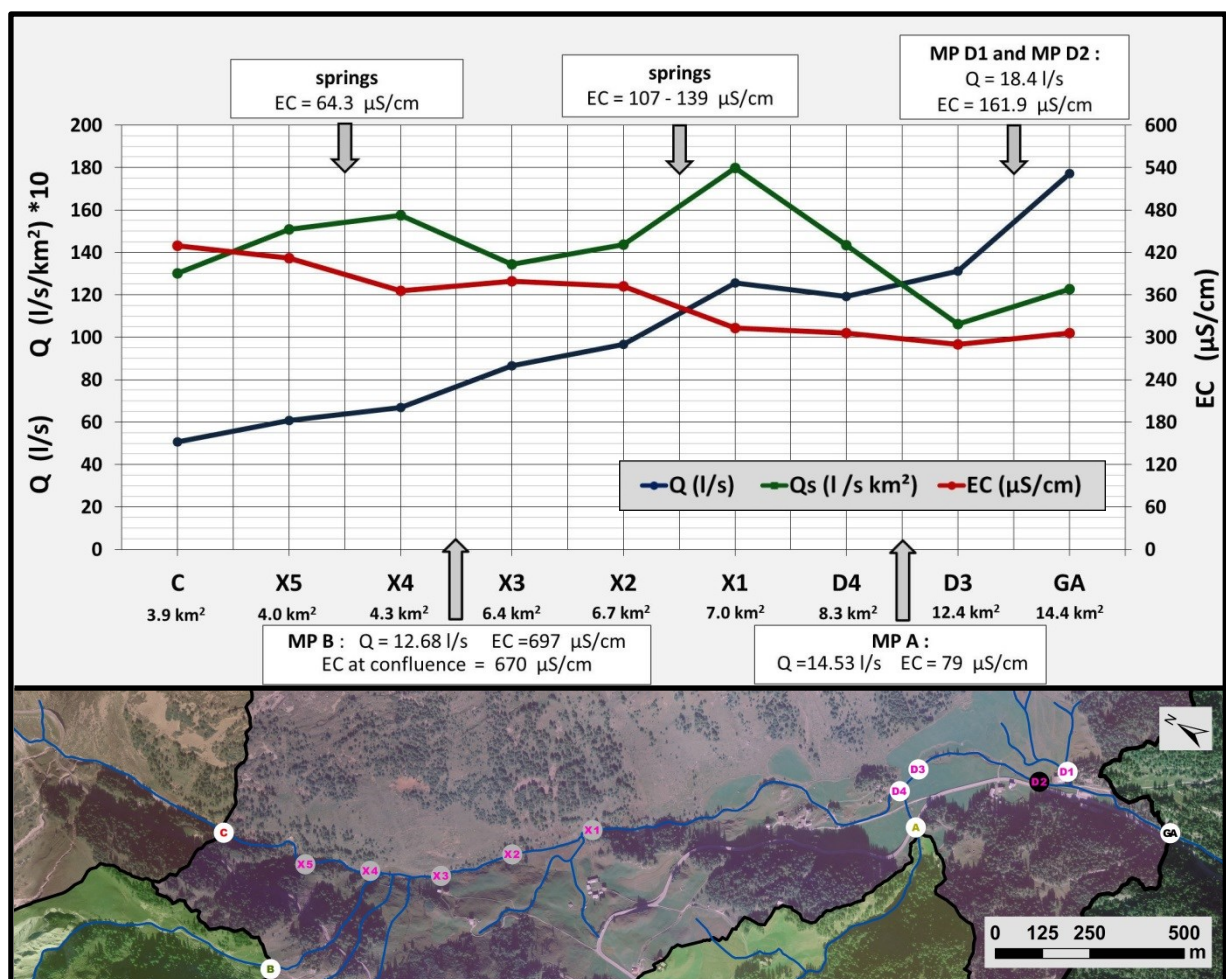


**Figure 39:** Variation of discharge (Q), specific discharge ( $Q_s$ ) and electric conductivity (EC) along Poschiavino from measurement point C to the gauging station on 22 February 2014

One can identify two main source areas, one between measurement points C and X5, the second between MP X2 and X1. Regarding existing geo(morpho)logical maps and field observations a rockslide (C to X5) and an area of creeping landmasses (X2 to X1) can be

identified as main points of contribution. Additionally subcatchment D1/ D2 and the area between D4 and the gauging station show specific discharge exceeding the mean value.

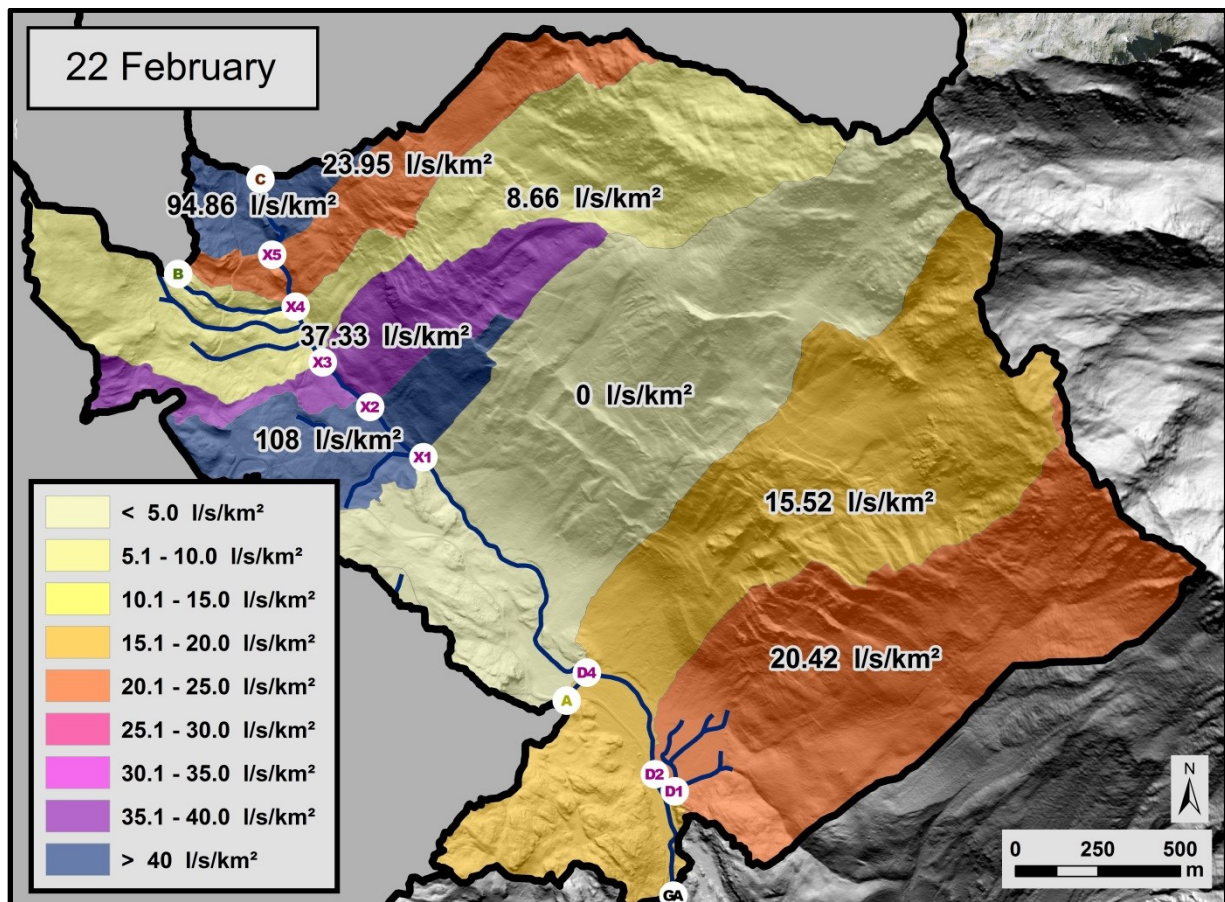


**Figure 40:** Spatial variation of specific discharge ( $Q_s$ ) for every single MP in subcatchment D on 22 February based on subcatchment areas defined by surface topography

Point sources are the main contributors to the river network. The hillshade of subcatchment D (Figure 41) shows linear faults interpreted as cracks and neotectonics. The whole slope on the orographic left side is covered by thick deposits. There is no recent river network visible on the slope, even fossil river channels are missing. This is evidence for the existence of subsurface flow resulting in uncertainties when deriving topographic catchment borders. It is unlikely to have a slope without any discharge (between X1 and D4) next to it a small subcatchment with extremely high specific discharge (X2 to X1). Therefore the topographic catchment areas do not coincide with subsurface watersheds. The sediment layers but also cracks and neotectonics (Figure 41) can transfer water beneath surface and therefore determine the catchment borders differently. Due to deposits on the slopes next to the alluvial plain, it is suggested that water is transported to the alluvial plain directly. So much water appears only after “Plain LaRösa” at the gauging station.

Between MP X2 and X1 the creeping landmasses have an exceptionally high contribution due to many small springs. Also the rockslide area, in the upper part of catchment D, more or

less derived by high fractured rocks with concentrated flow paths and few point source outlets, shows high contribution.

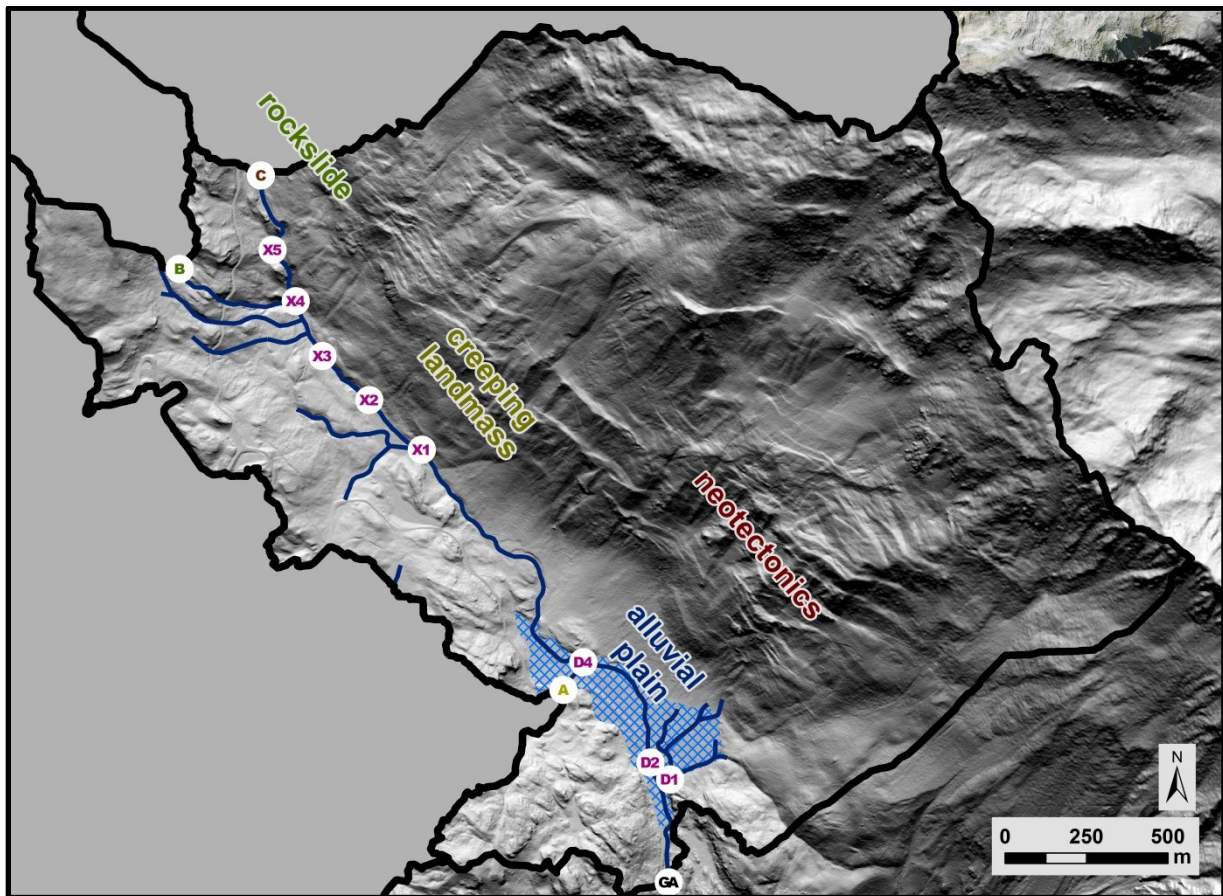


Figure 41: Hillshade of subcatchment D

### 5.3.2 Variation of ion composition along Poschiavino

Ion composition was analyzed between 06 January and 12 March 14 for several measurement points within the research area. Here some results of ion chromatography are presented. Figure 42 shows the evaluation for five ions (Mg, Na, Cl, Ca and  $\text{SO}_4$ ) along the main river in mg/l. X7 is the highest sampling point situated in subcatchment C, GA the lowest at the gauging station. Main sampling points along Poschiavino are also visualized in the map, additional samples were taken at PO2 – PO8 and furthermore tributaries are drawn.

Downriver concentrations of Mg, Ca and  $\text{SO}_4$  are decreasing, with an exception between MP X4 and MP X3 where the main creek from subcatchment B merges with Poschiavino. Especially sulfate concentration is extraordinary high, decreasing downriver, suggesting that  $\text{SO}_4$  contribution comes from the headwater area and subcatchment B.  $\text{SO}_4$  is mainly responsible for the high electric conductivity in subcatchments C and B. It suggests that the high amount of Mg, Ca and  $\text{SO}_4$  comes from the sedimentary rock layers. Another interesting

result is that Na and Cl concentration are rising after the confluence of the main creek with subcatchment A (see chapter 5.4.2). Also influence of the other tributaries on the ion composition in the main river network is visible.

The amount of ions decreases downriver, mainly because the discharge from sedimentary rocks in subcatchments B and C shows the highest ion concentration. High  $\text{SO}_4$  concentration from gypsum layers is responsible for the high electric conductivity in the headwater area.

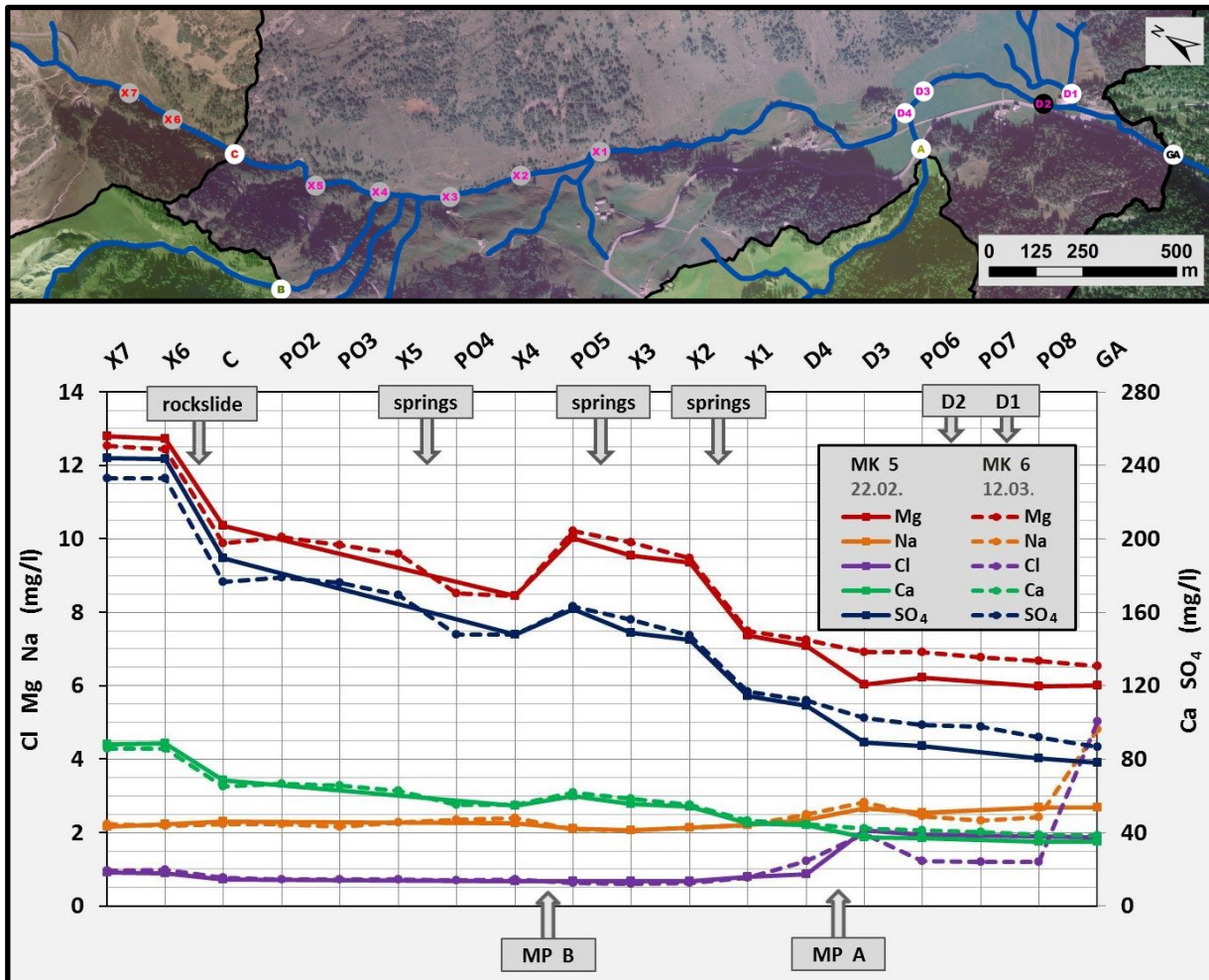
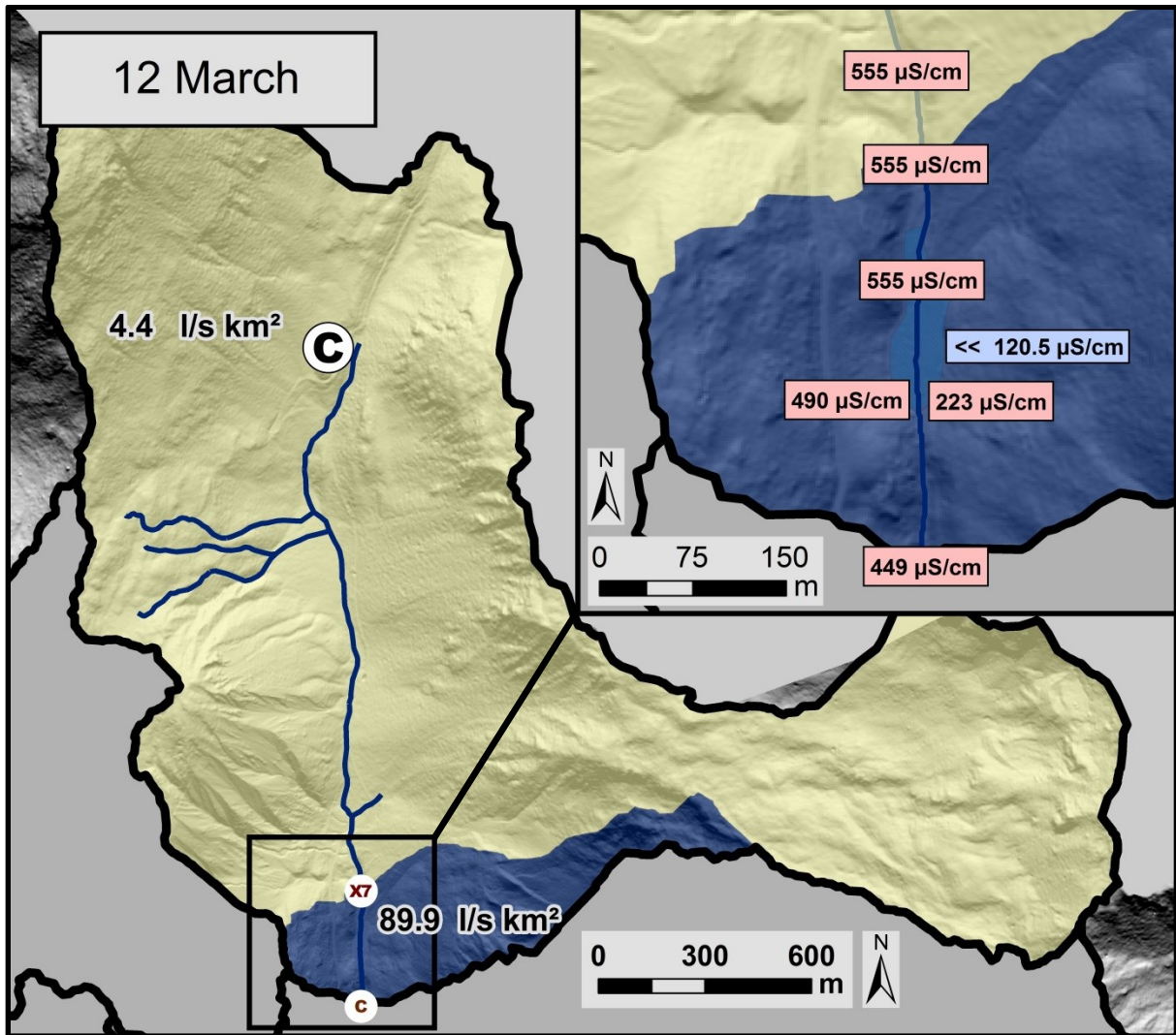


Figure 42: Variation of water chemistry along Poschiavino between 22 February 13 and 12 March 14

### 5.3.3 Influence of the rockslide area

At the border between subcatchment C and D rockslide material is deposited on the orographic left side of the main creek. An estimation of the contribution of this area to the discharge of subcatchment C is tried here, using product equations of discharge and electric conductivity.



**Figure 43:** Variation of specific discharge and electrical conductivity in subcatchment C on 12 March 14

Due to sediment accumulation along the main creek in subcatchment C the river flows not always on the surface. Unfortunately it was not possible to measure discharge in the upper part of subcatchment C due to avalanche risk and massive snow accumulation. The specific discharge for measurement point X7 is only  $4.4 \text{ l/s km}^2$  compared to  $89.9 \text{ l/s km}^2$  for MP C on 12 March. Based on this measurements contribution from the rockslide area could be calculated and interpreted. Above the rockslide area (MP X7) electric conductivity in the main creek is much higher than below (MP C) ( $555 \text{ µS/cm}$  vs.  $449 \text{ µS/cm}$ ) (see Figure 43). Along the alluvial plain between MP X7 and C variation in electric conductivity can be measured. One spring can be identified with a very low EC of  $120.5 \text{ µS/cm}$  originating from the rockslide (orographic left). Measured discharge rises from  $16 \text{ l/s}$  to  $44 \text{ l/s}$  between X7 and C. Although some undercurrent could occur at MP X7, it seems that the rockslide area is the main contributor to discharge measured at MP C.



As conductivity decreases and discharge increases in the creek passing the rockslide area the amount of water contributed from the two areas can be assessed with a simple product equation:

$$Q_{\text{Rockslide}} * EC_{\text{Rockslide}} + Q_{\text{between X7 and C}} * EC_{\text{between X7 and C}} = Q_C * EC_C - Q_{X7} * EC_{X7}$$

$$Q_{\text{Rockslide}} + Q_{\text{between X7 and C}} = Q_C - Q_{X7}$$

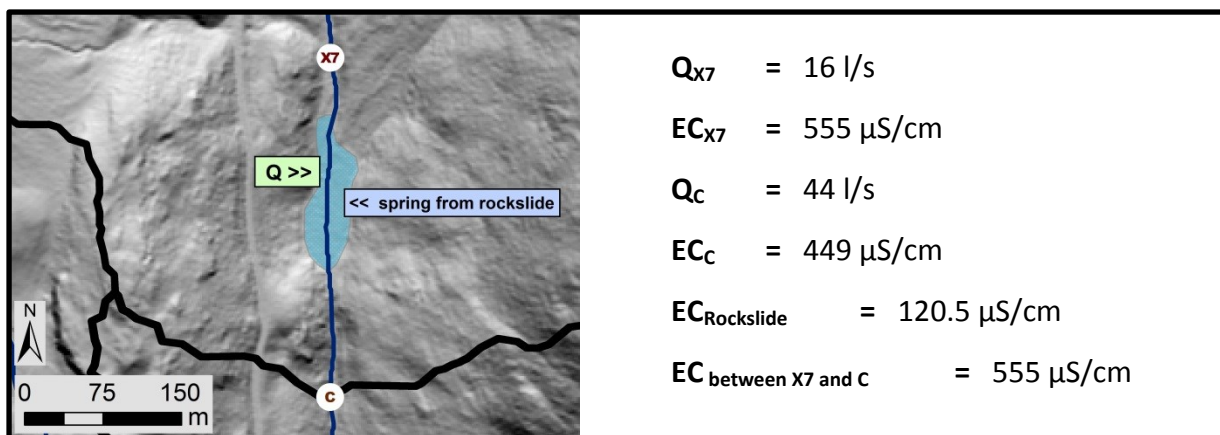


**Figure 44:** Measured values of EC and Q between X7 and C

Applying these equations using measured values from 12 March suggests that approximately 10 l/s come from the rockslide area and 18 l/s are coming from orographic left (sedimentary rocks) or from undercurrent at MP X7.

The rockslide area covers approximately 1 km<sup>2</sup>. The whole catchment area of the rockslide was calculated regarding topographic criteria to be about 1.7 km<sup>2</sup>. To compare the contribution from the rockslide area to the discharged volume of catchment C the derived value was extrapolated: Estimating that 10 l/s is the mean discharge from the rockslide area, the total discharged volume during the observations (27 November 13 until 12 March 14) would be 53 mm, which is far below the average of subcatchment C (190 mm). Also when estimating that a fifth of discharge (as in the example of 12 March) measured at MP C comes from the rockslide area all winter long, the discharged volume would only be 87 mm. Further influence of the rockslide area, like springs beneath MP C, could not be identified. Also electric conductivity in the main creek does not change downstream of MP C. Therefore the main source of subcatchment C is subsurface inflow from the sedimentary rocks orographic right and from identified storages upstream and not from the rockslide area.

### 5.3.4 The influence of Raibler sediment series on discharge behavior

Runoff from subcatchments B and C has a high electric conductivity due to the high amount of  $\text{SO}_4$ , Ca and Mg ions found in the water samples from these areas. These three ions are main components of marine sediments. According to the geological map, approximately 1.5  $\text{km}^2$  belong to the Lower East Alpine sediments (Raibler Series) in subcatchments B and C. The majority of water derives from gypsum ( $\text{CaSO}_4 \cdot 2\text{H}_2\text{O}$ ) and dolomite ( $\text{CaMg}(\text{CO}_3)_2$ ) layers, known as potent water storages, due to cavities.

**Table 3:** Estimated discharge from Raibler sediment series from ion composition from January 14 to March 14

Date	MP	$\text{SO}_4$	Ca	Mg	$Q_{\text{measured}}$	$Q_{\text{SED}}$	$Q_{\text{SED}}$
		mg/l	mg/l	mg/l	l/s	l/s	%
<b>MK Jan</b>	<b>B</b>	261	100	21	14.7	5.6	37.8
<b>MK Feb</b>	<b>B</b>	292	111	23	12.7	5.3	41.8
<b>MK Mar</b>	<b>B</b>	297	114	23	11.9	5.0	42.2
<b>MK Jan</b>	<b>C</b>	166	62	9	79.1	15.8	19.9
<b>MK Feb</b>	<b>C</b>	180	66	10	50.8	11.1	21.8
<b>MK Mar</b>	<b>C</b>	189	69	10	43.5	9.8	22.5
<b>MK Jan</b>	<b>X7</b>	181	67	10	-	-	-
<b>MK Feb</b>	<b>X7</b>	233	86	13	17.3	4.9	28.3
<b>MK Mar</b>	<b>X7</b>	244	88	13	15.6	4.5	29.1
<b>MK Jan</b>	<b>D4</b>	104	42	7	164.9	22.0	13.4
<b>MK Feb</b>	<b>D4</b>	112	45	7	122.5	18.0	14.7
<b>MK Mar</b>	<b>D4</b>	109	44	7	118.9	16.9	14.2
<p><math>Q_{\text{measured}}</math> ... measured discharge at the MP  <math>Q_{\text{SED}}</math> ... calculated Q from sedimentary rocks</p>							

Maximum  $\text{SO}_4$  saturation of water originating from gypsum is 1450 mg/l  $\text{SO}_4$  and 650 mg/l Ca (EUROGYPSUM, 2010), maximum Mg saturation of water from dolomite is 106 mg/l (PAVUNZA and TRAINDL, 1983). Assuming that water discharged from gypsum series is fully saturated with  $\text{SO}_4$  ions, runoff from dolomite layers is fully saturated with Mg ions and only these layers contribute Mg and  $\text{SO}_4$ , discharge from gypsum and dolomite can be calculated (see Table 3). The amount of water discharged from these layers is estimated for three dates based on measured concentration at the sampling points B, C, X7 and D4 (see Figure 45). For example if a concentration of 100 mg/l  $\text{SO}_4$  can be measured at a discharge of 10 l/s only 6.9% of the water are fully saturated with  $\text{SO}_4$  ions.

In subcatchment B the amount of water from sedimentary rocks (Table 3 -  $Q_{SED}$  l/s) is nearly constant over the observation period, a decrease can be observed in subcatchment C. Referring to specific discharge the whole area covered by sedimentary rocks in the subcatchments B and C shows decrease from 14 l/s km<sup>2</sup> to 10 l/s km<sup>2</sup> (from 08 January to 13 March 14).

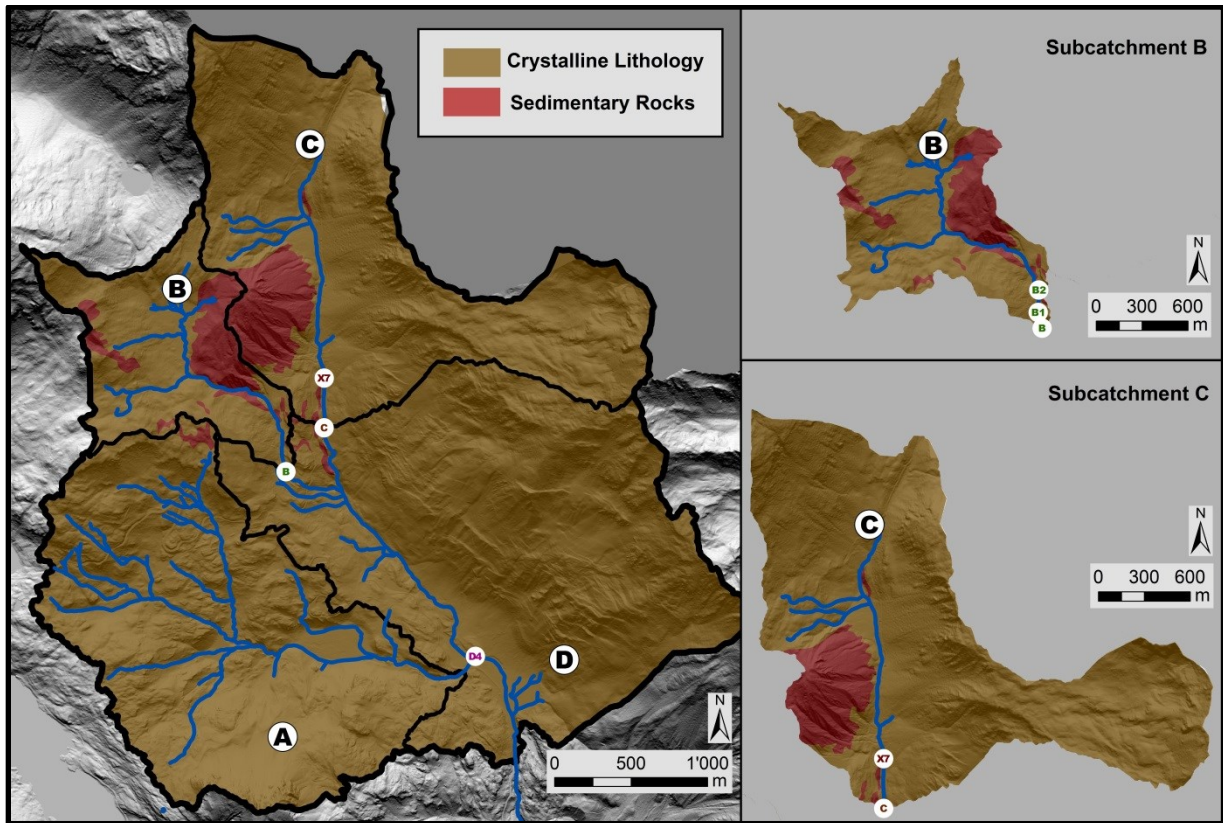


**Figure 45:** Area covered by sedimentary rocks and crystalline lithology and relevant sampling points

The percentage of water discharged from sedimentary rocks (Table 3 -  $Q_{SED}$  %) is around 40% in subcatchment B, around 20% in subcatchment C at MP C and 30% at MP X7. (see Figure 45). Although only 7 % of the whole catchment is covered by the Raibler Series, 14% of the discharge is coming from these sedimentary rocks. This value is estimated based on the assumption that water originating from the Raibler Series is completely saturated. The amount could be even higher when the water is not completely saturated.

To verify the obtained results also discharge from sediment series for MP D4 downstream was calculated assuming full  $SO_4$  and Mg saturation. It is estimated that below the measuring points B and C only little water containing  $SO_4$  or Mg is discharged. Therefore the sum of discharge from sedimentary rocks at MP B and MP C should be the same as the discharge from sedimentary rocks at MP D4. During the measuring campaign in January the sum from MP B and MP C was 21.4 l/s, at MP D4 22 l/s were calculated. So about 97% of the discharge from sedimentary rocks at MP D4 could already be measured at MP B and MP C.

However the percentage is decreasing to 91% during the measuring campaign in February and to 87.5 in March. The increasing difference between MP D4 and the sum of MP B and C could be a result of decreasing water storage in the cavities of the sedimentary rocks. It is estimated that with a lower water table in the cavities, more water is discharged below the measurement points B and C and could only be measured at point D4. Uncertainties when comparing the results occur, because water samples were not always taken at the same day at all sampling points and because of the unknown state of saturation of the water discharged from sedimentary rocks.

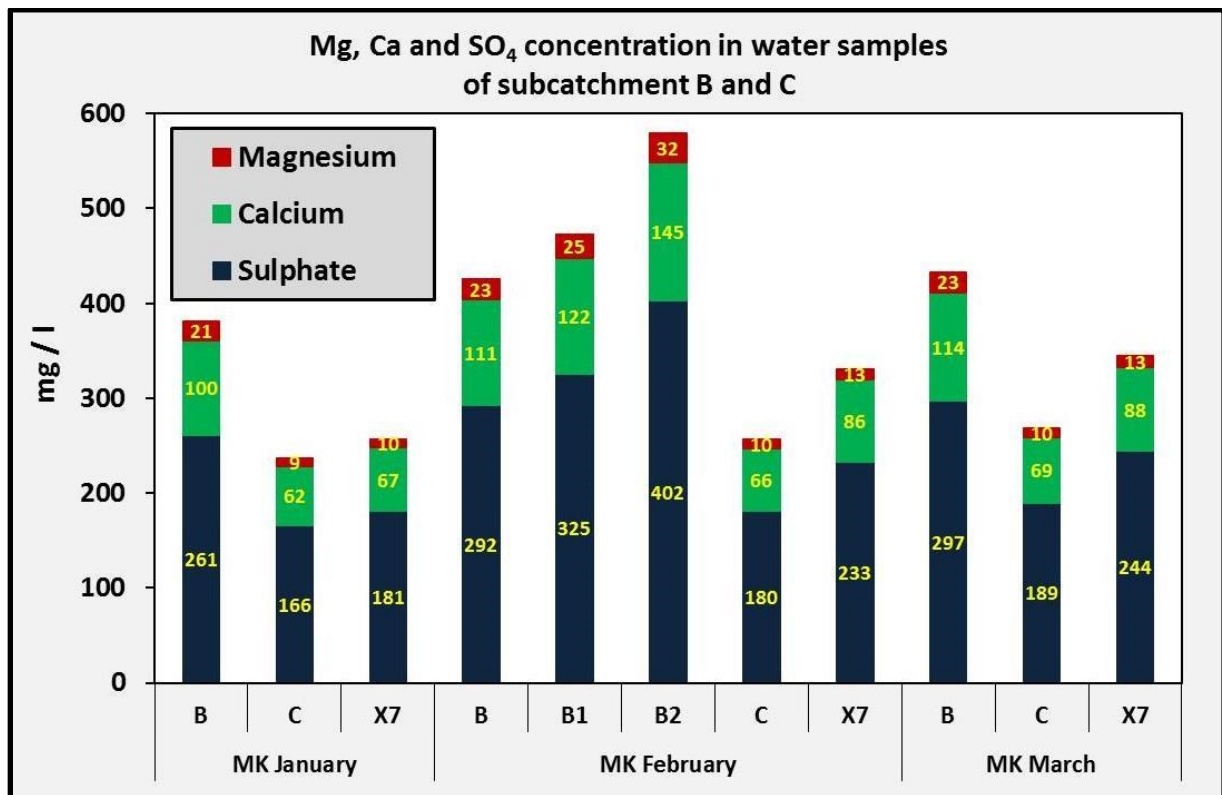


**Figure 46:** Total amount (mg/l) of Mg, Ca and SO<sub>4</sub> ions at sampling points in subcatchment B and C

Figure 46 shows the total amount of Mg, Ca and SO<sub>4</sub> ions in the subcatchments B and C. In both watersheds concentration increases upstream (see Figure 45 for location of the sampling points), confirming the significance of water from the sediment series sustaining baseflow during recession.

## 5.4 Additional results

### 5.4.1. Evaluation of influence of snowmelt

Hourly values of electric conductivity probes were used to evaluate the influence of snowmelt during the measurement period. Meltwater flowing into the creeks has a lower electric conductivity than water from the subsurface storages, therefore snowmelt results in decreasing electric conductivity measurable in the creek. In subcatchment A and in the lower parts of subcatchment D along the pass road, snowmelt is characterized by increasing electric conductivity, because the salt applied along the pass road leads to meltwater with a higher electrical conductivity than the baseline conductivity of the water in the creek (see chapter 5.4.2 for further explanation). After most of the salt is washed out into the river network, also in the parts along the pass road, meltwater leads to decreasing electric conductivity.

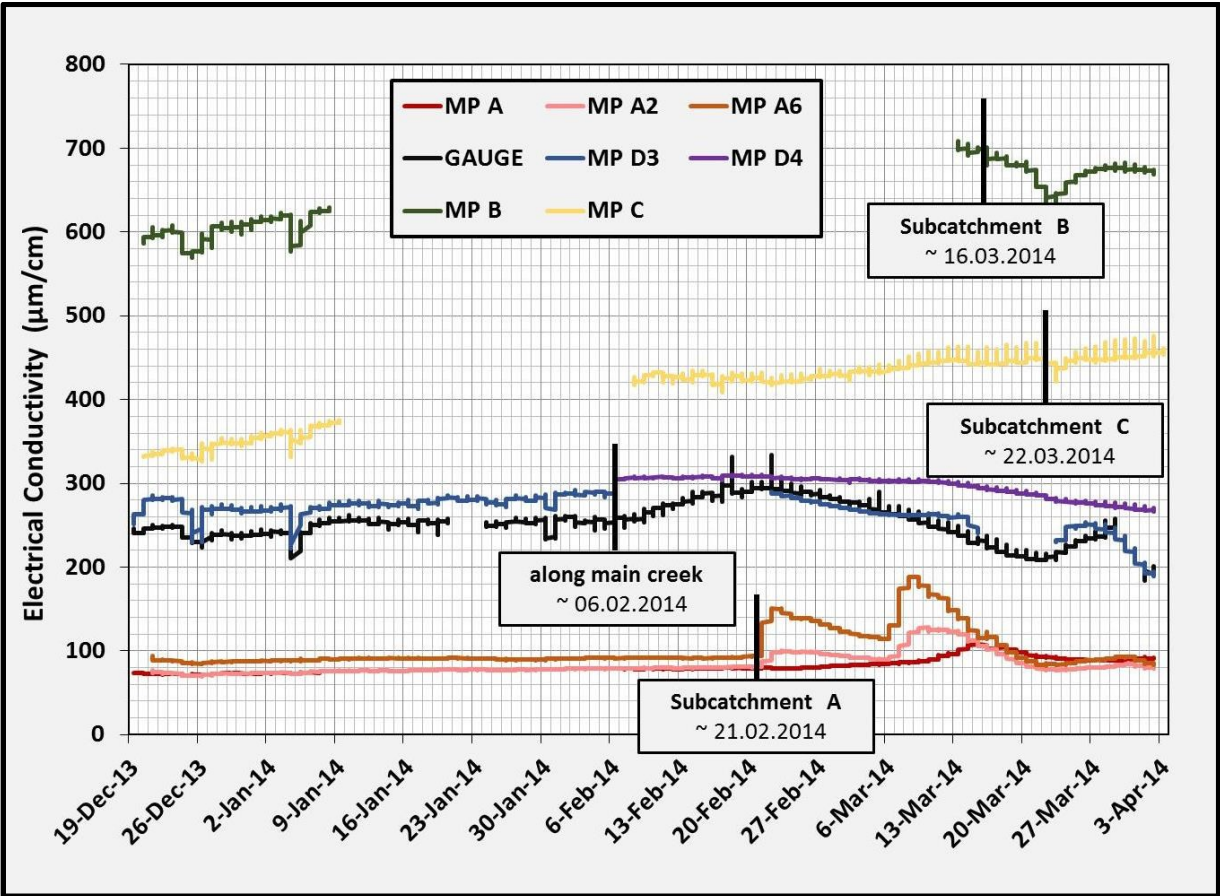


Figure 47: Evaluation of the electric conductivity probes for the main measurement points between 19 Dec until 03 April 14

To guarantee validity of calibration, probes were planned to be read out during every measurement campaign, but it was noticed that removing them from the water destroyed the calibration. Therefore many values had to be removed and the datasets produced have

---

high uncertainty. From the remaining data at least the point when major snowmelt insets could be identified. In some parts of the catchment also small melting events could be observed in some parts of the catchment (Figure 47).

Major influence of snowmelt could be seen in subcatchment A starting on 21 February. This event appears is well recorded by the three probes along the main creek with the same behavior. At the gauging station LaRösa and at the two measurement points along the main creek at low altitude (D4 - before merging with subcatchment A, D3 after merging with A) influence of snowmelt could be observed starting on 06 February (+ / - 2 days). In subcatchment C influence of meltwater in the creek can be observed starting on 22 March for three days. Afterwards electric conductivity increases again. Starting 8 March subcatchment C shows a higher day night variation of up to 40 $\mu$ S/cm, suggesting snowmelt during the day. Although discharge is still decreasing and electric conductivity is still increasing, day night variation has minor influence on the recession behavior. In subcatchment B removal of the probes for calibration led to major uncertainties, therefore a lot of values had to be removed. Snowmelt in subcatchment B is estimated to start on 16 March (+/-3 days).

Two periods of decreasing electric conductivity could be observed in subcatchments B, C and D. One around 26 December and another around 5 January, which could be assigned to two heavy snowfall events in the catchment. These snowfall events are not visible in the electric conductivity timeseries of subcatchment A, which is attributed to the low baseline conductivity in the creek. At MP D3 and the gauging station an additional snowfall event (around 31 January) was recorded (see Figure 47).

#### **5.4.2 Influence of the pass road on ion composition**

In this chapter the influence of the Bernina pass road in subcatchment A and along the lower parts of subcatchment D on ion composition is evaluated (see Figure 48). The drainage system of the street is speeding up the reaction of discharge during snowmelt due to direct inflow from the drainage system into the river network. During the measurement campaigns also influences on water chemistry could be observed.

According personal information from the company responsible for snow removal at the Bernina pass road (Fratelli Lanfranchi - <http://www.fratelli-lanfranchi.ch/>) mostly gravel split is used to prepare the lanes roadworthy due to the low air temperatures during winter months. In the winter season 2013 /14 about 15 tons of salt were applied between LaRösa and Passo di Bernina. With snowmelt, the salt is transported into the river network and can be measured in the water samples.

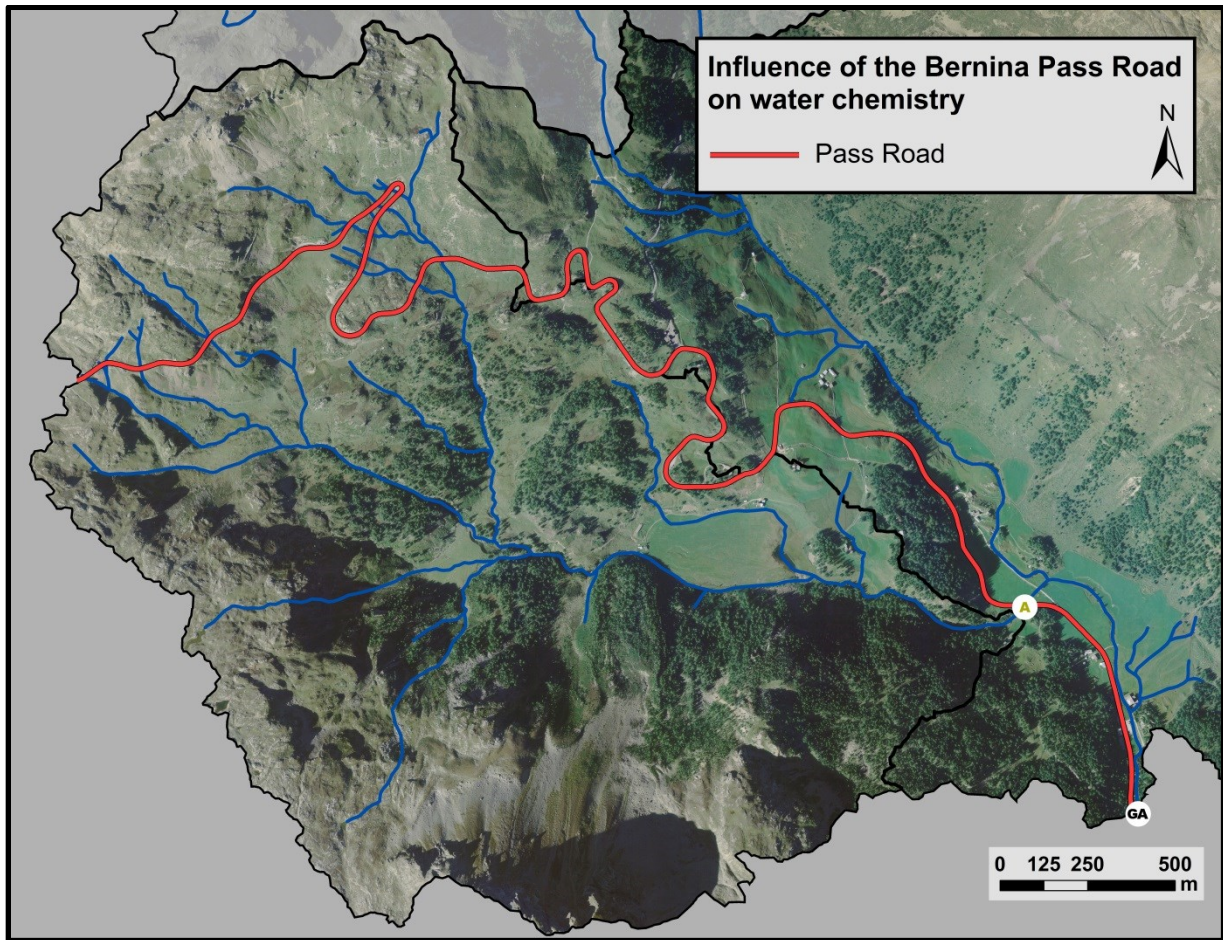


Figure 48: The Bernina Pass Road in the upper Poschiavino area

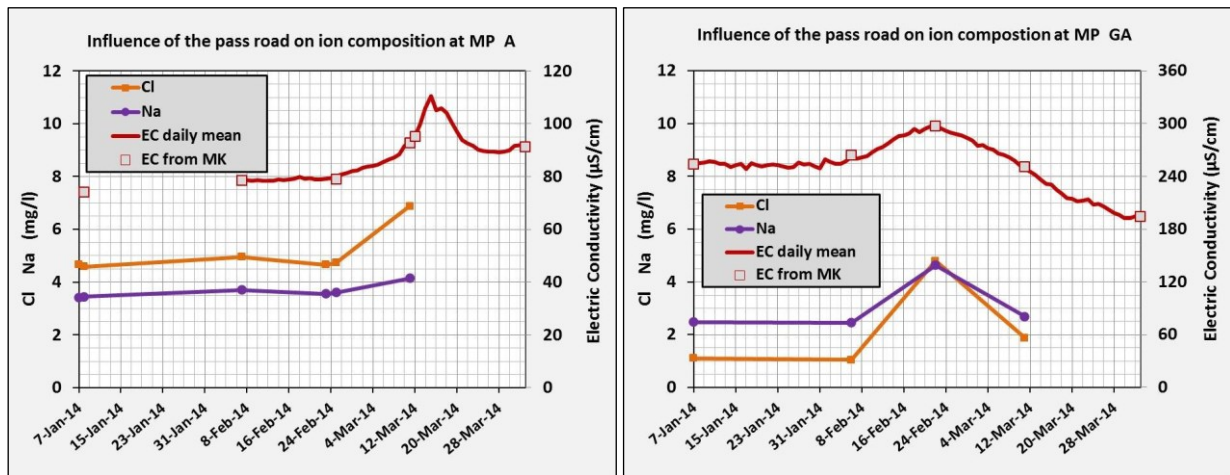


Figure 49: Variation of Na, Cl and EC during snowmelt at MP A and the gauging station

It is estimated that along the street snow is melting quicker than in parts with a continuous snow cover. With beginning snow melt first salty snow from along the road is transported into the river network leading to an increase in electric conductivity in the creeks. After the first flush of salty snow EC is decreasing due to the lower conductivity of meltwater.

---

Figure 49 shows the variation of Na, Cl and EC from 07 January to 2 April 14 for the sampling points MP A and at the gauging station: In subcatchment A an increase in electric conductivity could be observed between the measurement campaigns of 25 February and 17 March rising from 79  $\mu\text{S}/\text{cm}$  to 106  $\mu\text{S}/\text{cm}$ . Sodium concentration is rising by 0.5 mg/l, chloride concentration by 2 mg/l in this period. On 11 March a total amount of approximately 6.7 kg of Na and Cl were additionally added to the river network of subcatchment A in only one day.

At the gauging station influence could be measured earlier than in subcatchment A due to the lower altitude of the areas along the road. Increase in EC and the amount of Na and Cl ions could be observed between the MK of 7 February and 22 February. EC was rising from 264  $\mu\text{S}/\text{cm}$  to 297  $\mu\text{S}/\text{cm}$ , sodium concentration was rising by 2.2 mg/l, chloride concentration by 3.8 mg/l in this period. On 22 February a total amount of approximately 92 kg of Na and Cl were additionally added to the river network of the catchment.



---

## 6 Interpretation and discussion

### 6.1 Spatial variability in discharge during recession

Low flow recession proved to be highly variable within the research area. At subcatchment scale, variations from 54mm up to 194mm discharged in subcatchment A and D in the observation period were found. Different discharged volumes and variable recession behavior were assigned to different storage elements. Variety in discharge behavior during the winter season 2013/14 can be attributed to the mapped storage potential. Due to unfavorable conditions (9-10m of snow accumulation, air temperature up to -29°C) during the measurement campaigns, results have higher uncertainties. However the measurement errors were minimized by frequent calibration of the devices, detailed preparation of field campaigns and selection of appropriate observation sites in autumn.

As snowmelt during the winter months is small, storage refill was negligible, resulting in an undisturbed recession period. However minor contribution to the storages from snowmelt can not be totally excluded during the observation period: Heat fluxes from soil to snow cover may melt the snow from below. Especially in the swampy areas of subcatchment A a thinner snow cover could be observed, which suggests melting influence at least above soils actively converting organic matter during the winter months. Another point derived from observations was the influence of snow-free areas (e.g. along the pass road or along avalanche tracks of subcatchment D) which expanded due to melting of the surrounding areas happening also during periods with low temperatures due to influence of albedo. To evaluate these influences, electric conductivity probes were installed throughout the river network, because water from snowmelt would lead to decreasing electric conductivity. For subcatchment A, where the mentioned influences mainly occur, evaluation of electric conductivity did not show any interference of snowmelt.

The whole catchment was classified regarding geomorphological type, thickness and permeability. As main results the spatial distribution of storages contributing to low flow discharge could be derived and recession behavior could be assigned to the thickness of the contributing storages. Storage volume could be estimated within a certain range applying generalized assumptions on thickness and permeability. The suggested mapping methodology, based on existing data and field observations, could be applied in inaccessible terrain with modest outlay. As merely surface observations were done, main uncertainties derive from unknown subsurface flow paths and watersheds leading to unknown interactions between the single storages. However, small scale spatial variability of bedrock cracks and fractures can be neglected until a certain spatial scale of the research area. Heterogeneous storage properties can not be captured applying the developed

---

methodology. Observations were done in a mainly crystalline watershed, but have not been tried in other geological settings or within geological more heterogeneous alpine catchments.

Winter discharge observations at high altitude allowed obtaining recession curves for up to four months without interruption. This dataset helps understanding storage and drainage processes in alpine catchments during periods without storage refill. It was possible to obtain high spatial resolution information on the variability of contribution during low flow periods within a small catchment. With the developed mapping method the contributing storages can be identified, classified and an approximation of their volumes can be done.

## **6.2 Spatial scale issues**

Complex subsurface flow is leading to point source contributions often limiting the possible spatial scale of hydrological research. When trying to identify single storages on a small scale, computation of topographic catchment borders leads to uncertainties. All measuring points were chosen carefully in autumn after field observation, additionally considering high resolution data from different sources. When looking at catchment and subcatchment scale topographic borders could be derived with a high reliability. On smaller scale, when bounding the watersheds of nested subcatchments or single storages on topographic criteria uncertainties came up. The research area is characterized by thick deposits, therefore subsurface flow occurs. Additional influence of cracks and fractioned bedrock hides further uncertainties when trying to understand discharge and drainage behavior of the catchment. Due to the lack of information on subsurface flow processes, watersheds were derived based on surface topography. Variation in specific discharge between neighboring watersheds varied from 0 to 108 l/s km<sup>2</sup>. It indicates that research on storages is limited to a minimum scale on which research is possible; otherwise time-consuming tracer experiments would be necessary to define the accurate watershed of the different storages.

However the high resolution information on discharge and storage properties gathered for the project helped to assess rational catchment areas including the mentioned subsurface flow processes. This backward approach – from discharge behavior and storage properties to catchment area – could help resolving limiting scale issues in hydrological research, so catchment estimation would not only depend on tracer experiments.

---

### 6.3 Different storage types

A few methods were tried, separating different storage types regarding their contribution to low flow discharge: Water originating from sedimentary rocks could be identified using ion composition. Although no springs could be identified and diffuse inflow to the river network is dominant, contribution from Raibler series could be estimated by assuming full saturation of  $\text{SO}_4$  and Mg ions. Due to large differences in electric conductivity and variation of ion composition between water from crystalline geology and sedimentary rocks the applied quantification of the discharged volumes showed reliable results. Uncertainties derive from estimating full  $\text{SO}_4$  and Mg saturation of water from Raibler sediment series, however at least the minimum contribution from those layers can be calculated with the presented approach.

Contribution from the rockslide deposition area on the orographic left in the lower part of subcatchment C was quantified for one measurement campaign. The product of electric conductivity and discharge at the points above and below the rockslide area and electrical conductivity at a spring from the rockslide were used to calculate the discharge. Applying the presented calculations it could be shown that high winter discharge in subcatchment C does not come from the area where rockslide material is deposited. Due to massive snow accumulation during the winter the spring could first be detected in March and product equations could only be used for this measurement campaign, which is leaving a lot of uncertainties especially when extrapolating the derived results over the whole winter season.

---

## 7 Perspectives and summary

### 7.1 Perspectives

The collected data in the upper Poschiavino area give a good insight in complex storage mechanisms and the different drainage behavior of various catchment parts during low flow conditions. The observed hydrological behavior can be assigned to physical properties of the landscape, however these findings should be extended to other alpine watersheds in different geological settings and with diverse storage distribution. This would improve our knowledge on the complex interactions determining discharge behavior in high mountain areas.

The attained qualitative information on the storage and drainage mechanisms will be used to develop mathematical equations for a storage-based low flow model approach. A mapping methodology should be developed and validated in various alpine catchments. What are similarities and differences in storage composition and the drainage behavior during low flow conditions? The aim should be to explain discharge behavior by landscape properties that can be mapped, including available information and field investigations, as a fundamental for the model approach. The gathered information and additional investigation on discharge recession and water chemistry in various watersheds should be used to develop mathematical equations stating relations of storage and drainage interaction. The final outcome should be a storage-based model for low flow discharge in alpine watersheds.

The dataset of upper Poschiavino area shows a high variability in residence times within a small area. Although storages are relatively small, compared to lower altitude areas, water can be stored for long time periods, however yet no satisfactory approach for estimating this residence times could be found. By the means of knowledge on storage processes and the physical properties of these reservoirs more reliable statements on the residence times are possible.

A rough separation of different storage types can be done based on the dataset of electric conductivity and discharge calculating tracer balance. The approach can only be a first rough approximation on separation of discharge from different storages, however the dataset is an important base for further research on storage and drainage behavior of alpine catchments. Further attempts of storage quantification and separation could also improve flood prediction in alpine watersheds. It remains an open question to which extend storages responsible for sustaining baseflow during low flow conditions are also important retention features during flood events. Information on infiltration capacity of geomorphological properties, travel times and the drainage behavior is still little investigated, however further investigation of low flow recession enables to gather more reliable information.

Accuracy of winter discharge observations in high alpine regions during hostile conditions can be increased significantly when preparing for the observation campaigns regarding the

---

experiences of winter season 2013/14. This information can be used to find more accurate discharge measurement techniques on higher temporal and spatial resolution and improve observation of electric conductivity.

## 7.2 Summary

Even steep slopes can react damped to precipitation events and sustain baseflow significantly due to large storage volume. Not only storage, but also the time scale of drainage is important to understand recession dynamics. Winter months provide good opportunities to study flow recession in alpine catchments because there is little groundwater recharge from rainfall and snowmelt. Detailed field observation during the winter season 2013/14 helped understanding the complex hydrological interactions during low flow recession in upper Poschiavino area. Discharge was measured every three weeks at up to 58 measurement locations during recession. Additionally electrical conductivity and various ion composition were measured to identify different storages and the origin of the water. Sediment deposits were mapped regarding type, thickness and permeability, allowing a classification of storage potential throughout the catchment. The contribution from different storages regarding volume and drainage time could be estimated. Applying different approaches discharge from sedimentary rocks, a rockslide area and slow, medium and quick draining storages could be divided and their volumes were estimated.

Results were presented mainly based on four different subcatchments. These subcatchments have different storage potential due to different depth of sediment deposits, leading to different recession and drainage timescales. In the eastern part large storages could be identified, showing higher low flow and discharged water volume during the observation period (194mm in subcatchment D vs. 54mm in A discharged in 104 days). Drainage was quicker and the discharged volume was less in the western subcatchments (A and B). Point sources were limiting the spatial resolution of the hydrological research. The nested subcatchments show high variation in specific discharge, suggesting that topographic catchments do not coincide with the hydrological catchments. Subsurface flow and point source contribution are limiting the spatial resolution of the measurements, on the other hand high resolution information on discharge and storage properties could improve small scale catchment bordering. High electrical conductivity in subcatchments B and C could be traced back to sedimentary rocks covering about 7% of the catchment area. Estimating full saturation of  $SO_4$  and Mg ions contribution could be quantified. At least 14% of the total discharge of the catchment during recession derives from these sedimentary rocks. The contribution of a rockslide area could be estimated by product equations. Regarding the drainage time three storage types – quick, medium and slow – could be divided and an approximation of the volumes of these storage types was tried.

---

Low flow discharge in the crystalline upper Poschiavino area proved to be highly variable. This variability in recession and drainage behavior could be assigned to spatial distribution and depth of storages. Point sources, subsurface flow and the resulting uncertainties when deriving topographic catchment borders limit the spatial resolution of the investigations. Natural ion tracers and product equations of electric conductivity and discharge can be used to identify and separate contributions of different geological origin. The obtained results suggest that improved understanding of storage and drainage behavior of areas with large storage potential helps assessing catchment scale low flow problems.

---

## 8 References

**ASCHWANDEN, H. (1992).** Die Niedrigwasserabflussmenge Q347 - Bestimmung und Abschätzung in alpinen schweizerischen Einzugsgebieten (Bern).

**ASCHWANDEN, H., and KAN, C. (1999).** Die Abflussmenge Q347 - Eine Standortbestimmung (Eidgenössisches Department des Inneren, Landeshydrologie und -geologie).

**ASCHWANDEN, H., and WEINGARTNER, R. (1986).** Die Abflussregimes der Schweiz (Bern: Geographisches Institut der Universität Bern).

**BLUME, H.-P., BRÜMMER, G.W., HORN, R., KANDELER, E., KÖGEL-KNABNER, I., KRETZSCHMAR, R., STAHR, K., and WILKE, B.-M. (2010).** Scheffer/Schachtschabel: Lehrbuch der Bodenkunde. 16.Auflage;

**BOTTER, G., BERTUZZO, E., and RINALDO, A. (2011).** Catchment residence and travel time distributions: The master equation. *Geophysical Research Letters* 38, L11403.

**BOUSSINESQ, J. (1877).** Essai sur la theorie des eaux courantes du mouvement nonpermanent des eaux souterraines. *Acad. Sci. Inst. Fr.* 23, 252–260.

**BRUTSAERT, W. (2005).** Hydrology - An introduction (UK: Cambridge University Press).

**DAY, T.J. (1976).** On the precision of salt dilution gauging. *Journal of Hydrology* 31, 293–306.

**DAY, T.J. (1977).** Observed mixing lengths in mountain streams. *Journal of Hydrology* 35, 125–136.

**EUROGYPSUM (2010).** Fact sheet on: Gypsum and Water (Brussels: EUROGYPSUM - The voice of the european gypsum industry).

**FEDOTOVA, N., and GÜNTHER, D. (2013).** Ionenchromatographie (IC) - Bestimmung von Anionen in Wasser (Zürich: ETH Zürich).

**FLORIANCIC, M., SMOORENBURG, M., MARGRETH, M., and NAEF, F. (2014a).** Can we relate flood and low flow behavior to spatial distribution of thick quaternary deposits? Case study of the 14 km<sup>2</sup> alpine Poschiavino catchment, Switzerland. In AGU Chapman Conference, (Luxembourg City),.

**FLORIANCIC, M., SMOORENBURG, M., MARGRETH, M., and NAEF, F. (2014b).** Which hillslopes sustain baseflow during low flow conditions? Lessons from winter discharge observations in the alpine Poschiavino catchment,Switzerland. In *Geophysical Research Abstracts*, (Vienna),.

**JOHNSTON, R., and McCARTNEY, M. (2010).** Inventory of Water Storage Types in the Blue Nile and Volta River Basins (Colombo, Sri Lanka: International Water Management Institute).

- 
- KIENZLER, P.M., and NAEF, F. (2008).** Subsurface storm flow formation at different hillslopes and implications for the “old water paradox.” *Hydrol. Process.* 22, 104–116.
- KIRCHNER, J.W. (2006).** Getting the right answers for the right reasons: Linking measurements, analyses, and models to advance the science of hydrology. *Water Resources Research* 42, W03S04.
- KIRCHNER, J.W. (2009).** Catchments as simple dynamical systems: Catchment characterization, rainfall-runoff modeling, and doing hydrology backward. *Water Resour. Res.* 45, 34.
- KITE, G. (1989).** An extension to the salt dilution method of measuring streamflow. *International Journal of Water Resources Development* 5, 19–24.
- MAILLET, E. (1905).** *Essais d’hydraulique souterraine et fluviale.* Librairie Sci. 218.
- MARGRETH, M., NAEF, F., and SCHERRER, S. (2013).** Pilotstudie zur Anwendung von Abflussprozesskarten im Niedrigwasserbereich (Bern: Bundesamt für Umwelt (BAFU)).
- MENZEL, L., LANG, H., and ROHMANN, M. (1999).** Mittlere jährliche aktuelle Verdunstungshöhen 1973–1992.
- MOORE, R.D. (2004).** Introduction to salt dilution gauging for streamflow measurement. *Streamline - Watershed Management Bulletin* 7, 20–23.
- MOORE, R.D. (2005).** Slug Injection Using Salt in Solution. *Streamline - Watershed Management Bulletin* 8, 1–6.
- NAEF, M.H. (1987).** Ein Beitrag zur Stratigraphie der Trias-Serien im Unterostalpin Graubündens (Grisoniden). PhD Thesis. ETH Zürich.
- OUYANG, Y. (2012).** A potential approach for low flow selection in water resource supply and management. *Journal of Hydrology* 454–455, 56–63.
- PAVUNZA, R., and TRAINDL, H. (1983).** Über Dolomitkarst in Österreich. *Die Höhle* 34, 15–25.
- PFISTER, L., KLAUS, J., HISSLER, C., IFFLY, J.F., GOURDOL, L., MARTINEZ-CARRERAS, N., and McDONNELL, J.J. (2014).** A new perspective on catchment storage gained from a nested catchment experiment in Luxembourg (Europe). In *Geophysical Research Abstracts*, (EGU 2014),.
- PUSHPALATHA, R., PERRIN, C., LE MOINE, N., MATHEVET, T., and ANDREASSIAN, V. (2011).** A downward structural sensitivity analysis of hydrological models to improve low-flow simulation. *Journal of Hydrology* 411, 66–76.
- RANTZ, S.E. (1982).** Measurement and computation of streamflow: Volume 1 - Measurement of stage and discharge (Washington: USGS - U.S. Geological Survey).



---

**SAYAMA, T., MC DONNELL, J.J., DHAKAL, A., and SULLIVAN, K. (2011).** How much water can a watershed store? *Hydrological Processes* 25, 3899–3908.

**SCHERRER, S., and NAEF, F. (2003).** A decision scheme to indicate dominant hydrological flow processes on temperate grassland. *Hydrol. Process.* 17, 391–401.

**SCHERRER, S., NAEF, F., FAEH, A.O., and CORDERY, I. (2007).** Formation of runoff at the hillslope scale during intense precipitation. *Hydrol. Earth Syst. Sci.* 11, 907–922.

**SCHMOCKER-FACKEL, P., NAEF, F., and SCHERRER, S. (2007).** Identifying runoff processes on the plot and catchment scale. *Hydrol. Earth Syst. Sci.* 11, 891–906.

**SINGH, V.P., and FREVERT, D.K. (2002).** *Mathematical Models of Small Watershed Hydrology and Applications.*

**SMOORENBURG, M., VOLZE, N., MARGRETH, M., SCHERRER, S., and NAEF, F. (2013).** How do storage and drainage processes influence extreme floods in the Swiss Alps? In *Geophysical Research Abstracts*, (Vienna: EGU 2013),.

**SUMMERFIELD, M.A. (1987).** Neotectonics and landform genesis. *Progress in Physical Geography* 11, 384–397.

**TALLAKSEN, L.M. (1995).** A review of baseflow recession analysis. *Journal of Hydrology* 165, 349–370.

**TURNIPSEED, P., and SAUER, V. (2010).** *Discharge Measurements at Gaging Stations* (Virginia: USGS - U.S. Geological Survey).

**UHLENBROOK, S., FREY, M., LEIBUNDGUT, C., and MALOSZEWSKI, P. (2002).** Hydrograph separations in a mesoscale mountainous basin at event and seasonal timescales. *Water Resources Research* 38, 31–1.

**WEILER, M., and NAEF, F. (2003).** An experimental tracer study of the role of macropores in infiltration in grassland soils. *Hydrol. Process.* 17, 477–493.

**WOOD, P. and DYKES, A. (2002).** The use of salt dilution gauging techniques: ecological considerations and insights. *Water Research* 36, 3054–3062.

---

**Online references:** (last access 21.10.2014)

<http://map.geo.admin.ch>

<http://www.hydrodaten.admin.ch/de/>

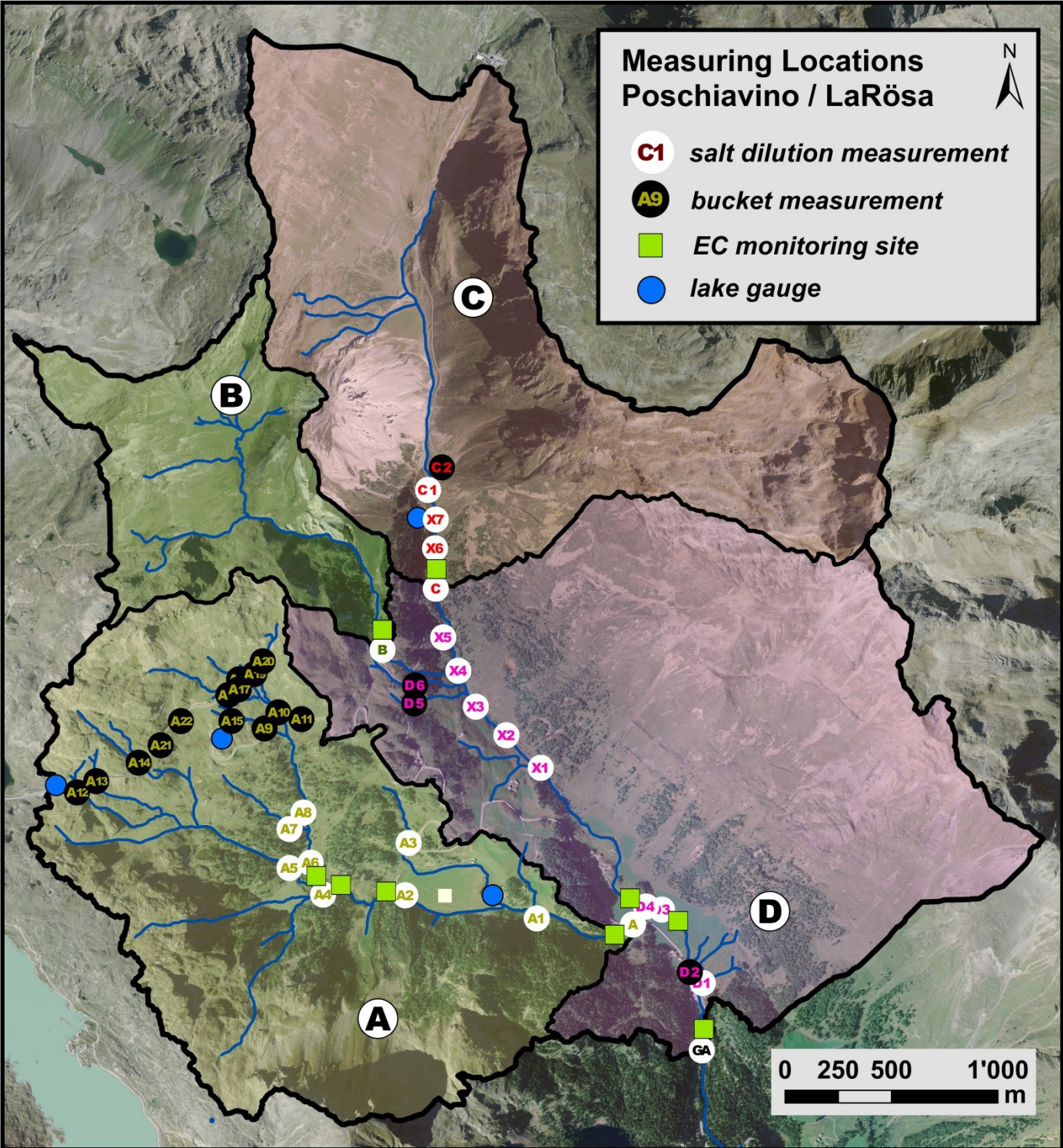
<http://www.meteosuisse.admin.ch/>

<http://www.fratelli-lanfranchi.ch/>

<http://www.swisstopo.admin.ch/internet/swisstopo/de/home/products/maps/geology/accessories.html>

# 9 Appendix

## Measurement Locations



### Measuring Point A\_1a

X (GIS) 801313  
 Y (GIS) 142670  
 Altitude (m) (GIS) 1930  
 Catchment (km<sup>2</sup>) 3.7  
 Method SALT  
 Description TEZG A after Campasc  
 before side torrent



Method	SD	SD	SD
Date	12.11.2013	26.11.2013	21.12.2013
I / s	175.8	48.4	20.3
Conductivity	61.2	71.9	73.1
Temperature	1.9	0.3	1.9
I / km <sup>2</sup>	47.1	13.0	5.4

### Measuring Point A\_1b

X (GIS) 801313  
 Y (GIS) 142670  
 Altitude (m) (GIS) 1930  
 Method SALT  
 Description TEZG A after Campasc  
 after side torrent



Method	SD
Date	26.11.2013
I / s	49.9
Conductivity	70.8
Temperature	0.1

### Measuring Point A\_2

X (GIS) 800622  
 Y (GIS) 142760  
 Altitude (m) (GIS) 1960  
 Catchment (km<sup>2</sup>) 3.0  
 Method SALT  
 LF Sonde A2  
 Description TEZG A before Campasc



Method	SD	SD
Date	27.11.2013	21.12.2013
I / s	21.3	10.8
Conductivity	67.2	74.3
Temperature	0.0	1.1
I / km <sup>2</sup>	7.2	3.6

**Measuring Point U\_PEG**

X (GIS) 802127  
 Y (GIS) 141706  
 Catchment (km<sup>2</sup>) 15.2  
 Method SALT  
 Description at street below gauging station



Method	SD
Date	12.03.2014
l / s	183.3
Conductivity	251
Temperature	
l / km <sup>2</sup>	12.0

**Measuring Point - GAUGING STATION**

X (GIS) 807295  
 Y (GIS) 158534  
 Altitude (m) (GIS) 1810.8  
 Catchment (km<sup>2</sup>) 14.44  
 Method SALT  
 LF Sonde PEGEL  
 Description Gauging Station Poschiavino / La Rōsa



Method	SD	SD	SD	SD	SD	SD	SD	SD	SD
Date	09.11.2013	12.11.2013	25.11.2013	19.12.2013	07.01.2014	06.02.2014	22.02.2014	11.03.2014	02.04.2014
l / s	1266.6	736.9	391.5	255.0	231.7	181.9	177.1	183.6	345.9
Conductivity	160.3	236	270	244	254	264	306	251	194.2
Temperature	3.4	2.4	0.4	1.6	1.9	1.1	1.1	3.5	4.5
l / km <sup>2</sup>	87.7	51.0	27.1	17.7	16.0	12.6	12.3	12.7	24.0

**Measuring Point A**

X (GIS) 801774  
 Y (GIS) 142589  
 Altitude (m) (GIS) 1890  
 Catchment (km<sup>2</sup>) 4.04  
 Method SALT  
 LF Sonde A  
 Description TEZG A before junction with Poschiavino



Method	SD	SD	SD	SD	SD	SD	SD	SD	SD
Date	01.11.2013	12.11.2013	25.11.2013	19.12.2013	08.01.2014	07.02.2014	25.02.2014	11.03.2014	02.04.2014
l / s	310.5	187.3	56.1	22.9	19.0	19.9	14.5	31.0	97.5
Conductivity	59.7	60.8	68.9	73.8	74.2	78.6	79.0	92.7	91.2
Temperature	5.1	1.8	1.4	0.9	1.1	0.6	0.9	1.5	1.7
l / km <sup>2</sup>	76.9	46.3	13.9	5.7	4.7	4.9	3.6	7.7	24.1

### Measuring Point A\_1a

X (GIS) 801313  
Y (GIS) 142670  
Altitude (m) (GIS) 1930  
Catchment (km<sup>2</sup>) 3.7  
Method SALT  
Description TEZG A after Campasc  
before side torrent



Method	SD	SD	SD
Date	12.11.2013	26.11.2013	21.12.2013
I / s	175.8	48.4	20.3
Conductivity	61.2	71.9	73.1
Temperature	1.9	0.3	1.9
I / km <sup>2</sup>	47.1	13.0	5.4

### Measuring Point A\_1b

X (GIS) 801313  
Y (GIS) 142670  
Altitude (m) (GIS) 1930  
Method SALT  
Description TEZG A after Campasc  
after side torrent



Method	SD
Date	26.11.2013
I / s	49.9
Conductivity	70.8
Temperature	0.1

### Measuring Point A\_2

X (GIS) 800622  
Y (GIS) 142760  
Altitude (m) (GIS) 1960  
Catchment (km<sup>2</sup>) 3.0  
Method SALT  
LF Sonde A2  
Description TEZG A before Campasc



Method	SD	SD
Date	27.11.2013	21.12.2013
I / s	21.3	10.8
Conductivity	67.2	74.3
Temperature	0.0	1.1
I / km <sup>2</sup>	7.2	3.6

### Measuring Point A\_3

X (GIS) 800748  
Y (GIS) 143049  
Altitude (m) (GIS) 2000  
Catchment (km<sup>2</sup>) 0.19  
Method SALT  
Description TEZG A next to street / conveyor Campasc



Method	SD	SD
Date	27.11.2013	20.12.2013
I / s	2.0	0.9
Conductivity	96.6	88.2
Temperature	0.1	0.6
I / km <sup>2</sup>	10.4	4.9

### Measuring Point A\_4a

X (GIS) 800197  
Y (GIS) 143428  
Altitude (m) (GIS) 2130  
Catchment (km<sup>2</sup>) 0.69  
Method SALT  
Description



Method	SD	SD
Date	26.11.2013	21.12.2013
I / s	9.1	3.2
Conductivity	38.3	41.1
Temperature	2.3	3.0
I / km <sup>2</sup>	0.6	0.2

### Measuring Point A\_4b

X (GIS) 800197  
Y (GIS) 143428  
Altitude (m) (GIS) 2130  
Catchment (km<sup>2</sup>) 1.7  
Method SALT  
LF Sonde A5 II  
Description



Method	SD	SD
Date	26.11.2013	21.12.2013
I / s	22.4	7.5
Conductivity	80.3	87.5
Temperature	0.3	1.5
I / km <sup>2</sup>	13.6	4.6

### Measuring Point A\_5

X (GIS) 800370  
 Y (GIS) 142755  
 Altitude (m) (GIS) 2020  
 Catchment (km<sup>2</sup>) 1.0  
 Method SALT  
 Description



Method	SD	SD	SD
Date	12.11.2013	26.11.2013	21.12.2013
l / s	34.6	8.8	2.5
Conductivity	69.9	68.5	94.6
Temperature	1.0	0.1	0.5
l / km <sup>2</sup>	34.0	8.6	2.4

### Measuring Point A\_6

X (GIS) 800377  
 Y (GIS) 142778  
 Altitude (m) (GIS) 2020  
 Catchment (km<sup>2</sup>) 0.62  
 Method SALT  
 LF Sonde A6  
 Description



Method	SD	SD	SD
Date	12.11.2013	26.11.2013	21.12.2013
l / s	41.2	8.8	2.7
Conductivity	69.7	78.9	92.7
Temperature	1.4	0.3	0.2
l / km <sup>2</sup>	66.4	14.2	4.3

### Measuring Point A\_7

X (GIS) 800248  
 Y (GIS) 142808  
 Altitude (m) (GIS) 2050  
 Catchment (km<sup>2</sup>) 0.13  
 Method SALT  
 Description



Method	CAL	SD
Date	12.11.2013	26.11.2013
l / s	18.9	1.7
Conductivity		97.7
Temperature		0.3
l / km <sup>2</sup>	145.5	12.8



### Measuring Point A\_8

X (GIS) 800291  
 Y (GIS) 142845  
 Altitude (m) (GIS) 2050  
 Catchment (km<sup>2</sup>) 0.49  
 Method SALT  
 Description



Method	SD	SD
Date	12.11.2013	26.11.2013
l / s	22.3	6.4
Conductivity	71.1	79.4
Temperature	1.4	0.1
l / km <sup>2</sup>	45.4	13.1

### Measuring Point A\_9a

X (GIS) 800061  
 Y (GIS) 143533  
 Altitude (m) (GIS) 2160  
 Catchment (km<sup>2</sup>) 0.03  
 Method BUCKET  
 Description small catchment from swamp



Method	BUCKET (old)	BU new	BU new
Date	11.11.2013	27.11.2013	20.12.2013
l / s	4.5	0.6	0.1
Conductivity	-	90.0	104.2
Temperature	-	0.8	0.5
l / m <sup>2</sup>	150.0	20.3	3.3

### Measuring Point A\_9b

X (GIS) 800061  
 Y (GIS) 143533  
 Altitude (m) (GIS) 2160  
 Method BUCKET  
 Description small sub catchment side torrent - oro left from KL / HS



Method	ESTIMATION	BU new	BU new
Date	09.11.2013	27.11.2013	20.12.2013
l / s	2.0	< 0.01	no Q
Conductivity	17.5	-	-
Temperature	3.8	-	-

**Measuring Point A\_10a**

X (GIS) 800133  
 Y (GIS) 143601  
 Altitude (m) (GIS) 2160  
 Catchment (km<sup>2</sup>) 0.45  
 Method BUCKET  
 Description Main torrent A15-A20



Method	ESTIMATION	ESTIMATION	BU big	BU big	BU big
Date	01.11.2013	08.11.2013	27.11.2013	20.12.2013	08.01.2014
l / s	15.0	10.0	4.1	1.3	1.2
Conductivity	39.4	46.5	64.9	78.7	82.3
Temperature	6.5	2.9	0.4	0.5	1.0
l / km <sup>2</sup>	33.3	22.2	9.0	3.0	2.7

**Measuring Point A\_10b**

X (GIS) 800087  
 Y (GIS) 143599  
 Altitude (m) (GIS) 2160  
 Method BUCKET  
 Description Drainage between A9a - A10a



Method	BU small	BU small
Date	08.11.2013	27.11.2013
l / s	1.0	no Q
Conductivity	24.9	-
Temperature	3.5	-

**Measuring Point A\_11a**

X (GIS) 800176  
 Y (GIS) 143607  
 Altitude (m) (GIS) 2160  
 Method BUCKET  
 Description Side torrent from HS above the street I



Method	BUCKET (old)	BU NaCl	BU NaCl	BU NaCl
Date	11.11.2013	27.11.2013	20.12.2013	08.01.2014
l / s	1.5	0.1	< 0.01	no Q
Conductivity	15.2	18.0	-	-
Temperature	3.0	1.2	-	-

**Measuring Point A\_11b**

X (GIS) 800176  
 Y (GIS) 143607  
 Altitude (m) (GIS) 2160  
 Method BUCKET  
 Description Side torrent from HS above the street II



Method	BU new	BU NaCl	BU NaCl
Date	27.11.2013	20.12.2013	08.01.2014
I / s	0.09	0.03	no Q
Conductivity	31.4	37.3	-
Temperature	3.4	2.3	-

**Measuring Point A\_12a**

X (GIS) 799173  
 Y (GIS) 143323  
 Altitude (m) (GIS) 1885  
 Method BUCKET  
 Description TEZG A 12 / torrent in HS  
 outflow of small lakes + small catchment



Method	BUCKET (old)
Date	08.11.2013
I / s	no Q
Conductivity	-
Temperature	-

**Measuring Point A\_12b**

X (GIS) 799173  
 Y (GIS) 143323  
 Altitude (m) (GIS) 1885  
 Method BUCKET  
 Description TEZG A 12 / torrent in HS  
 NR 272



Method	BUCKET (old)	BU new
Date	08.11.2013	24.11.2013
I / s	0.2	no Q
Conductivity	39.1	-
Temperature	3.4	-

**Measuring Point A\_13a**

X (GIS) 799173  
 Y (GIS) 143323  
 Altitude (m) (GIS) 1885

Method SALT  
 Description torrents from HS / KL  
 Schacht - NR 271



Method Date	BUCKET (old) 08.11.2013	BU small 24.11.2013	BU NaCl 18.12.2013	BU NaCl 06.01.2014
I / s	0.9	0.09	0.01	no Q
Conductivity	94.8	57.8	102.5	-
Temperature	3.0	2.0	1.2	-

**Measuring Point A\_13b**

X (GIS) 799173  
 Y (GIS) 143323  
 Altitude (m) (GIS) 1885

Method SALT  
 Description torrents from HS / KL



Method Date	BU small 24.11.2013	BU new 18.12.2013	BU NaCl 06.01.2014
I / s	0.14	0.06	no Q
Conductivity	61.5	61.5	-
Temperature	2.3	2.6	-

**Measuring Point A\_14**

X (GIS) 799466  
 Y (GIS) 143376  
 Altitude (m) (GIS) 2300  
 Catchment (km<sup>2</sup>) 0.1  
 Method BUCKET  
 Description beneath junction of EZG A14  
 2 torrents (a + b) NR 265



(a) oro left Date	COND 24.11.2013	BU NaCl 18.12.2013
I / s	-	0.06
Conductivity	43.5	42.0
(b) oro right Date	COND 24.11.2013	COND 18.12.2013
I / s	not pos.	not pos.
Conductivity	-	-
TOTAL MP A14 Date	BU med 24.11.2013	BU med 18.12.2013
I / s	0.47	not pos.
Conductivity	49.8	-

**Measuring Point A\_15a**

X (GIS) 799911  
 Y (GIS) 143609  
 Altitude (m) (GIS) 2200  
 Method BUCKET  
 Description small torrent from HS and KL



Method Date	BU NaCl	BU NaCl
	24.11.2013	18.12.2013
I / s	0.53	no Q
Conductivity	79.9	-
Temperature	0.2	-

**Measuring Point A\_15b**

X (GIS) 799883  
 Y (GIS) 143537  
 Altitude (m) (GIS) 2200  
 Method BUCKET  
 Description small drainage from HS and KL



Method Date	BU NaCl
	18.12.2013
I / s	< 0.01
Conductivity	133.5
Temperature	3.0

**Measuring Point A\_16a**

X (GIS) 799869  
 Y (GIS) 143702  
 Altitude (m) (GIS) 2240  
 Method BUCKET  
 Description creek A16 - upper part



Method Date	ESTIMATION	ESTIMATION	BU med
	01.11.2013	08.11.2013	24.11.2013
I / s	7.5	5.0	no Q
Conductivity	30.0	29.6	-
Temperature	5.9	3.4	-

**Measuring Point A\_16b**

X (GIS) 799928  
 Y (GIS) 143675  
 Altitude (m) (GIS) 2220

Method Description BUCKET  
 creek A16 - lower part



Method Date	ESTIMATION 08.11.2013	BU med 24.11.2013	BU med 18.12.2013
l / s	10.0	2.0	0.4
Conductivity	42.3	47.4	58.2
Temperature	3.3	0.3	1.6

**Measuring Point A\_17**

X (GIS) 799944  
 Y (GIS) 143714  
 Altitude (m) (GIS) 2240

Method Description BUCKET  
 Spring of HS and KL



Method Date	BUCKET (old) 08.11.2013	BU med 24.11.2013	BU new 18.12.2013
l / s	0.3	0.17	0.13
Conductivity	192.1	163.6	132.0
Temperature	5.4	0.7	2.8

**Measuring Point A\_18a**

X (GIS) 799943  
 Y (GIS) 143765  
 Altitude (m) (GIS) 2250

Method Description BUCKET  
 creek 18 - upper part



Method Date	BUCKET (old) 01.11.2013	BUCKET (old) 08.11.2013	BU med 24.11.2013	BU med 18.12.2013
l / s	5.50	5.00	1.24	0.18
Conductivity	30.0	32.0	33.9	35.8
Temperature	7.0	3.8	0.7	1.2

**Measuring Point A\_18b**

X (GIS) 799967  
 Y (GIS) 143748  
 Altitude (m) (GIS) 2240

Method BUCKET  
 Description creek 18 - lower part



Method	EC	BU NaCl (GRAV)
Date	08.11.2013	18.12.2013
l / s	-	0.37
Conductivity	45.0	44.0
Temperature	3.1	-

**Measuring Point A\_19**

X (GIS) 799975  
 Y (GIS) 143801  
 Altitude (m) (GIS) 2230

Method BUCKET  
 Description



Method	EC	BU new	BU NaCl
Date	08.11.2013	27.11.2013	20.12.2013
l / s	-	0.24	0.19
Conductivity	56.6	47.4	54.6
Temperature	4.9	1.5	1.8

**Measuring Point A\_20**

X (GIS) 800045  
 Y (GIS) 143799  
 Altitude (m) (GIS) 2220

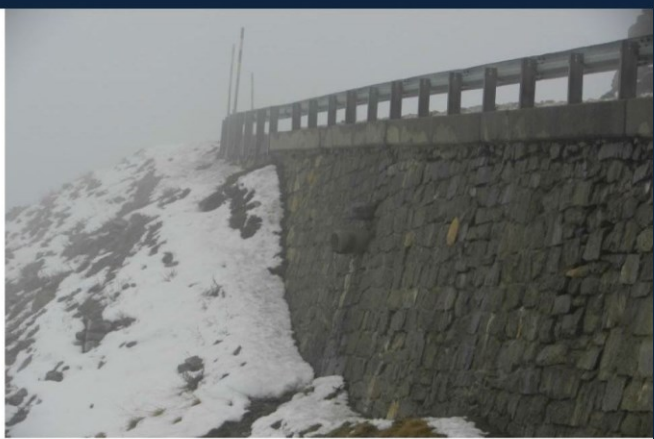
Method SALT  
 Description Torrent 20



Method	ESTIMATION	SALT
Date	07.11.2013	20.12.2013
l / s	2.0	no Q
Conductivity	18.7	-
Temperature	2.7	-

**Measuring Points A\_21a**

X (GIS) 799703  
Y (GIS) 143608  
Altitude (m) (GIS) 2260  
Method BUCKET  
Description Drainages between A14 and A16



Method BU small  
Date 24.11.2013

I / s no Q  
Conductivity -  
Temperature -

**Measuring Points A\_21b**

X (GIS) 799703  
Y (GIS) 143608  
Altitude (m) (GIS) 2260  
Method BUCKET  
Description Drainages between A14 and A16



Method BU NaCl BU small  
Date 24.11.2013 18.12.2013

I / s 0.02 no Q  
Conductivity 114.5 -  
Temperature 2.3 -

**Measuring Points A\_22a**

X (GIS) 799703  
Y (GIS) 143608  
Altitude (m) (GIS) 2260  
Method BUCKET  
Description Drainages between A14 and A16



Method BU NaCl  
Date 24.11.2013

I / s no Q  
Conductivity -  
Temperature -



**Measuring Points A\_22a**

X (GIS) 799703  
 Y (GIS) 143608  
 Altitude (m) (GIS) 2260  
 Method BUCKET  
 Description Drainages between A14 and A16



Method	BU NaCl
Date	24.11.2013
I / s	no Q
Conductivity	-
Temperature	-

**Measuring Points A\_22b**

X (GIS) 799703  
 Y (GIS) 143608  
 Altitude (m) (GIS) 2260  
 Method BUCKET  
 Description Drainages between A14 and A16



Method	BU NaCl	BU small
Date	24.11.2013	18.12.2013
I / s	0.26	no Q
Conductivity	39.3	-
Temperature	4.6	-

**Measuring Point B**

X (GIS) 800681  
 Y (GIS) 143844  
 Altitude (m) (GIS) 2190  
 Catchment (km<sup>2</sup>) 1.4  
 Method SALT  
 LF Sonde B3  
 Description Main torrent TEZG B



Method	SD	SD	SD	SD	CAL	SD	SD	SD
Date	12.11.2013	27.11.2013	20.12.2013	08.01.2014	06.02.2014	23.02.2014	13.03.2014	03.04.2014
I / s	71.6	25.3	17.1	14.7	13.4	12.7	11.9	16.9
Conductivity	290	494	588	629		697	708	669
Temperature	3.0	-	2.3	2.5		2.3	2.5	2.6
I / km <sup>2</sup>	5.0	1.8	1.2	1.0	9.6	0.9	0.8	1.2

### Measuring Point C

X (GIS) 800971  
 Y (GIS) 143777  
 Altitude (m) (GIS) 1980  
 Catchment (km<sup>2</sup>) 3.9  
 Method SALT  
 LF Sonde B4  
 Description Poschiavino at beginning of gorch



Method	SD	SD	SD	SD	SD	SD	SD
Date	25.11.2013	20.12.2013	09.01.2014	06.02.2014	24.02.2014	13.03.2014	03.04.2014
l / s	165.9	103.3	79.1	58.5	50.8	43.5	45.3
Conductivity	408	332	376	417	430	449	461
Temperature	1.1	2.3	3.1	2.3	3.0	3.4	3.3
l / km <sup>2</sup>	11.5	7.2	5.5	4.1	3.5	3.0	3.1

### Measuring Point C\_1a

X 800838  
 Y 144675  
 Altitude (m) 2080  
 Catchment (km<sup>2</sup>) 2.6  
 Method SALT  
 Description Main torrent TEZG C / Bridge Forcola di Livigno



Method	SD	SD	SD
Date	12.11.2013	25.11.2013	20.12.2013
l / s	107.3	57.1	50.4
Conductivity	612	677	452
Temperature	3.7	2.1	2.7
l / km <sup>2</sup>	7.4	4.0	3.5

### Measuring Point C\_1b

X 800838  
 Y 144675  
 Altitude (m) 2080  
 Method BUCKET  
 Description Spring out of tube - right of street



Method	BUCKET (old)	BU NaCl	BU NaCl
Date	01.11.2013	25.11.2013	20.12.2013
l / s	1.6	1.4	0.00
Conductivity	270	182.1	-
Temperature	3.5	3.1	-

### Measuring Point C\_2a

X 800838  
 Y 144675  
 Altitude (m) 2080  
 Method BUCKET  
 Description Outflow - under Livigno street



Method	BU NaCl	BU NaCl
Date	25.11.2013	20.12.2013
I / s	2.9	no Q
Conductivity	181.5	-
Temperature	1.0	-

### Measuring Point C\_2b

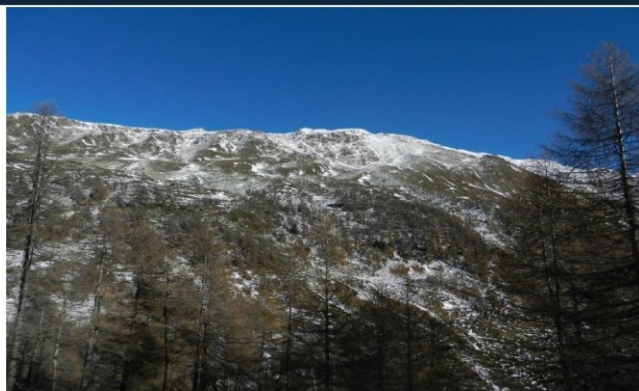
X 800838  
 Y 144675  
 Altitude (m) 2080  
 Method ESTIMATION  
 Description Springs - under Livigno street



Method	ESTIMATION	ESTIMATION	ESTIMATION
Date	01.11.2013	12.11.2013	25.11.2013
I / s	5	6	not pos
Conductivity	240	180	-
Temperature	3.5	4.0	-

### Discharge Catchment D

Catchment (km<sup>2</sup>) 5.1  
 Method CALCULATION A  
 Description PEGEL - (MP\_A + MP\_B + MP\_C)  
 Method CALCULATION B  
 Description D3 - (MP\_A + MP\_B + MP\_C) + D1 + D2



Method	CAL_A	CAL_A	CAL_A	CAL_A	CAL_A	CAL_A	CAL_A
Date	24.11.2013	20.12.2013	08.01.2014	06.02.2014	24.02.2014	12.03.2014	03.04.2014
I / s	144.1	111.8	118.9	90.1	99.1	97.2	186.3
I / km <sup>2</sup>	10.0	7.7	8.2	6.2	6.9	6.7	12.9
Method	CAL_B	CAL_B	CAL_B	CAL_B	CAL_B	CAL_B	CAL_B
Date	24.11.2013	20.12.2013	08.01.2014	06.02.2014	24.02.2014	12.03.2014	
I / s	116.2	85.7	88.8	71.4	72.2	63.4	
I / km <sup>2</sup>	8.1	5.9	6.2	4.9	5.0	4.4	

**Measuring Point D\_1**

X (GIS) 800971  
 Y (GIS) 143777  
 Altitude (m) (GIS) 1980  
 Method Description SALT  
 small torrent under Chalet Post



Method Date	SD 25.11.2013	SD 19.12.2013	SD 09.01.2014	SD 07.02.2014	SD 22.02.2014	SD 11.03.2014
l / s	10.6	7.6	6.5	6.1	5.8	5.5
Conductivity	119.0	126.2	130.2	173.3	138.0	140.0
Temperature	2.1	3.7	3.8	3.5	3.4	3.6

**Measuring Point D\_2a**

X 800838  
 Y 144675  
 Altitude (m) 2080  
 Method Description Bucket gravimetric  
 small tube / under Chalet Post



Method Date	BU med 25.11.2013	BU med (GRAV) 19.12.2013	BU med (GRAV) 07.01.2014	BU med (GRAV) 22.02.2014	BU med (GRAV) 11.03.2014
l / s	6.2	6.2	6.1	5.0	4.5
Conductivity	166.0	169.8	170.4	174.0	179.4
Temperature	5.2	4.2	2.4	3.2	4.5

**Measuring Point D\_2b**

X 800838  
 Y 144675  
 Altitude (m) 2080  
 Method Description Bucket gravimetric  
 big tube / under Chalet Post



Method Date	BU med 25.11.2013	BU big (GRAV) 19.12.2013	BU med (GRAV) 07.01.2014	BU med (GRAV) 22.02.2014	BU med (GRAV) 11.03.2014
l / s	11.8	11.4	10.2	8.2	8.0
Conductivity	163.0	170.2	169.0	172.0	175.5
Temperature	2.9	3.2	2.4	3.1	3.6

**D\_1\_2 (D1 + D2a + D2b)**

X (GIS) 800971  
 Y (GIS) 143777  
 Altitude (m) (GIS) 1980  
 Catchment (km<sup>2</sup>) 0.93  
 Method SALT  
 Description C1 + C2a + C2b



Method Date	CAL 25.11.2013	CAL 19.12.2013	CAL 09.01.2014	CAL 22.02.2014	CAL 11.03.2014
I / s	28.6	25.2	22.8	18.9	17.9
Conductivity	147.4	156.9	158.4	162.1	165.6
I / km <sup>2</sup>	30.7	27.1	24.5	20.3	19.3

**Measuring Point D\_3**

X (GIS) 801849  
 Y (GIS) 142707  
 Altitude (m) (GIS) 1885  
 Catchment (km<sup>2</sup>) 12.4  
 Method SALT  
 LF Sonde AB  
 Description MP A and B after confluence

D\_3 is calculated by:  
 (measured value D\_3 + (measured value A + measured value D\_4))/2



Method Date	CAL 24.11.2013	SD 19.12.2013	SD 07.01.2014	SD 06.02.2014	SD 22.02.2014	SD 11.03.2014	SD 02.04.2014
Measurement	-	183.6	173.1	135.6	131.2	157.5	281.0
MP A + MP D4	356.8	217.9	183.9	149.6	137.0	149.9	257.3
I / s	356.8	200.7	178.5	142.6	134.1	153.7	269.2
Conductivity		257	271	286	290	264	194.9
Temperature		1.6	2.1	1.4	1.3	2.4	3.1
I / km <sup>2</sup>	24.7	13.9	12.4	9.9	9.3	10.6	18.6

**Measuring Point D\_4**

X (GIS) 801849  
 Y (GIS) 142707  
 Altitude (m) (GIS) 1885  
 Catchment (km<sup>2</sup>) 8.3  
 Method SALT  
 LF Sonde B  
 Description TEZG B C and D / before junction with Berninabach



Method Date	SD 12.11.2013	SD 25.11.2013	SD 19.12.2013	SD 08.01.2014	SD 06.02.2014	SD 22.02.2014	SD 25.02.2014	SD 11.03.2014	SD 02.04.2014
I / s	454.2	300.7	195.0	164.9	129.7	122.5	119.2	118.9	159.8
Conductivity	314	322	273	285	303	308	306	303	270
Temperature	3.8	1.1	1.8	2.5	1.8	1.3	2.0	2.6	4.0
I / km <sup>2</sup>	31.5	20.8	13.5	11.4	9.0	8.5	8.3	8.2	11.1

**Measuring Point D\_5a**

X (GPS) 807028  
 Y (GPS) 157721  
 Altitude (m) (GPS) 1820  
 Method BUCKET  
 Description Side torrent I TEZG B / tube beneath Forcola di Livigno



Method Date	Bucket (old) 12.11.2013	BU med 25.11.2013	BU NaCl 19.12.2013	BU NaCl 09.01.2014
I / s	3.5	0.5	0.1	0.0
Conductivity	64.3	61.6	224.0	
Temperature	3.2	0.3	0.1	

**Measuring Point D\_5b**

X (GPS) 807028  
 Y (GPS) 157721  
 Altitude (m) (GPS) 1820  
 Method BUCKET  
 Description Side torrent II TEZG B / tube beneath Forcola di Livigno



Method Date	BU NaCl 25.11.2013	BU NaCl 19.12.2013	BU NaCl 09.01.2014
I / s	0.20	0.04	0.00
Conductivity	73.1	423.0	
Temperature	1.4	1.3	

**Measuring Point D\_6a**

X (GPS) 807028  
 Y (GPS) 157721  
 Altitude (m) (GPS) 1820  
 Catchment Size  
 Method BUCKET  
 Description Side torrent III TEZG B / tube beneath Forcola di Livigno



Method Date	BU NaCl 25.11.2013	BU NaCl 19.12.2013	BU NaCl 09.01.2014
I / s	0.06	0.03	0.00
Conductivity	71.3	92.9	
Temperature	1.0	0.8	

**Measuring Point D\_6b**

X (GPS) 807028  
 Y (GPS) 157721  
 Altitude (m) (GPS) 1820  
 Catchment Size  
 Method BUCKET  
 Description Side torrent IV TEZG B / tube beneath Forcola di Livigno



Method Date	ESTIMATION 12.11.2013	BU med 25.11.2013	BU new 19.12.2013
I / s	4.00	1.97	0.52
Conductivity	41.2	55.1	74.1
Temperature	5.0	0.4	0.7

**Measuring Point X\_1**

X (GIS) 801363  
 Y (GIS) 143343  
 Catchment (km<sup>2</sup>) 7.0  
 Method SALT  
 Description After springs from creeping landmasses from oro. left



Method Date	SD 23.02.2014	SD 12.03.2014
I / s	125.6	119.5
Conductivity	313	311
Temperature		
I / km <sup>2</sup>	8.70	8.28

**Measuring Point X\_2**

X (GIS) 801196  
 Y (GIS) 143494  
 Catchment (km<sup>2</sup>) 6.7  
 Method SALT  
 Description Before springs from creeping landmasses from oro. Left



Method Date	SD 23.02.2014	SD 12.03.2014	SD 03.04.2014
I / s	96.7	92.7	108.5
Conductivity	372	372	342
Temperature			
I / km <sup>2</sup>	14.4	13.8	16.1

**Measuring Point X\_3**

X (GIS) 801056  
 Y (GIS) 143640  
 Catchment (km<sup>2</sup>) 6.4  
 Method SALT  
 Description after confluence with creek B



Method	SD	SD
Date	23.02.2014	12.03.2014
l / s	86.6	86.0
Conductivity	380	381
Temperature		
l / km <sup>2</sup>	13.4	13.4

**Measuring Point X\_4**

X (GIS) 800971  
 Y (GIS) 143804  
 Catchment (km<sup>2</sup>) 4.3  
 Method SALT  
 Description before confluence with creek B



Method	SD	SD	SD
Date	23.02.2014	12.03.2014	03.04.2014
l / s	67.0	62.1	
Conductivity	366	371	
Temperature			
l / km <sup>2</sup>	15.8	14.6	

**Measuring Point X\_5**

X (GIS) 800911  
 Y (GIS) 143957  
 Catchment (km<sup>2</sup>) 4.0  
 Method SALT  
 Description after terrain rim



Method	SD
Date	23.02.2014
l / s	60.8
Conductivity	412
Temperature	
l / km <sup>2</sup>	15.1



**Measuring Point X\_6**

X (GIS) 800860  
 Y (GIS) 144375  
 Catchment (km<sup>2</sup>) 3.6  
 Method SALT  
 Description above MP C



Method	SD	SD
Date	23.02.2014	12.03.2014
l / s	17.3	11.6
Conductivity	531	555
Temperature		
l / km <sup>2</sup>	4.8	3.2

**Measuring Point X\_7**

X (GIS) 800864  
 Y (GIS) 144510  
 Catchment (km<sup>2</sup>) 3.6  
 Method SALT  
 Description above MP C



Method	SD	SD
Date	12.03.2014	03.04.2014
l / s	15.6	15.8
Conductivity	555	572
Temperature		
l / km <sup>2</sup>	4.4	4.4

## Electric conductivity ( $\mu\text{S}/\text{cm}$ )

Measuring Point	FS	MA	MC 1	MC 2	MC 3	MC 4	MC 5	MC 6	MC 7
u_PEG								253	
PEGEL		236	271	244	252	263	289	250	194
A	60	61	69	74	74	79	79	93	91
A_1a		61	72	73					
A_1b			71						
A_2			67	74					
A_3			97	89					
A_4a			38	41					
A_4b			80	88					
A_5		70	87	95					
A_6		70	79	93					
A_7			98						
A_8		71	79						
A_9a		103	90	104					
A_9b		18							
A_10a	39	47	65	79	82				
A_10b		25							
A_11a		15	18						
A_11b			31	37					
A_12a									
A_12b		39							
A_13a			58	103					
A_13b			62	62					
A_14			50						
A_14a			44	42					
A_14b									
A_15a			80						
A_15b				134					
A_16a	30	30							
A_16b		42	47	58					
A_17		192	164	132					
A_18a	30	32	34	36					
A_18b		45		44					
A_19		57	47	55					
A_20		19							
A_21a									
A_21b			115						
A_22a									
A_22b			39						
B		290	494	583	629		697	708	669
above MP_B_oro_left							889		
above MP_B_oro_right							390		
B_plain_above							755		
B_at_confluence_to_main_creek							670	620	
C			412	329	373	417	430	449	461
C_1a		615	677	488					

C_1a_conveyor_oro_right				553					
C_1b	270	200	182						
C_2a			182						
C_2b	240	180							
above_C1				643					
X6							531	555	
X7							532	556	572
plain_above_MP_C_side								492	
plain_above_MP_C_main								550	
conveyor_from_oro_left_I							139	145	
conveyor_from_oro_left_at spring								120	
D									
D_1			119	126	130	173	138	140	
D_2a			166	170	170		174	179	
D_2b			163	170	169		172	176	
after_D1_li							271	241	
after_D1_re								255	
after_D2							282		
before_D2_li							278	259	
before_D2_re							283	262	
spring_of_MP_D1_I								213	
spring_of_MP_D1_II								210	
D_3				257	268	286	290	264	195
D_4	304	314	321	273	285	303	306	303	270
PO1							424		
PO2							425		
PO3							440		
X5							425		
ZU 2							64		
PO 4							368		
X4							368	372	
PO 5							405	392	
ZU 3							64	65	
X3							378	383	
X2							372	372	342
springs_from_landslide_oro_left_I							107		
springs_from_landslide_oro_left_II							117		
springs_from_landslide_oro_left_III							132	127	
springs_from_landslide_oro_left_IV							133		
springs_from_landslide_oro_left_V							140		
springs_from_landslide_oro_left_VI							139		
springs_from_landslide_oro_left_VII							137	135	
X1							312	310	
conveyor_at_X1								126	
D_5a		64	62	224					
D_5b			73	423					
D_6a			71	93					
D_6b		41	55	74					

## Ion capacity

Sampling location	January 07 - 09								
	Fluoride mg/l	Chloride mg/l	Bromide mg/l	Nitrate mg/l	Sulphate mg/l	Sodium mg/l	Potassium mg/l	Calcium mg/l	Magnesium mg/l
	along main creek (in flow direction)								
MP_X6	0.72	0.92	0.00	0.93	200.84	2.20	2.57	73.95	10.91
plain_above_MP_C_main	0.69	0.86	0.00	0.99	180.50	2.13	2.46	66.85	10.09
plain_above_MP_C_side	0.66	0.82	0.00	1.14	155.74	2.15	2.18	59.30	9.09
MP_C	0.56	0.73		0.97	146.17	1.91	2.02	53.70	8.16
MP_D4	0.39	0.72	0.02	0.66	104.13	2.28	1.89	41.78	6.66
MP_D3	0.36	0.92	0.02	0.69	96.31	2.32	2.13	39.28	6.37
MP_D2a	0.22	0.67	0.12	1.07	36.30	2.22	2.32	22.85	5.09
MP_D2b	0.24	0.51	0.12	0.82	40.36	2.48	2.81	21.92	4.88
MP_D1	0.13	0.28	0.11	1.22	23.00	2.06	2.64	17.66	3.58
PEGEL	0.32	1.10	0.05	0.96	83.74	2.47	1.89	36.55	6.22
	Subcatchment A								
MP_A	0.03	4.62	0.04	1.43	7.25	3.41	0.98	9.67	1.61
	Subcatchment B								
MP_B	0.40	0.14	0.11	0.83	260.71	0.46	3.53	99.59	20.93
SNOW_at_MP_B	0.08	4.58	0.04	0.27	0.36	2.80	1.54	1.73	0.22

Sampling location	February 07 - 08								
	Fluoride mg/l	Chloride mg/l	Bromide mg/l	Nitrate mg/l	Sulphate mg/l	Sodium mg/l	Potassium mg/l	Calcium mg/l	Magnesium mg/l
	along main creek (in flow direction)								
MP_C	0.59	0.74	0.00	1.08	171.41	2.20	2.37	63.83	9.62
MP_D4	0.36	0.58	0.01	0.67	110.65	2.16	2.09	44.30	7.14
MP_D3	0.33	0.92	0.00	0.77	102.28	2.29	1.90	41.68	6.70
PEGEL	0.30	1.08	0.03	0.98	86.81	2.46	1.93	37.59	6.56
	Subcatchment A								
MP_A	0.03	4.95	0.04	1.45	7.59	3.70	0.93	10.33	1.63

Sampling location	February 22 - 24								
	Fluoride mg/l	Chloride mg/l	Bromide mg/l	Nitrate mg/l	Sulphate mg/l	Sodium mg/l	Potassium mg/l	Calcium mg/l	Magnesium mg/l
	<b>along main creek (in flow direction)</b>								
PO_1	0.74	0.95	0.00	1.14	232.91	2.22	2.67	85.90	12.54
MP_X6	0.75	0.98	0.00	1.11	232.88	2.19	2.54	85.94	12.43
tributary_oro_left_I	0.17	0.31	0.00	1.02	52.30	2.57	1.73	17.09	3.43
MP_C	0.57	0.71	0.00	1.08	172.63	2.23	2.12	63.65	9.71
PO_2	0.59	0.72	0.00	1.08	178.94	2.23	2.38	66.57	10.04
PO_3	0.58	0.72	0.00	1.04	176.04	2.15	2.08	65.63	9.84
MP_X5	0.56	0.73	0.00	1.04	169.30	2.29	2.35	62.97	9.59
tributary_oro_left_II	0.19	0.23	0.00	0.76	21.41	2.48	1.48	6.60	1.48
PO_4	0.52	0.70	0.00	1.02	148.08	2.36	1.93	55.07	8.51
MP_X4	0.51	0.72	0.00	1.03	147.96	2.40	2.31	55.29	8.44
PO_5	0.49	0.63	0.00	1.06	162.99	2.09	2.33	61.74	10.21
tributary_oro_left_III	0.20	0.21	0.00	0.65	22.05	2.68	1.42	6.45	1.46
MP_X3	0.47	0.60	0.00	0.95	156.01	2.06	1.98	58.43	9.91
MP_X2	0.45	0.63	0.00	0.92	147.14	2.14	2.13	55.02	9.47
springs_landslide_oro_left_I	0.14	0.38	0.03	0.74	29.63	2.52	2.08	16.06	1.29
springs_landslide_oro_left_II	0.12	0.46	0.06	0.78	33.35	2.45	2.35	20.02	1.30
springs_landslide_oro_left_III	0.14	0.48	0.06	0.85	34.05	2.41	2.97	21.09	1.27
springs_landslide_oro_left_IV	0.11	0.36	0.06	0.88	34.11	2.18	2.71	22.30	1.25
springs_landslide_oro_left_V	0.11	0.32	0.06	0.90	35.74	2.09	2.81	23.70	1.33
springs_landslide_oro_left_VI	0.11	0.29	0.06	0.93	35.00	2.09	2.73	22.44	1.25
Springs_landslide_oro_left_VII	0.11	0.22	0.05	0.91	34.62	2.00	2.57	22.58	1.22
MP_X1	0.37	0.77	0.02	0.82	116.89	2.20	2.41	46.72	7.50
MP_D4	0.35	1.22	0.01	0.83	111.99	2.48	2.09	44.62	7.26
MP_D3	0.32	1.96	0.02	0.88	102.55	2.84	2.31	42.37	6.92
PO6	0.32	1.22	0.04	0.85	98.72	2.45	2.57	41.40	6.90
MP_D2a	0.22	0.61	0.10	0.99	37.60	2.32	2.08	23.89	5.07
MP_D2b	0.23	0.45	0.09	0.79	41.35	2.45	2.77	22.92	4.96
PO7	0.31	1.20	0.04	0.86	97.52	2.33	2.38	40.10	6.77
MP_D1	0.15	0.29	0.09	1.17	24.73	2.27	2.64	18.94	3.88
PO8	0.30	1.21	0.05	0.86	92.00	2.41	2.14	38.79	6.68
PEGEL	0.30	5.04	0.05	0.86	86.67	4.81	2.39	38.23	6.52
	<b>Subcatchment A</b>								
MP_A	0.03	4.70	0.07	1.49	7.77	3.56	1.09	10.12	1.75
	<b>Subcatchment B</b>								
B_plain_above	0.48	0.19	0.14	0.84	325.25	0.47	4.58	122.01	25.32
above MP_B_oro_left	0.15	0.26	0.18	1.60	119.99	0.52	2.59	63.35	9.56
above MP_B_oro_right	0.92	0.47	0.18	0.82	402.46	0.72	5.46	145.02	32.11
MP_B	0.39	0.14	0.11	0.97	292.74	0.48	4.39	111.81	22.74
B_at_main_creek	0.36	0.29	0.10	1.04	276.32	0.57	2.48	107.68	22.06

Sampling location									
March 11 - 13									
	Fluoride mg/l	Chloride mg/l	Bromide mg/l	Nitrate mg/l	Sulphate mg/l	Sodium mg/l	Potassium mg/l	Calcium mg/l	Magnesium mg/l
<b>along main creek (in flow direction)</b>									
PO_1	0.73	0.91	0.00	1.26	243.78	2.16	3.00	87.86	12.80
MP_X6	0.73	0.88	0.00	1.24	243.31	2.23	3.08	88.68	12.72
tributary_oro_left_I	0.17	0.30	0.00	1.07	53.87	2.56	2.05	17.35	3.49
tributary_oro_left_I_spring	0.14	0.40	0.00	1.00	45.70	2.68	1.79	13.60	2.92
MP_C	0.59	0.73	0.00	1.17	189.48	2.30	2.72	68.56	10.35
MP_X4	0.48	0.67	0.00	1.12	148.05	2.24	2.64	54.83	8.44
PO_5	0.46	0.68	0.00	1.22	161.60	2.10	2.29	60.09	10.03
MP_X3	0.43	0.67	0.00	1.14	148.74	2.07	2.60	55.72	9.53
MP_X2	0.42	0.66	0.00	1.10	145.11	2.13	2.19	54.18	9.36
springs_landslide_oro_left_III	0.12	0.20	0.00	0.66	33.03	2.37	2.32	19.25	1.29
springs_landslide_oro_left_VII	0.11	0.24	0.02	0.85	33.94	2.38	2.07	20.99	1.09
MP_X1	0.34	0.79	0.00	1.05	114.17	2.21	2.68	45.18	7.36
MP_D4	0.33	0.87	0.00	1.01	109.23	2.35	2.61	43.99	7.08
MP_D3	0.27	2.07	0.00	1.12	88.89	2.65	1.93	37.24	6.02
PO6	0.27	1.95	0.00	1.07	87.00	2.54	2.03	36.81	6.22
MP_D2a	0.23	0.72	0.07	0.97	39.37	2.43	2.47	23.93	5.15
MP_D2b	0.23	0.43	0.06	0.78	41.94	2.43	3.05	22.67	5.00
spring_of_MP_D1_I	0.31	0.26	0.07	0.44	53.15	2.87	3.75	26.67	6.56
spring_of_MP_D1_II	0.29	0.28	0.07	0.46	52.92	2.83	3.83	26.47	6.59
MP_D1	0.15	0.44	0.07	1.19	24.81	2.21	2.86	18.54	3.70
PO8	0.26	1.89	0.02	0.98	80.57	2.68	2.23	35.12	5.99
PEGEL	0.26	1.88	0.02	0.98	78.27	2.68	2.12	34.95	6.01
uPEG	0.27	2.32	0.02	0.91	78.91	3.00	2.31	35.44	6.22
<b>Subcatchment A</b>									
MP_A	0.03	6.88	0.03	1.52	8.46	4.15	0.97	11.34	1.93
<b>Subcatchment B</b>									
MP_B	0.37	0.20	0.02	1.05	296.79	0.54	3.50	113.75	22.79
SNOW_at_MP_B	0.06	4.86	0.14	0.03	0.65	4.06	1.66	18.16	1.07



## **Which hillslopes sustain baseflow during low flow conditions? Lessons from winter discharge observations in the alpine Poschiavino catchment, Switzerland**

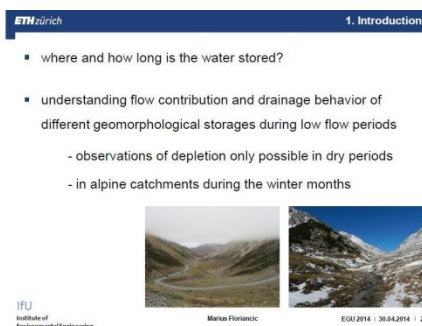
Marius Floriancic (1), Maarten Smoorenburg (1), Michael Margreth (2), and Felix Naef (1)

(1) Institute for Environmental Engineering, ETH Zurich, Zurich, Switzerland, (2) Soilcom GmbH, Zurich, Switzerland

Estimation of water availability during low flow conditions is important for many economic and environmental services. Yet, particularly in mountainous terrain, knowledge of which areas in a catchment store water long enough to sustain streamflow during low flow conditions is very limited. Not only the storage volume, but also the drainage time scale is important for understanding recession dynamics. To identify how alpine hillslopes contribute to baseflow recession at the catchment scale, a detailed field study of winter low flows was conducted in the 14.1km<sup>2</sup> upper Poschiavino catchment in southeast Switzerland. Winter discharge observations in alpine catchments are particularly suitable for studying drainage behavior because there is little recharge and groundwater reservoirs are depleted by drainage only.

The upper Poschiavino catchment with its crystalline geology is an interesting research area because of its high winter discharge ( $Q_{95}$  approximately 10 l/s/km<sup>2</sup>). Based on geo(morpho)logical maps, digital elevation model, aerial photographs and field observations a variety of geomorphological storages, like glacial, rockfall and fluvial deposits, was identified. Frequent discharge measurements during winter allowed obtaining a baseflow recession time series for nested subcatchments in various geomorphological settings. The discharge observations were augmented with electrical conductivity measurements and analysis of stream water chemistry.

These observations form a spatial dataset of low flow distribution in the river network that allows identifying the drainage timescales and the storages involved. We found much variation in the contribution of these hillslopes and tried to attribute these variations to properties of the storages, like catchment area, geomorphology and physical parameters of the sediments. A classification of the different storage types regarding capacity and drainage behavior was developed. This classification formed the basis for a geomorphological mapping scheme for low flow estimation that was evaluated using the discharge observations. The developed methodology may help to estimate the magnitude of low flow in ungauged alpine catchments.





**Can we relate flood and low flow behavior to spatial distribution of thick quaternary deposits? Case study of the 14 km<sup>2</sup> alpine Poschiavino catchment, Switzerland**

**Marius Floriancic<sup>1</sup>, Maarten Smoorenburg<sup>1</sup>, Michael Margreth<sup>2</sup> and Felix Naef<sup>1</sup>**

(1) ETH Swiss Federal Institute of Technology, Zurich, Switzerland (2) Soilcom GmbH, Zurich, Switzerland

Better understanding of water storage timescales of soils and quaternary deposits may improve flood prediction and low flow estimation in mountainous catchments. Even steep slopes can react damped to precipitation events and sustain baseflow during dry periods due to large storage. It remains an open question to what extent short term storage mechanisms that dampen flood runoff are also responsible for sustaining baseflow. Therefore we explored how flood and low flow behavior relate to spatial organization of storage potential in the upper Poschiavino, a 14km<sup>2</sup>basin with strongly contrasting subcatchments.

Winter months provide good opportunities for studying flow recession in alpine catchments because there is little groundwater recharge from rainfall and snowmelt. Therefore, discharge time series were obtained for different nested subcatchments in 7 campaigns throughout the 2013/14 winter season. Stream water electrical conductivity and various ion composition were measured to identify different drainage types and their origin.

To study the effect of storage on low flow, sediment cover type and thickness were mapped. This allowed classifying storage potential throughout the catchment. Alongside, contribution to flood formation was evaluated for different slopes using a recently developed tool for geomorphology-based classification of dominant runoff formation processes in mountainous terrain.

We found substantial spatial variation in drainage timescales and contributed volumes between the different subcatchments (54mm vs. 200mm discharged in four months). Subsurface flow and point source contributions complicate small scale studies of recession flow, suggesting this process should be studied at subcatchment rather than hillslope-scale. The recession analyses combined with time series of ion composition allowed detecting different drainage timescales and an estimation of storage volumes. The variability of low flow discharge and differences in recession behavior can be attributed to the mapped storage potential. Flood runoff behavior could be linked to the mapped distribution of storages, but also requires understanding of drainage mechanisms not only during recession but also during flood formation. Short and long term storage do not necessarily share the same mechanisms but can be related in some areas (strong runoff response - substantially lower winter discharge). Our observations suggest that understanding storage and drainage behavior of areas with large storage potential helps assessing catchment-scale flood and low flow problems.



# Can we relate low flow recession to depth of deposits?

## Case study: 14 km<sup>2</sup> alpine Poschiavino catchment, Switzerland

Marius Floriancic<sup>1</sup>, Maarten Smoorenburg<sup>1</sup>, Michael Margreth<sup>2</sup>, Felix Naef<sup>1</sup>

### Introduction

Even steep slopes can **react damped** to precipitation events and sustain baseflow significant due to **large storage volumes**. Not only storage, but also **time scale of drainage** is important to understand recession dynamics. Winter months provide good opportunities to study flow recession in alpine catchments because there is little groundwater recharge from rainfall and snowmelt.

#### Study area upper Poschiavino:

area	14 km <sup>2</sup>
altitude	1860 – 3032 m asl
precipitation	1738 mm
Q <sub>95</sub>	10 l/s km <sup>2</sup>

We explored how low flow behavior relates to spatial organization of storage potential in crystalline upper Poschiavino basin. **Discharge time series** were obtained for different nested subcatchments in 8 campaigns at up to 54 measurement points throughout the 2013/14 winter season. Stream water **electrical conductivity** and various **ion composition** were also measured to identify different storages and the origin of water. Sediment cover and thickness were mapped, allowing a **classification of storage potential** throughout the catchment.

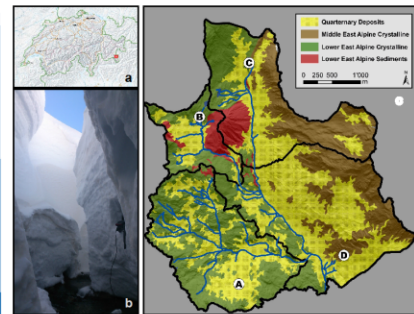


Fig. 1a: Location of the study area Fig. 1b: Snow accumulation during winter season 2013/14 Fig. 1c: Tectonic map of Poschiavino / LaRösa

### Results

#### Different storages – different drainage behavior

The four subcatchments have different storage potential due to different depth of sediment deposits (Fig.2). This leads to different recession and drainage timescales. In the eastern part huge storages could be identified (C and D) leading to higher low flow and discharged water volume (194 mm in D vs. 54 mm in A discharged in 104 days). Drainage is quicker in the western subcatchments.

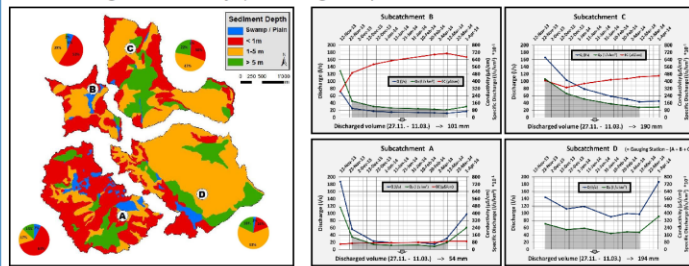


Fig. 2: Distribution of sediments with different depth in the four subcatchments and discharge (l/s), specific discharge (l/s km<sup>2</sup>) and electrical conductivity (µS/cm) in winter 2013/14

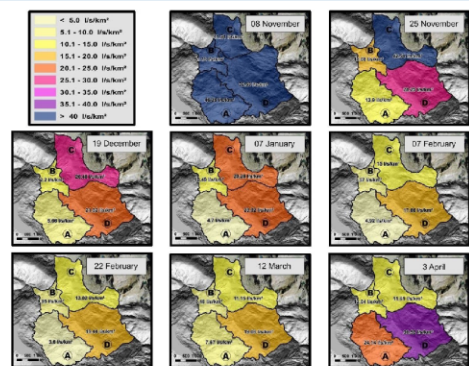


Fig. 3: Specific discharge (l/s km<sup>2</sup>) in the four main subcatchments (A, B, C and D) for every measurement campaign

Recession differs in the four subcatchments during winter season 2013/14.

#### Natural ion tracer experiment

High electrical conductivity in subcatchments B and C derives from sedimentary rocks (Fig. 1c), mainly gypsum and dolomite covering 7% of the catchment. Estimating full saturation of SO<sub>4</sub> and Mg ions quantification of their contribution was done. About 14% of total discharge of the catchment derive from sedimentary rocks (Fig. 5). The amount is even higher in sub-catchment B and C.

Date	MP	SO <sub>4</sub>		Mg		Q <sub>SO<sub>4</sub></sub>		Q <sub>Mg</sub>		Q <sub>sum</sub>	Q <sub>sum</sub> / Q <sub>sum</sub>
		mg/l	mg/l	l/s	mg/l	l/s	l/s	%			
MC Jan	B	261	21	147	5.6	37.8					
MC Feb	B	292	23	127	5.3	41.8					
MC Mar	B	297	23	119	5.0	42.2					
MC Jan	C	166	9	791	15.8	19.9					
MC Feb	C	180	10	50.8	11.3	21.8					
MC Mar	C	189	10	43.5	9.8	22.5					
MC Jan	D4	104	7	164.9	22.0	13.4					
MC Feb	D4	113	7	123.5	18.0	14.7					
MC Mar	D4	109	7	118.9	16.9	14.2					

Fig. 5: Estimated contribution from sedimentary rocks, for subcatchments A, B and the whole catchment (D4)

#### Point sources limiting spatial resolution

Subcatchment D is showing the highest contribution / slowest drainage during recession. However higher resolution measurements for subcatchment D show high spatial variation in specific discharge (Fig. 4). Topographic catchments do not coincide with the hydrological catchments. Subsurface flow and point source contribution are limiting the possible spatial resolution.

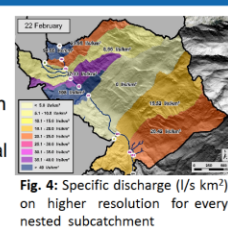


Fig. 4: Specific discharge (l/s km<sup>2</sup>) on higher resolution for every nested subcatchment

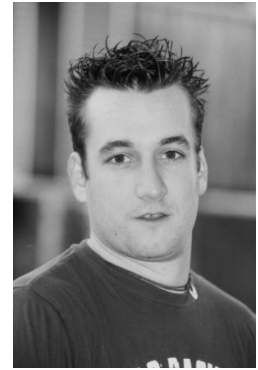
### Conclusions

- low flow discharge in crystalline headwaters proved to be highly variable
- variability in recession and drainage behavior could be assigned to spatial distribution and depth of storages
- point source contribution and uncertain catchment borders limit the spatial resolution of hydrological research
- natural tracers can be used to identify contributions of different geological origin
- understanding storage and drainage behavior of areas with large storage potential helps assessing catchment scale flood and low flow problems



---

# Curriculum Vitae - Marius Günter Floriancic



---

## Ausbildung

- 2012 - 2014**     **Universität für Bodenkultur – Wien**  
**Masterstudium Hydrologie und alpine Naturgefahren**  
*Schwerpunkte:* Hydrologie und wasserwirtschaftliche Planung, Landeskulturelle Wasserwirtschaft, Konstruktiver Wasserbau, Risikomanagement und Ressourcenschutz , Niederschlag-Abfluss Modellierung und Feststofftransport in Wildbächen
- 2012 - 2014**     **Universität Wien / Masterstudium Angewandte Geographie**  
*Schwerpunkte:* Geomorphologie, Pedologie und Hydrologie
- 2007 - 2012**     **Universität Wien / Bachelorstudium Physische Geographie**  
*Bachelorarbeit:* Trinkwasserversorgung von Ballungsräumen – Herausforderungen und Entwicklungspotentiale für Mexico City, Sanaa, Las Vegas und Wien
- 06/2006**         **AHS Matura – AHS BG Peraustraße, Villach**

---

## Studienbegleitende Berufserfahrung

- seit 10/2013**     **Projektassistent am Institut für Umweltingenieurwissenschaften / ETH Zürich**  
Arbeitsgruppe Hydrologie – Dr.Felix Naef  
Abflussmessungen, Kartierung und GIS-gestützte Analysen im Rahmen des Niederwasserprojekts am oberen Poschiavino
- 07-08/2013**     **Abteilung 8 des Landes Kärnten – Umwelt, Wasser und Naturschutz**  
Unterabteilungen Umweltdaten & KAGIS und Schutzwasserwirtschaft  
Umstellung von KAGIS auf ArcGis Server, Validierung von schutzwasserwirtschaftlichen Maßnahmen, GIS-gestützte Hochwasserereignisdokumentation
- 10/2012 – 05/2013**     **Projektassistent der Arbeitsgruppe ENGAGE**  
Institut für Geographie und Regionalforschung – Universität Wien  
GIS-gestützte Risikoanalysen, Geländekartierung, Erstellung von Prozesskarten und Gefahrenkarten im Rahmen der EU-Projekte SEERisk
- 07/2012**         **Forsttechnischer Dienst für Wildbach und Lawinenverbauung**  
Gebietsbauleitung Gailtal und oberes Drautal  
Wildbachkartierungen, Bauwerkszustandserhebungen, Abflussmodellierung und CAD gestützte Erstellung von Prozesskarten, Durchflussprofilen u. Gefahrenzonenplänen

---

## Projektarbeit

---

- 2012 / 13**     **Projektmitarbeiter – Physiographisches Labor Universität Wien**  
Probennahme und physikalische und chemische Laboranalytik  
im Auftrag u.a. von: Ökoregion Kaindorf, Bioforschung Austria, NUA;
- 09/2013**     **Soilcom GmbH, Scherrer AG**  
Profilaufnahmen zur Validierung der Abflussprozesskarte Vinschgau / Südtirol im Auftrag  
der autonomen Provinz Bozen
- 10-11/2012**   **NUA – Umweltanalytik GmbH**  
Bodenbeweissicherung von Rekultivierungsflächen im Rahmen des Baus der S10  
Mühlviertler Schnellstraße

---

## Wissenschaftliche Publikationen

---

**FLORIANCIC, Marius; SMOORENBURG, Maarten; MARGRETH, Michael; NAEF, Felix; (in prep.)**  
Evaluating capacity and drainage behavior of alpine groundwater storages – winter recession  
observations in the upper Poschiavino Area / Switzerland; Hydrological Processes;

**Conference abstracts:**

**FLORIANCIC, Marius; SMOORENBURG, Maarten; MARGRETH, Michael; NAEF, Felix; (2014)** Which  
hillslopes sustain baseflow during low flow conditions? Lessons from winter discharge observations in  
the alpine Poschiavino catchment.- In: European Geoscience Union (Eds.): Abstracts Vol.16; General  
Assembly, Vienna (Austria) 27.April - 02. Mai 2014;

**FLORIANCIC, Marius; SMOORENBURG, Maarten; MARGRETH, Michael; NAEF, Felix; (2014)** Can we  
relate flood and low flow behavior to spatial distribution of thick quaternary deposits? Case study of the  
14 km<sup>2</sup> alpine Poschiavino catchment, Switzerland. In: American Geoscience Union (Eds.): AGU Chapman  
Conference, Luxembourg City (Luxembourg) 23.September - 26.September 2014;

---

## Mitgliedschaften

---

American Geoscience Union (AGU)  
European Geoscience Union (EGU)  
Österreichische Gesellschaft für Hydrologie (ÖGH)

---

## Sonstiges

---

**Kinderuni (2012 u. 2013)** – Lehrveranstaltungsgestaltung „Jetzt tauts – Wasser marsch statt Pistenspaß“

**Tutorium: Fachexkursion - Die Wiener Wasserversorgung** – Universität Wien / WS 2012

**2010/11** **Auslandssemester in Rom** - Studium der Geographie an der Universität „La Sapienza“

**2009** **pm basic Zertifikat** – Projekt Management Austria